

**OPTIMIZATION OF THE CUTTING ACTION OF A
SPRING SUPPORTED SASH SAW THROUGH
COMPUTER SIMULATED TOOTH TRACE ANALYSES**

CENTRE FOR NEWFOUNDLAND STUDIES

**TOTAL OF 10 PAGES ONLY
MAY BE XEROXED**

(Without Author's Permission)

E. S. LARGE

OPTIMIZATION OF THE CUTTING ACTION
OF A SPRING SUPPORTED SASH SAW
THROUGH COMPUTER SIMULATED TOOTH TRACE ANALYSES

by
(c) E. S. Large, B. Eng.

A thesis submitted to the School of graduate.

Studies in partial fulfillment of the
requirements for the degree of

Master of Engineering

Department of Engineering and Applied Science

Memorial University of Newfoundland

December 1986

St. John's

Newfoundland

Canada

Permission has been granted to the National Library of Canada to microfilm this thesis and to lend or sell copies of the film.

The author (copyright owner) has reserved other publication rights, and neither the thesis nor extensive extracts from it may be printed or otherwise reproduced without his/her written permission.

L'autorisation a été accordée à la Bibliothèque nationale du Canada de microfilmer cette thèse et de prêter ou de vendre des exemplaires du film.

L'auteur (titulaire du droit d'auteur) se réserve les autres droits de publication; ni la thèse ni de longs extraits de celle-ci ne doivent être imprimés ou autrement reproduits sans son autorisation écrite.

ISBN 0-315-43347-7

In memory of my father, Edward Christopher Large,
who sparked my unending quest for knowledge

Abstract

The influences of various factors on the mechanics of wood cutting by a spring-supported, vertically oscillating frame saw are examined. These include saw tooth pitch, tooth gullet depth and capacity, saw blade overhang, oscillation frequency and amplitude, and log feed speed.

The efficiency and effectiveness of the cutting process are dependent primarily on the relative path of motion taken by each tooth through the wood during sawing; thus it is the tooth traces upon which the attention of this study is focused. The factors listed above govern the shapes of these traces, and thus it is the determination of optimum values for some of these factors which is the main objective here.

For the purpose of tooth trace analyses, a computer program has been developed which, when coupled with plotting facilities, allows the user to view a set of simulated relative tooth paths. The program incorporates features which accommodate the other than normal kinematic characteristics of the plate spring supported sash, and combines these influences with those of the factors listed above. Most importantly it allows for the introduction of a non-constant log feed speed function, specifically one which combines a constant with a sinusoidal portion.

A detailed analysis of the produced plots with a view to solution to inherent sash saw problems comprises the final portion of this paper. From specific observations and assumptions with respect to the mechanics of cutting of the saw teeth, simultaneous equations are developed and solved for three system variables. Finally, conclusions are drawn and recommendations made with respect to the development of a more efficient MUN (Memorial University of Newfoundland) Sash Saw design.

Acknowledgements

The paper to follow was completed at the Faculty of Engineering and Applied Science, Memorial University of Newfoundland, over the period fall 1983 to spring 1986. The author wishes to thank the university for its fellowship and graduate supplement support during the first and last periods of study, and the Natural Sciences and Engineering Research Council of Canada for its support during the second year.

The author greatly appreciates the advice, guidance, and moral support provided by his supervisor, Professor W. G. (Bill) Smith, throughout the term of his graduate program. Thanks are also in order to Dr. G. R. Peters, Dean of Engineering, and to Dr. T. R. Chari, Associate Dean of Engineering, for facilities provided and support given. Finally, the assistance and patience of the support and technical staff of the university are gratefully acknowledged.

Table of Contents

ABSTRACT	iii
ACKNOWLEDGEMENTS	v
LIST OF TABLES	viii
LIST OF FIGURES	ix
NOMENCLATURE	xi
1. INTRODUCTION	1
1.1. SAWMILLING MACHINES - A BRIEF HISTORY	1
1.2. BACKGROUND TO THE PROJECT	3
1.3. OBJECTIVES OF THIS STUDY	10
2. COMPUTER SIMULATION	12
2.1. PLATE DEFLECTION ANALYSIS	12
2.2. PLATE VIBRATION ANALYSIS	23
2.2.1. Simple beam-girder approximation	24
2.2.2. Improved beam-girder approximation	26
2.2.3. Computer frequency analysis	29
2.3. LOG FEED INCORPORATION	32
2.4. SAW BLADE AND MOUNTING GEOMETRY	33
3. SAWING OPTIMIZATION	35
3.1. EQUATION GENERATION	35
3.2. EXPERIMENTAL EXAMINATION	39
3.3. DOWNWARD STROKE ANALYSIS	41
3.3.1. Area calculation	43
3.3.2. Integration of centre tooth trace equation	47
3.3.3. Integration of adjacent tooth trace equation	50
3.4. UPWARD STROKE ANALYSIS	54
3.4.1. Interference assessment	54
3.4.2. Return stroke assessment	59
3.5. EQUATION SOLUTIONS - INITIAL	62
3.5.1. Variable reduction	62
3.5.2. Assignment of objective values	64
3.5.3. Matrix solution of equations	66
3.6. EQUATION SOLUTIONS - RE-ITERATION	71
3.7. EQUATION SOLUTIONS - DEEPER GULLETS	76

4. SUMMARY AND CONCLUSIONS	88
4.1. Results of study	88
4.2. The future of the MUN Sash Saw	89
REFERENCES	93
Appendix A. COMPUTER PROGRAM LISTINGS	94
A.1. Tooth Trace Simulation Program	95
A.2. Strudl Analysis - Approach #1	99
A.3. Strudl Analysis - Approach #2	101
A.4. Strudl Analysis - Approach #3	103
A.5. Strudl Analysis - Approach #4	105
A.6. Fourier Series Fitting Program	107
A.7. System Equations Solution Program	109

List of Tables

Table 2-1:	Frequency Outputs from STRUDL Runs	31
Table 3-1:	Fourier Order vs. Compiled Error	37
Table 3-2:	Parameter Solutions - Initial	67
Table 3-3:	Parameter Solutions - Second Iteration	72
Table 3-4:	Gullet Areas (est.) for 1.25 inch Pitch	77
Table 3-5:	Parameter Solutions - Deeper Gullets	78

List of Figures

Figure 1-1:	Pit Saw	2
Figure 1-2:	Band Saw Strip Cutting	6
Figure 1-3:	Circular Saw Strip Cutting	6
Figure 1-4:	The MUN Sash Saw	8
Figure 1-5:	Kokum's Figure-8 Frame Travel	9
Figure 2-1:	Sash Mounting - Side View	13
Figure 2-2:	Plate Deflected Shape	13
Figure 2-3:	Plate Free-Body Diagram	14
Figure 2-4:	Infinitesimal Curve	16
Figure 2-5:	Existing Crank Drive	19
Figure 2-6:	Crank Drive/Sinusoid Deviation	20
Figure 2-7:	Flow Chart for Plate Deflection Data Generation	22
Figure 2-8:	GTStrudl Plate Division #1	30
Figure 2-9:	GTStrudl Plate Division #2	30
Figure 2-10:	GTStrudl Plate Division #3	30
Figure 2-11:	GTStrudl Plate Division #4	31
Figure 2-12:	Saw Blade Overhang and Pitch	33
Figure 3-1:	Plate End Deflection - Curve Shape	37
Figure 3-2:	Fourier Curve vs. Original Curve	38
Figure 3-3:	Experimental Set-Up	39
Figure 3-4:	Wax Sandwich Board Mounted on Feed Table	40
Figure 3-5:	Gullet Nomenclature and Area Determination	42
Figure 3-6:	Example Tooth Trace	44
Figure 3-7:	Kerf Profile After Cutting Stroke	45
Figure 3-8:	Tooth Vertical and Horizontal Offsets	50
Figure 3-9:	Interference Illustration - Wide View	55
Figure 3-10:	Interference Illustration - Isolation View	56
Figure 3-11:	Log Velocity vs. Sash Position	64
Figure 3-12:	Tooth Trace - 0.000 in. Interference	69
Figure 3-13:	Tooth Trace - Constant Log Feed Speed	70
Figure 3-14:	Tooth Trace - Revised Integration Limits	74
Figure 3-15:	Standard North American Band Saw Blade Gullets	76
Figure 3-16:	0.4375 in. Gullet - 0.000 in. Interference Trace	80
Figure 3-17:	0.4375 in. Gullet - 0.020 in. Interference Trace	81
Figure 3-18:	0.500 in. Gullet - 0.000 in. Interference Trace	82
Figure 3-19:	0.500 in. Gullet - 0.030 in. Interference Trace	83

Figure 3-20:	0.5625 in. Gullet - 0.000 in. Interference Trace	84
Figure 3-21:	0.5625 in. Gullet - 0.040 in. Interference Trace	85
Figure 3-22:	0.625 in. Gullet - 0.000 in. Interference Trace	86
Figure 3-23:	0.625 in. Gullet - 0.050 in. Interference Trace	87
Figure 4-1:	Saw Tooth Spring and Swage-Sets	91

NOMENCLATURE

β	blade overhang angle
θ	phase lag angle
ν	Poisson's ratio
$\psi(x)$	deflection shape function
ω	vibration frequency
ω_n	natural frequency
a_n	fourier function cosine coefficient
a_0	fourier offset constant
A	log feed constant component amplitude
A_a	area under adjacent tooth trace
A_c	area under centre tooth trace
A_f	area under feed function trace
A_{tot}	area between traces
b_n	fourier function sine coefficient
CK	crank length
CR	connecting rod length
D	plate flexural rigidity
e	fourier error

E	Young's modulus
EF	wood expansion factor
h	plate thickness
I	section modulus
k	spring stiffness constant
L	plate length
m_{eff}	total effective mass
m_I	effective inertial mass
m_s	sash mass
M	bending moment
p	tooth pitch
P	plate end load
R	log feed sinusoidal component amplitude
S_f	log net horizontal displacement
t	time
T	finite time period
v	vertical excursion
v_o	tooth vertical offset
V_f	total log feed speed
x	general horizontal position
x_a	horizontal position - adjacent tooth
x_c	horizontal position - centre tooth
x_L	plate horizontal span

x_0

tooth horizontal offset

X

plate cross-sectional area

Chapter 1

INTRODUCTION

1.1. SAWMILLING MACHINES - A BRIEF HISTORY

Saws in all forms throughout the ages have served one specific purpose; to alter the cross-section of a log from its natural round form to a shape, usually square or rectangular, better suited to the construction project at hand. The earliest saws known to man were reciprocating blades made from flint. Later, bronze blades were used, specifically in Egyptian hand saws, pulled in one direction only because of the lack of stiffness of the soft metal. Over the centuries larger saw types evolved, more efficient and complicated and requiring more power, in most cases of the animate type. In the pit saw method of producing boards and planks for example, a log sat horizontally over a pit while two men, one in the pit and one above, pulled the blade up and down. The log was shifted forward when necessary as the sawing progressed (see Fig. 1-1)¹. The process was backbreaking and the lumber produced was relatively inaccurate in terms of straightness and uniformity of thickness.

Over a period of time machines evolved in which blades were mounted in a frame or sash, guided mechanically in reciprocation for greater precision. Similarly mounted multiple blades enabled the production of multiple boards with

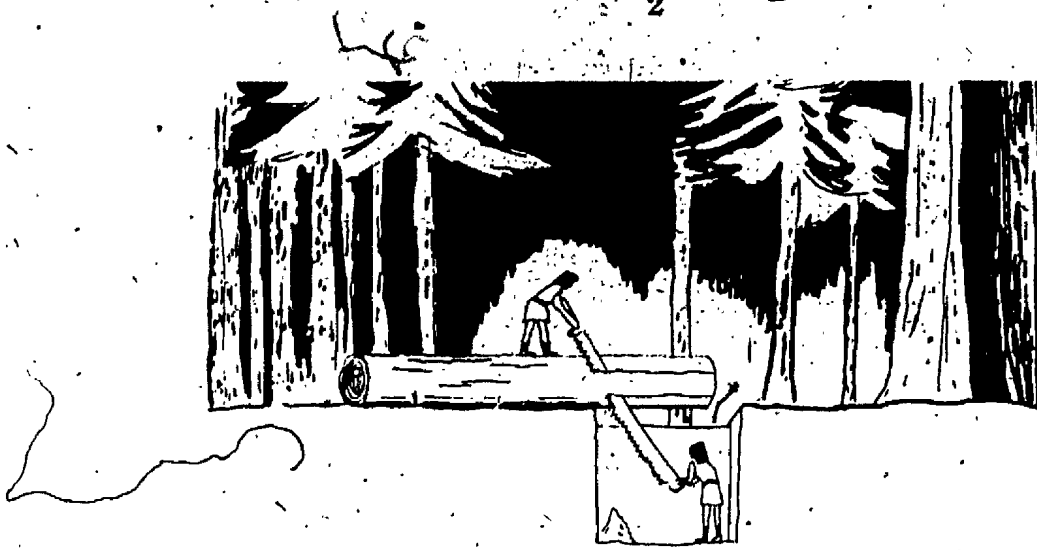


Figure 1-1: Pit Saw

a single pass of the log through the sash. Such saws have actually been in use for centuries. Developing in the meantime however were the two other staples of the sawmilling industry. The first, the circular saw, was patented in 1790². The early ones had blades four feet in diameter and three-eighths of an inch thick. Modern circular blades can be much larger in diameter, with thicknesses of 5/16 inch to 3/8 inch. The second development, introduced in 1890's, was the band saw, in which a toothed, endless belt of steel runs between two tensioning guide wheels. Modern band saw blades have very minimal thicknesses, as low as 1/32 inch.

All three machines have inherent advantages and disadvantages. The circular saw is the cheapest to purchase and install and is extremely rugged, and therefore requires minimal skills in operation and maintenance. However, geometry dictates the necessity of a relatively great blade thickness for cutting accuracy and durability, and thus a high wastage to production ratio is inevitable. The band saw produces a much thinner kerf, and can sustain great log feed rates through high blade speeds. However it is difficult to operate in gang format, and

thus only one board or cant is normally produced during a single pass. The modern sash or gang saw machine is a massive piece of machinery, requiring immense mounting foundations and sophisticated counterbalancing, as a heavy rigid frame is required to maintain the numerous blades in equal high tension. Its primary advantage is its low wastage level per blade, comparable to that of the band saw, while being able to produce accurate, multiple boards at a reasonable rate. As well, the blades are usually simple and easy to maintain and/or replace with minimum production downtime.

The following section elaborates on the pros and cons of the various saw types as a prelude to the development of the MUN sash saw.

1.2. BACKGROUND TO THE PROJECT

Studies performed during the 1970's indicated that about 1440 registered sawmills existed in the province of Newfoundland at the time, most of which were push-bench mills with large diameter circular blades. As such, they are extremely wasteful of raw materials and energy, due to wide kerf cuts and large planing allowances for lack of precision in cutting. Such observations were noted during an investigation into the industry by J. W. Church and L. M. Zeidler, whose report of March 1977 recommended that "a gang sash saw be developed for Newfoundland conditions"³. Such a machine, to be competitive with existing equipment, had to be reasonable in price, energy efficient, and easy to install and maintain, and thus involve a fairly low level of technology.

Under the auspices of the Memorial University Faculty of Engineering, and

the Federal Canadian Forestry Service, a project was initiated in August, 1979 to develop an improved sash saw, ie; one which would retain the advantages inherent in the sawing method while reducing or eliminating the negative aspects. In tailoring the design for Newfoundland operations, specifically for the sawing of relatively small diameter logs, a more radical sash suspension and drive, through which the design objectives could be reached, was realized.

Contemporary sash saw designs generally incorporate a simple sash travelling in vertical oscillation within vertical guides, driven by a motor, crank, and connecting rod arrangement. The full stroke travel in these machines is fairly large, to accomodate massive logs. The long sash travel dictates long free, or unguided blade spans, and thus high blade loads to maintain proper tensions for accurate sawing are necessary. Heavy rigid sash frames are common, with masses which can reach 400 kilograms in Swedish frame saw designs. With typical oscillation frequencies between 300 and 400 cycles per minute, combined with long strokes and massive frames, the inertia forces can reach 20 tonnes in the connecting rods, which can themselves weigh 250 kilograms. The end result is the first major disadvantage of the contemporary frame saw; it is a massive, non-portable piece of machinery which must be mounted on an immense concrete foundation, up to as much as 100 cubic metres in volume. In the Swedish sawmilling community, laws dictate that these saws be outside a set residential proximity, due to high generated noise and vibration levels. Multiple saws must be operated out of phase, or at different speeds, to prevent superimposed vibrational effects. As well, the concrete mounting foundations must not be connected directly to bedrock, through which vibrations could be transmitted to the surrounding countryside.

The second disadvantage of the standard sash saw design is also a consequence of large sash and connecting rod masses. Large forces and thus high power are required for high acceleration and deceleration during normal operating oscillation rates. In some cases complex and expensive counterbalancing equipment is incorporated, the driving of which requires some additional power.

The final problem with the conventional design is a consequence of the actual sawing motion. In band sawing each individual tooth will make a complete cut through a log, from top to bottom, removing a strip of material whose width is a function of the rate at which the log is fed into the blade (see Fig. 1-2). The most efficient and economical feed is realized when the volume of removed material matches the volume inside the tooth 'gullet', into which it must be stored while the tooth remains inside the log. A similar situation exists with the circular blade, where each tooth cuts an arc-shaped strip of a width dependent again on the log feed rate (see Fig. 1-3)¹. In both cases the cut material is expelled when the tooth leaves the log. In sash sawing however, due to the stroke reversal, a tooth may or may not make a complete pass through a log, depending on its position on the blade relative to the log. Thus a tooth will not have the opportunity to dump its respective cut material unless it completes its cutting stroke after exiting the log at the bottom. As well, it will not likely remove a continuous strip of material in any case, as the reciprocating motion of the blade leaves an irregular kerf shape behind after a cutting stroke. This irregular shape also induces back-cutting, or the driving of the backsides of the teeth into the kerf during the return stroke. Back-cutting can cause undue wear on the teeth, as well as produce an additional energy drain.

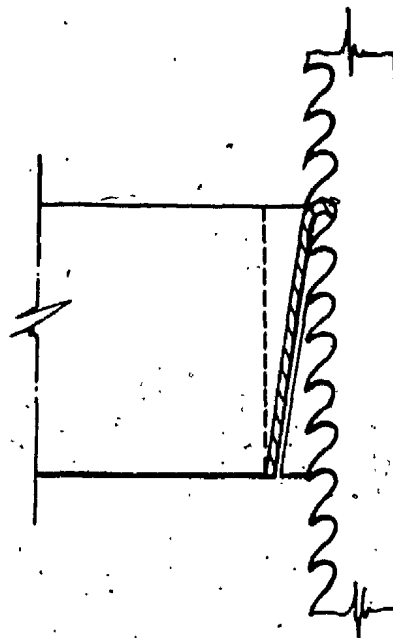


Figure 1-2: Band Saw Strip Cutting

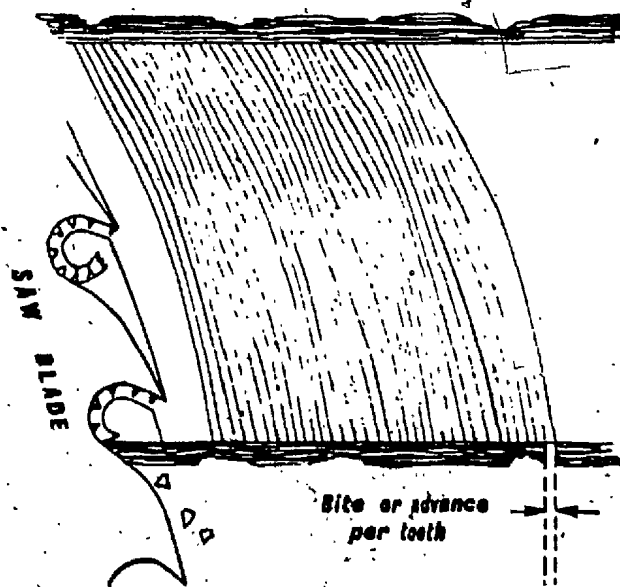


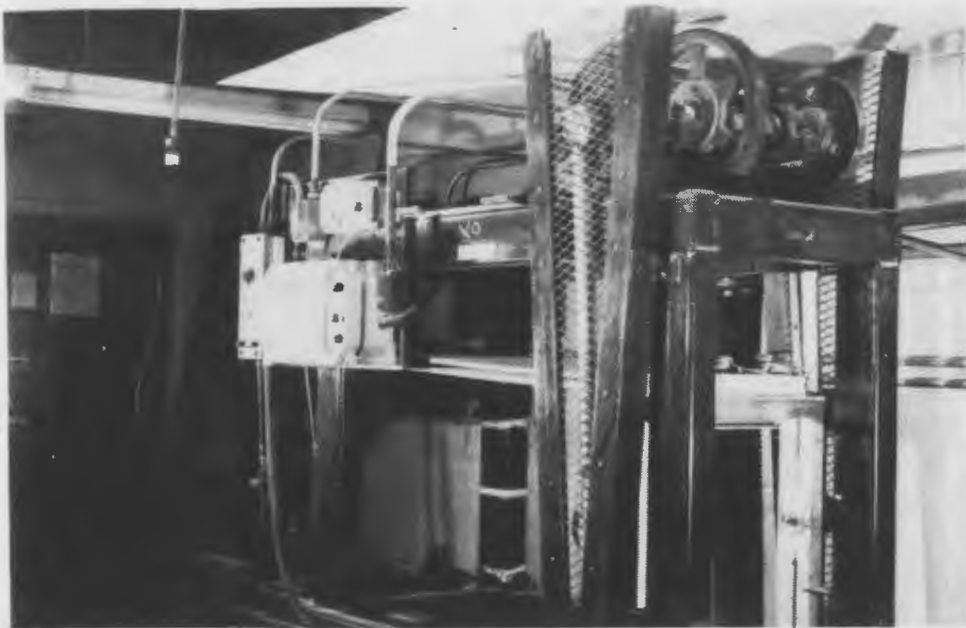
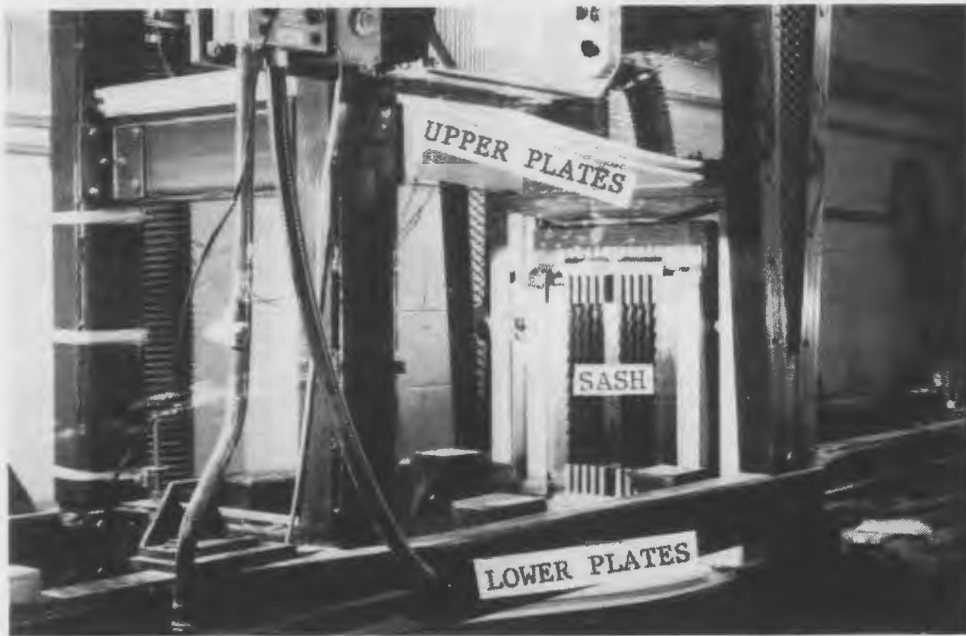
Figure 1-3: Circular Saw Strip Cutting

The MUN sash saw in its present form (illustrated in the photographs of Fig. 1-4) through making use of the property of torsional rigidity in parallel plates, has all of the advantages of the gang saw, and few of its disadvantages.

No precision guides are required to control the motion of the frame. Instead of using massive flywheels, the energy needed to assist in the reversal of the frame's motion at the end of each stroke is stored as potential elastic energy in deflected plates (see Fig. 1-4 and 2-1). This type of suspension provides sufficient stiffness to resist lateral and torsional deflections during sawing. In tuning the drive to the natural frequency of vibration of the plate spring system, energy input is required only for the actual sawing, and to overcome some small internal damping and windage losses. Thus connecting rods need not be unreasonably massive. In designing the saw for the cutting of smaller logs, stroke lengths are smaller, as are the blade free lengths. Thus the sash need not be so rigid, as lower blade loads should be required for accurate cutting. The end results of these modifications are much lower vibrational effects, negligible noise, and much lower power requirements. Combined with the minimal wastage of thin band-saw type blades, the MUN sash saw is an attractive, innovative piece of equipment.

The last design consideration, the one explored herein, is the final disadvantage of the frame saw; back-cutting effects. In conventional designs, no standard acceptable approach to the problem exists. In simpler machines and in the early years of frame sawing, saw overhang, or an inclination of the blade from the vertical was normally incorporated. It will be shown in this study that overhang alone is not a complete solution. In more complex machines, such as Kokum's Figure-8 model shown schematically in Figure (1-5), the frame ends travel in paths as suggested by the name, so that it is continuously swinging with respect to the vertical plane⁵. This allows the teeth to pull out and away from the kerf at the end of a cut. In other models, such as Esterer's Vollgatter gang

Figure 1-4: The MUN Sash Saw



saw, overhang is combined with an oscillating or intermittent log feed speed to reduce or eliminate back-cutting⁶.

Due to frame mounting constrictions in the MUN saw, swinging of the frame is not a practical solution. It is the final combination of overhang and variable log feed which has been evaluated. The following section introduces the approach taken in this study towards that goal.

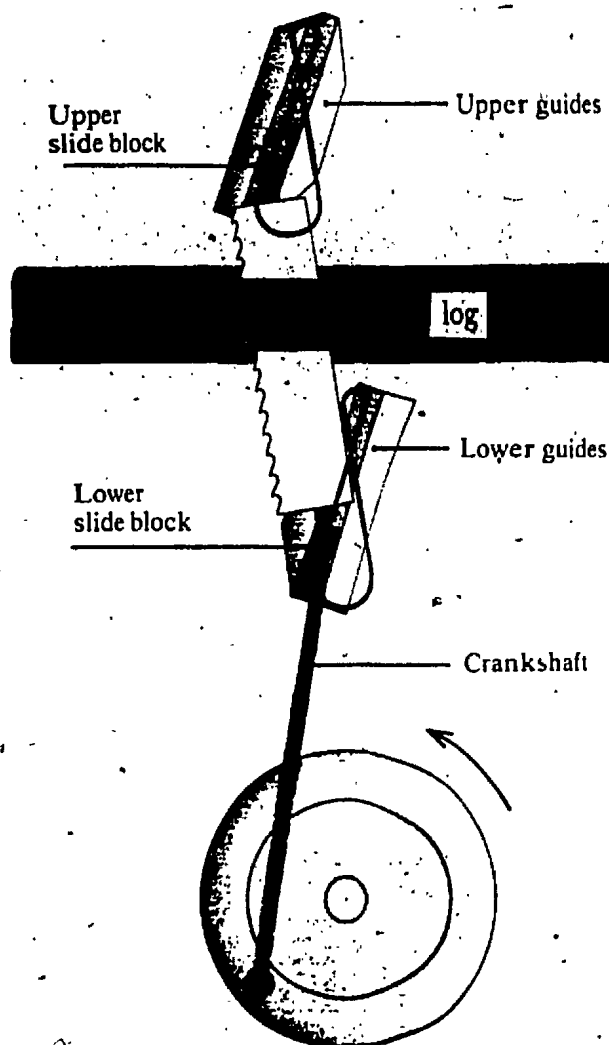


Figure 1-5: Kokum's Figure-8 Frame Travel

1.3. OBJECTIVES OF THIS STUDY

A project to study in detail the kinematics of motion of the frame during operation was initiated in the fall of 1983 as a topic of graduate research in mechanical engineering design. Detailed literature searches indicated that no such study had ever been documented, specific to a frame sawing situation. With no obvious starting point for the research, the onus lay in the development and substantiation of novel theories relating primarily to the MUN sash sawing concept. The material contained herein therefore relies very little upon and refers very seldom to background material.

The principal objective here is the qualification and quantification of the motion of the individual saw teeth with respect to the material being sawn, and the use of the developed equations in the determination of optimum sawing parameters. The first step towards this goal is a geometric and dynamic analysis of the plate spring support system of the saw, through mechanics of solids principles and vibration analysis techniques. These lead to the development of a computer program which produces traces simulating the relative paths of individual teeth as they cut their way through a log during the sawing process. The trace shapes are governed by input values of the system variables in question; log feed speed parameters, saw blade inclination, and tooth and gullet geometrical factors.

The second part of this study is the detailed analysis of the generated traces. The main focus is upon the shape of the face of the advancing log, or kerf profile, at different points in the sawing cycle. From a superposition of kerf shapes upon

the traces, it is possible to determine the shapes and amounts of material removed by an individual tooth. The kerf shape also indicates possible points of interference of the tooth during the non-sawing upstroke, as well as the clearance available for advance of the log.

After assignment of some system objective values, the end result is the derivation of system equations, solution to which provides numbers for the variables in question. Thus the objective of optimizing the cutting action of the saw, through determination of optimum system parameters, is realized. Note that throughout this paper, the British system of units is employed, as this is the form in which material properties, tooth characteristics, sawing stroke, etc. are expressed. The final results however, are shown in SI units primarily, and secondarily in British units.

Chapter 2

COMPUTER SIMULATION

Four geometric and/or dynamic characteristics of the system are involved in the development of the computer program, listed as A.1 in the appendix, which simulates and plots the relative motions of the saw blade teeth. These include the vertical and horizontal displacements of the saw blade cantilever support system, the frequency of oscillation of the cantilever plates, the log feed function specifics, and the saw blade and set-up geometry. Each topic will be explored and discussed in this chapter.

2.1. PLATE DEFLECTION ANALYSIS

As discussed, the saw operates by means of oscillatory displacements of flat plate springs in the vertical direction, within maximum amplitude limits. The situation is illustrated in Figure (2-1), $v(t)$ being a sinusoidal-shaped time-based function of frequency ' ω '. As shown in Figure (2-2), a vertical displacement is accompanied by a horizontal displacement $\Delta x(t)$, giving the attached blade-mounting sash a natural curved path of travel. It is this shape which most distinguishes the cutting action of this mechanism from that of a standard frame saw. It is also the reason that the cutting mechanics must be strictly examined and evaluated.

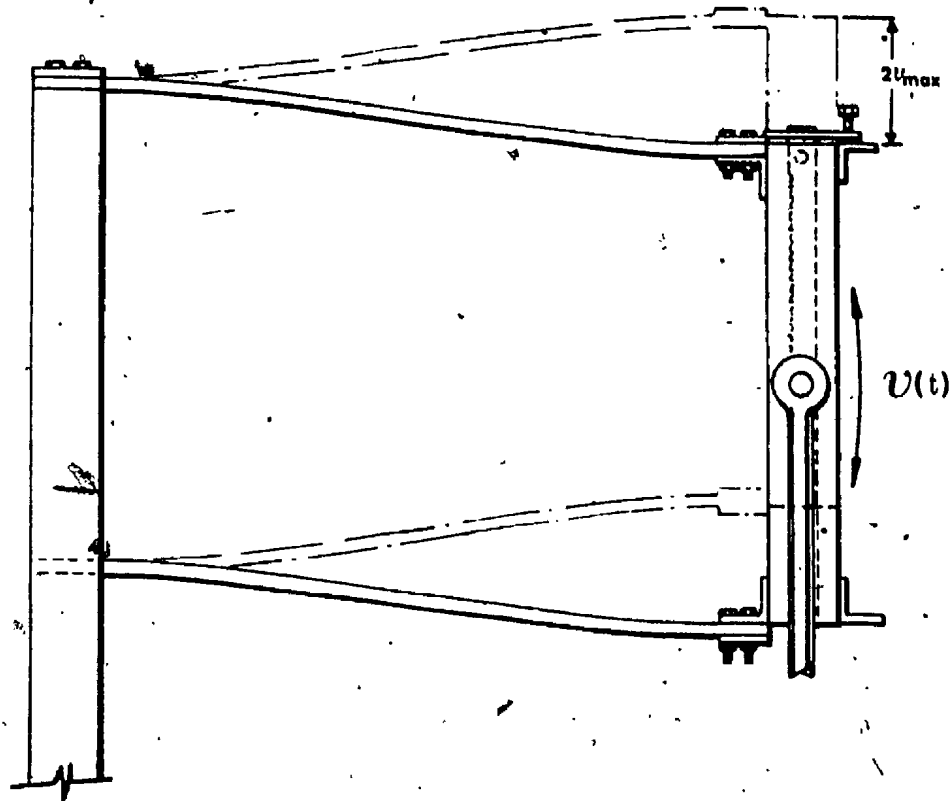


Figure 2-1: Sash Mounting - Side View

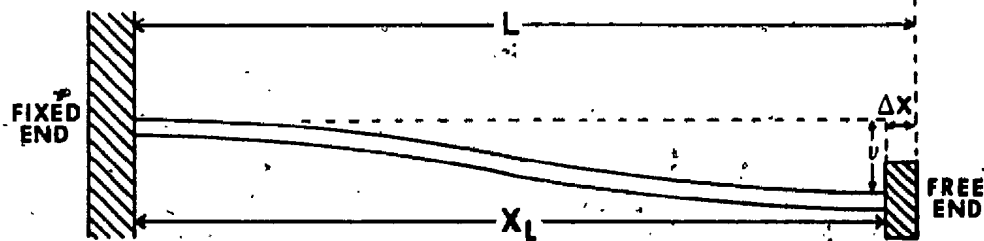


Figure 2-2: Plate Deflected Shape

The rigid clamping at both ends of the plate gives the deflected shape shown in Figure (2-2). The boundary conditions imposed, as functions of the horizontal distance from the left-hand end, are thus:

$$v(0) = 0$$

$$\frac{dv}{dx}(0) = 0$$

$$\frac{dv}{dx}(L) = 0. \quad (2.1)$$

$$\frac{d^2v}{dx^2}(L/2) = 0$$

where the first and second derivatives of vertical displacement represent respectively the slope and curvature at a point on the beam. The free-body diagram of the plate system is illustrated in Figure (2-3), with positive moment convention as shown. For an applied end load, assuming symmetry about the midpoint;

$$M_0 = M_L = \frac{PL}{2} \quad (2.2)$$

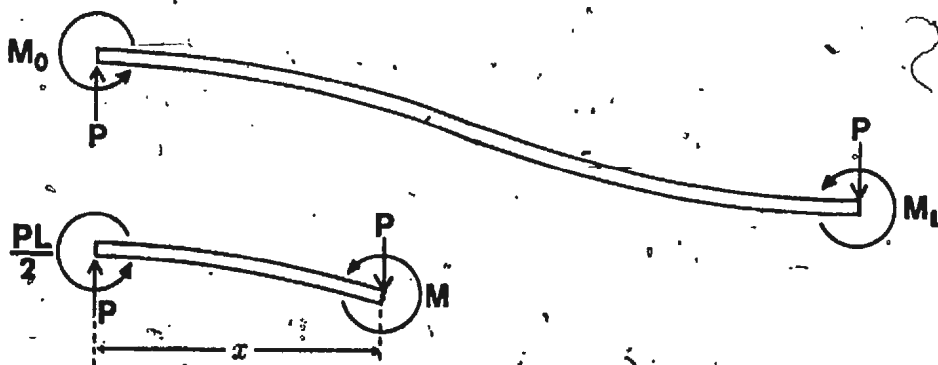


Figure 2-3: Plate Free-Body Diagram

At a distance 'x' from the left-hand end, equating the sum of the moments to zero, gives:

$$M + Px - \frac{PL}{2} = 0 \quad (2.3)$$

Knowing that (for a beam element) $\sum M = EI \frac{d^2v}{dx^2}$:

$$-Px + \frac{PL}{2} = EI \frac{d^2v}{dx^2} \quad (2.4)$$

Integrating once:

$$-\frac{Px^2}{2} + \frac{PLx}{2} + C_1 = EI \frac{dv}{dx} \quad (2.5)$$

From the second boundary condition; $C_1 = 0$. Integrating again:

$$-\frac{Px^3}{6} + \frac{PLx^2}{4} + C_2 = Elv \quad (2.6)$$

From the first boundary condition; $C_2 = 0$. The deflection of the beam at any point along its length is thus given as:

$$v(x) = \frac{1}{EI} \left(\frac{PLx^2}{4} - \frac{Px^3}{6} \right) \quad (2.7)$$

At $x = L$:

$$v = -\frac{PL^3}{12EI} \quad (2.8)$$

A value of horizontal displacement for a given vertical displacement 'v' can be obtained from the beam elastic curve, which from Equation (2.5) above is:

$$EI \frac{dv}{dx} = \frac{PLx}{2} - \frac{Px^2}{2} \quad (2.9)$$

From Pythagoras' Theorem, the length of the infinitesimal curve ' ds ', shown in Figure (2-4) is given as:

$$ds = \sqrt{dx^2 + dv^2}$$

or:

$$\frac{ds}{dx} = \sqrt{1 + (dv/dx)^2} \quad (2.10)$$

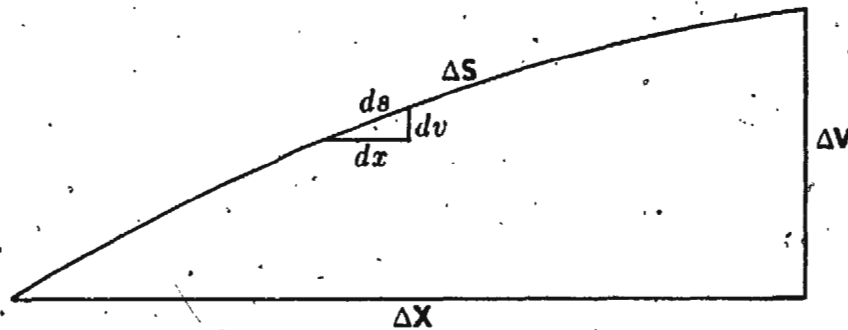


Figure 2-4: Infinitesimal Curve

' ds ' being approximated as a straight segment. Knowing that the length of the neutral central plane of the plate remains constant for any deflection shape, and restating Equation (2.9):

$$\frac{dv}{dx} = K (Lx - x^2) \quad (2.11)$$

where:

$$K = \frac{P}{2EI} \quad (2.12)$$

After substituting (2.11) into (2.10), the length of the plate, through integral summation, becomes:

$$\begin{aligned} L &= \int_A^B \sqrt{1 + (dv/dx)^2} dx \\ &= \int_0^{x_L} \sqrt{1 + [K(Lx - x^2)]^2} dx \\ &= \int_0^{x_L} \sqrt{K^2 x^4 - 2K^2 L x^3 + K^2 L^2 x^2 + 1} dx \end{aligned} \quad (2.13)$$

where ' x_L ' is the horizontal span of the plate under a reasonable state of distortion. The difference between the constant curve length, ie; the undistorted horizontal span ' L ', and the upper integral limit ' x_L ' is the amount of end horizontal displacement coincident with a specified end vertical displacement ' v ' of the plate.

To determine ' x_L ' for a specific ' v ', Equations (2.8) and (2.12) are first used to express ' K ' in terms of ' v ':

$$K = - \frac{6v}{L^3} \quad (2.14)$$

Equation (2.13) thus becomes:

$$L = \int_0^L \sqrt{\frac{36v^2x^4}{L^6} - \frac{72v^2x^3}{L^5} + \frac{36v^2x^2}{L^4} + 1} dx \quad (2.15)$$

It should be noted that this entire method is based upon mechanics of solids theories, which assume small deflections in beam elements. This situation does not fit clearly within those limitations, as plate elements rather than beams are involved, and the maximum end deflection is 3 inches for a plate length of 40 inches, or about 1 in 13. Non-linear behavior in terms of deflection versus load may normally be expected in such situations, but the sole concern of this analysis is geometry. All aspects of power and load are ignored. Stiffness factors 'E' and 'I', Young's modulus and bending moment of inertia, also cancel out of the final expression, negating the effects of stiffness variation between plate and beam elements. Assuming that the shape of Figure (2-2) remains accurate, Equation (2.15) describes accurately the plate's vertical and horizontal geometry.

Due to the crank drive of the existing mechanism, the plate end deflection varies from harmonic motion slightly during operation, and has been taken as²:

$$v(t) = CK \cos(\omega t) + CR \left(1 - \sqrt{1 - \frac{CK^2 \sin^2 \omega t}{CR^2}} \right) \quad (2.16)$$

which is specific to the case where the crank is mounted above the driven member (as in the existing equipment). The actual set-up is illustrated in the photograph

of Figure (2-5). Note that the second part of Equation (2.16) represents the deviation from harmonic motion, where 'CK' is the crank length. This deviation approaches zero rapidly as 'CR', the connecting rod length, increases with respect to 'CK'.

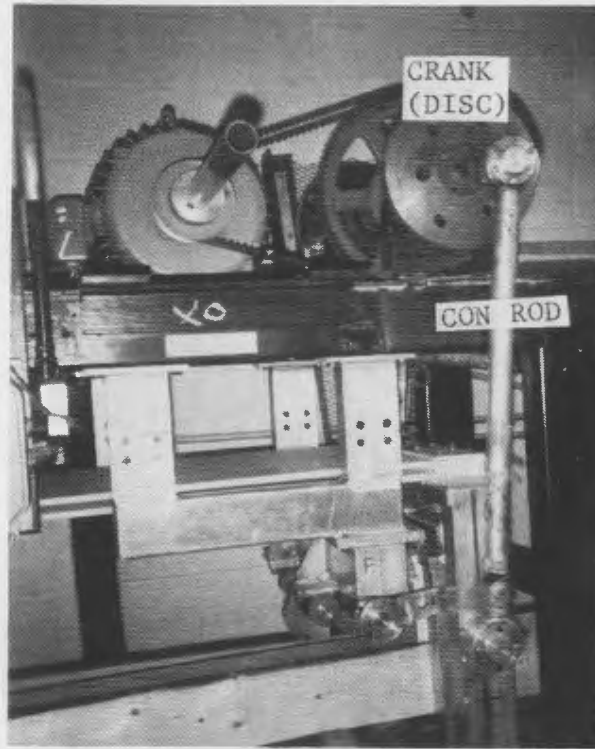


Figure 2-5: Existing Crank Drive

In the existing mechanism, 'CR' has been measured at 35.47 inches, while 'CK' is 3 inches, as mentioned. The maximum deviation, which will occur when $\omega t = \pi/2$, will be:

$$\begin{aligned}
 v(\pi/2) &= 0 + 35.47 \left(1 - \sqrt{1 - \frac{3^2}{35.47^2}} \right) \\
 &= 0.128 \text{ inch}
 \end{aligned}$$

where $v(\pi/2)$ would be zero for perfect harmonic motion. The deviation will tend to zero at the extremes, where $\omega t = 0, \pi, 2\pi, \dots$. A comparison between harmonic motion, and this specific crank drive motion is shown in Figure (2-6). The stroke top, midpoint, and bottom positions are located as shown.

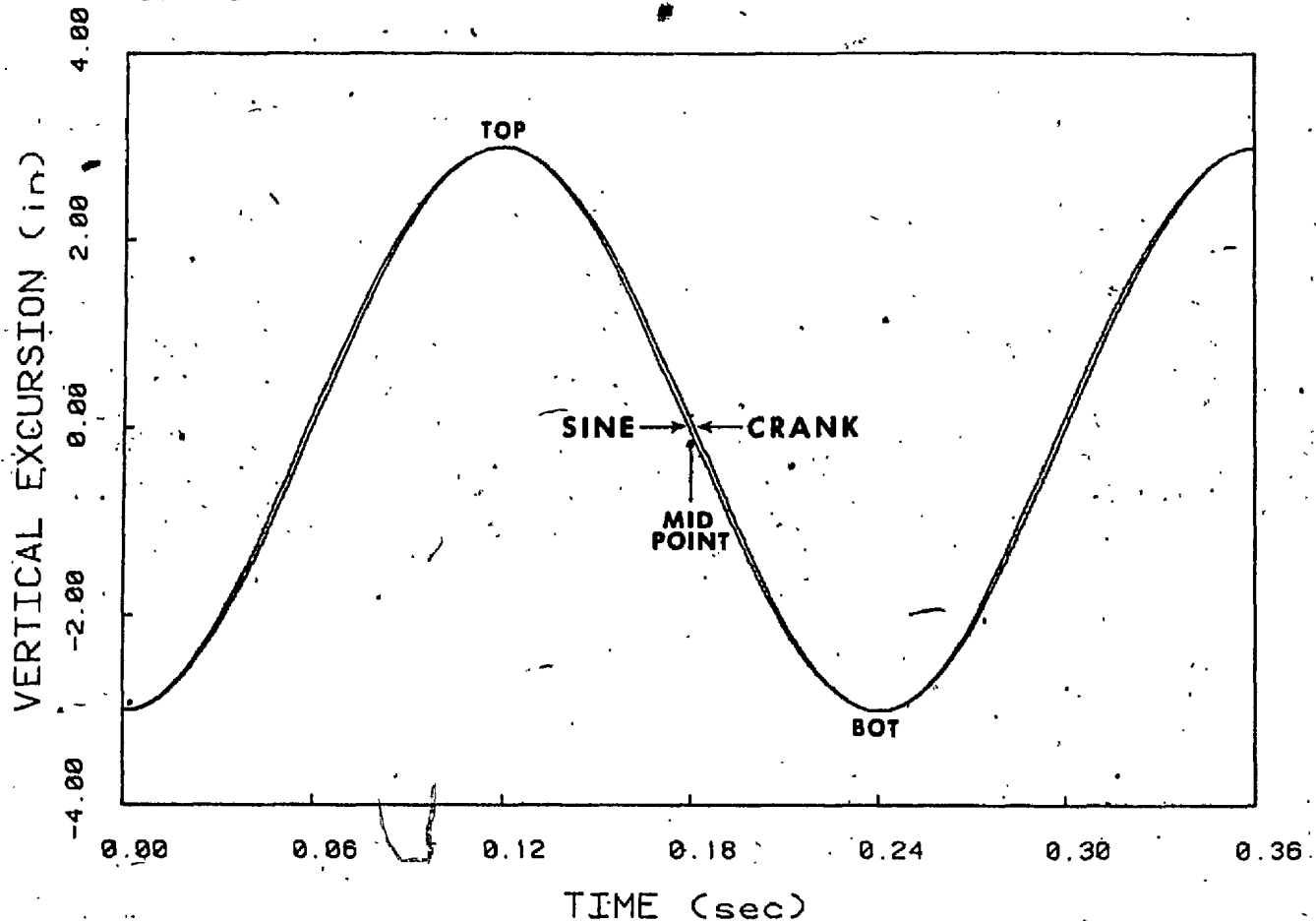


Figure 2-6: Crank Drive/Sinusoid Deviation

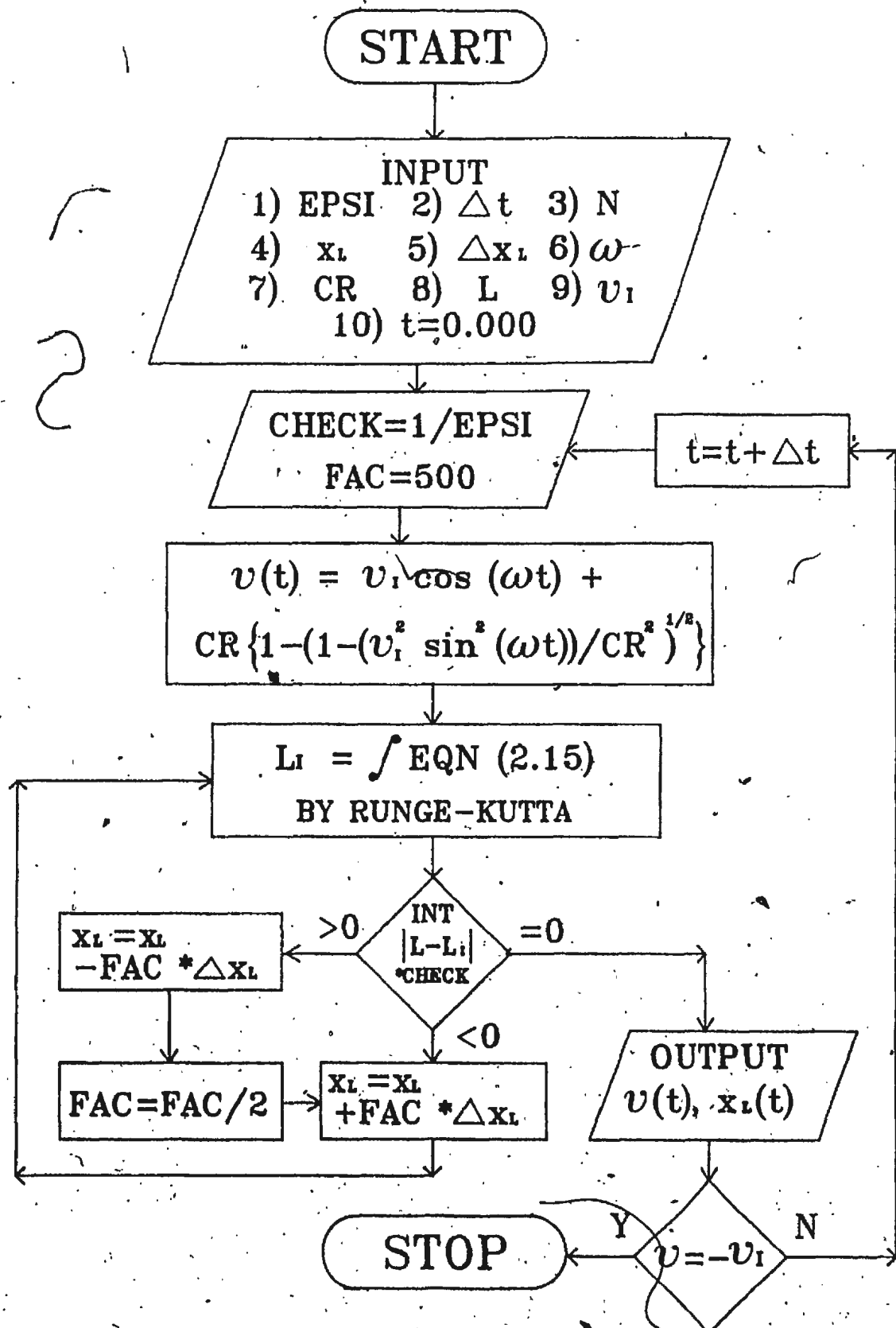
It should be further noted that due to some horizontal motion of the plate end, and therefore of the crank rod to sash connection, Equation (2.16) still is not absolutely precise. However, the maximum horizontal displacement will occur at the extremes, where the crank rod should be vertical. The expected small horizontal displacement of the plate end, and the comparatively long crank rod

combine to produce a very small angle with respect to the vertical, and thus minimum vertical positioning error. At the vertical midpoint, where the error of Equation (2.16) is greatest, the horizontal displacement of the plate end, and thus the equation error, are zero. The displacements given by the crank drive equation can now be used to provide more accurate results from the calculations of plate span values.

The form of Equation (2.15) is a type of elliptic integral, the exact solution of which would require considerable time and effort. As it is the purpose of this analysis to develop a computer program for saw blade motion simulation, a solution through computer numerical integration, though approximate, was deemed both convenient and adequately accurate. In this case the final numerical value of the integral is known, while the upper limit is to be determined. The procedure used to calculate this horizontal span thus employs an iterative step and check value, with an assumed initial ' x_L ', as shown in the flow chart of Figure (2-7). For each successive new assumed ' x_L ', a standard fourth-order Runge-Kutta method is used to evaluate the integral⁷. The number of intervals assumed (representing the number of strips of incremental length below the deflection curve) gives a compromise between accuracy and computer time employed. The flow chart shows the procedure followed in the generation of values for an entire sweep of the plate, from $v(t) = +3.0$ to -3.0 . At each incremental time ' $n\Delta t$ ' an end deflection $v(t)$ is calculated according to the crank drive equation described above, and a corresponding $x_L(t)$ output after the epsilon check is satisfied.

At this point, the vertical deflection and corresponding horizontal span for a

Figure 2-7: Flow Chart for Plate Deflection Data Generation



specified number of time points have been generated and stored, to be referenced later for addition of log feed and tooth offset influence values. The frequency ' ω ' shown above was determined beforehand, in the manner to be discussed in the following section.

2.2. PLATE VIBRATION ANALYSIS

The entire sash supporting structure can be considered a 'space frame' in the sense that its flexible plates have two dimensional properties, as opposed to beams, with one dimension in the axial direction. Four of these plates, of an acetal resin with the trade name 'Delrin', are mounted in closely spaced pairs in horizontal planes (in the undistorted mode). One pair above and one below support the sash or frame into which are mounted the straight band-saw section blades.

The frame is driven in vertical oscillation as discussed above by a motor-crank mechanism, approximating the motion described by Equation (2.16). As one outstanding feature of this device is the reduction in power consumption through the use of plate spring mountings to alternately store and expend deflection energy, it is desired to determine the frequency of operation at which this cycle is most efficient. This is of course the resonant frequency of the system, at which minimum input force will return maximum deflections. In this section various methods are employed, from basic approximations to computer algorithms, to determine the frequency of the first, and assumed only dominant mode of vibration; that which has the deflection shape shown in Figure (2-2).

2.2.1. Simple beam-girder approximation

The system may be analysed in simplest terms as a mass and spring, with the natural frequency of vibration approximated by:

$$\omega_n = \sqrt{\frac{k}{m}} \quad (2.17)$$

where ' k ' is the stiffness, or spring constant of the system, in force per distance units, and ' m ' is the system mass. Here, ' ω_n ' is the natural and, since damping is ignored, the resonant frequency. In this, and the subsequent methods of frequency analysis used, one single plate will be considered, assuming a lumped mass of one-quarter of that of the sash mounted at its 'free' end.

The stiffness ' k ' of one plate is defined as the force per unit deflection, or:

$$k = \frac{P}{v} \quad (2.18)$$

For a rectangular beam element, the stiffness is, from Equation (2.8):

$$k = \frac{12EI}{L^3} \quad (2.19)$$

where:

$$I_{\text{beam}} = \frac{bh^3}{12} \quad (2.20)$$

For beam dimensions $L = 40$ in., $h = 0.5$ in., $b = \text{width} = 19$ in., ' I ' is calculated to be 0.1979 in^4 . However, it is normally assumed that plate elements

have greater stiffness in bending than beam elements, although the point of transition between the two is not clearly defined. For plates, the flexural rigidity 'D' replaces the bending moment of inertia 'I', and is given, per unit width, as:

$$D = \frac{h^3}{12(1 - \nu^2)} \quad (2.21)$$

where ν = Poisson's ratio = 0.35 (for Delrin). For width 19 in. $D_{\text{plate}} = 0.2255$ in⁴. The plate element is thus about 14% stiffer than if assumed to have beam characteristics. Replacing 'I' in Equation (2.19) by the above value (with $E = 4.1(10^5)$ psi for delrin):

$$k = \frac{12(0.2255)(4.1(10^5))}{(40)^3}$$

$$= 17.339 \text{ lb/in}$$

Use of Equation (2.17) in the form shown infers that the plates are massless, 'm' being contributed by the sash frame only. For now, this will serve to provide first a rough approximation. The weight of the simple single-blade mounting sash currently in place is unknown; it will thus be assigned an arbitrary value of 10 pounds. The 'm' for Equation (2.17) per plate is thus:

$$m_s = \frac{1}{4}(10 \text{ lb}) \left(\frac{1}{32.2 \text{ ft/s}^2} \right) \left(\frac{1}{12 \text{ in/ft}} \right)$$

$$= 0.00647 \text{ lb-s}^2/\text{in}$$

A first approximation of the frequency is thus:

$$\begin{aligned}
 \omega_{n1} &= \sqrt{\frac{17.339}{0.00647}} \\
 &= 51.77 \text{ rad/s} \\
 &= 494.3 \text{ cycles/min}
 \end{aligned}$$

The shortcomings of this method are many. The assumption of massless spring elements is a gross underestimation, as a plate of the size in question has a weight of about 19.5 pounds. Any additional mass will affect a decrease in the frequency of a system. As well, the possible non-linearity in elasticity of the plate due to large deflections may affect the dynamics in a way which is difficult to predict. The later problem is beyond the scope of this study, but the former is resolved through the method to follow.

2.2.2. Improved beam-girder approximation

An improvement on the above method is the inclusion of the distributed mass of the plate with that of the sash frame, to give an 'effective' mass to be used in Equation (2.17). To begin, a separation of variables gives a generalized displacement, for any point along the beam⁸:

$$v(x,t) = \psi(x) \cdot v(t) \quad (2.22)$$

where $\psi(x)$ is a 'shape function' for the deflected plate, and $v(t)$ is the generalized displacement parameter. For the given boundary conditions of Equation (2.1), the shape function can be obtained directly from equations derived previously. Being

unitless, and attaining a maximum unit size, the shape function is expressed as the ratio of the general displacement to the end deflection. From Equations (2.7) and (2.8):

$$\begin{aligned}\psi(x) &= \frac{v(x)}{v(L)} = \frac{[PLx^2/4 - Px^3/6]/EI}{PL^3/12EI} \\ &= \frac{3x^2}{L^2} - \frac{2x^3}{L^3}\end{aligned}\quad (2.23)$$

The effective mass from distributed inertial forces for a slab or plate is⁸:

$$\begin{aligned}m_I &= \int_X m(x,z)[\psi(x,z)]^2 dX \\ &= \int_0^L \rho X \psi^2(x) dx\end{aligned}\quad (2.24)$$

where:

ρ = plate mass density
 X = cross-sectional area
 L = plate length

The second form of Equation (2.24) is valid when no bending occurs in the 'z' direction, or across the width of the plate in this case. Thus:

$$\begin{aligned}m_I &= \rho X \int_0^L \left(\frac{9x^4}{L^4} - \frac{12x^5}{L^5} + \frac{4x^6}{L^6} \right) dx \\ &= \rho X \left(\frac{9L}{5} - 2L + \frac{4L}{7} \right)\end{aligned}$$

For $L = 40$ inches, $\rho = 0.000133 \text{ lb-s}^2/\text{in}^4$, $X = 9.5 \text{ in}^2$; $m_1 = 0.01872 \text{ lb-s}^2/\text{in}$.

The total effective mass of the system may now be approximated as:

$$\begin{aligned} m_{eff} &= m_8 + m_1 \\ &= (0.00647) + (0.01872) \\ &= 0.02519 \text{ lb-s}^2/\text{in} \end{aligned}$$

The improved frequency approximation is thus:

$$\begin{aligned} w_{n2} &= \sqrt{17.339/0.0251} \\ &= 26.24 \text{ rad/s} \\ &= 250.5 \text{ cycles/min} \end{aligned}$$

It should be noted that due to its distribution, only 37% of the actual plate mass is combined with the lumped end mass, but it has the effect of dropping the frequency estimate by almost 50%. Error here may again be attributed to the linearity assumption of plate deflection. However, the integral formulations for stiffness and mass should provide an estimate as accurate as can be expected from hand calculations.

2.2.3. Computer frequency analysis

As a final check, the plate is analysed through a GTStrudl (Georgia Tech. Structural Design Language) routine. In this finite element approach, the member is manually subdivided into appropriately shaped and sized elements, each of which is assigned specific mass, spring, and damping values based upon input boundary conditions and mechanical properties. Solution of the resulting matrix equation(s) provides frequency values for the specified modes of vibration.

Three different element division types were tested initially, each more complex than the previous. It was assumed that since this is a 'finite' analysis, the closer one approached an 'infinite' analysis, the more precise the result would become; hence the dramatic increase in the number of elements. Young's modulus and Poisson values are as used above. The elements are assumed type 'SBHT6', or 'stretching and bending hybrid triangles with six degrees of freedom'. Also to be consistent with the above analyses, only the first, natural frequency is pursued. The sash weight is included as an inertial mass added, for 'x' and 'v' directions, to the two free-end nodes in each case, a node being the point of connection of any two or more element corners. The value of (2.5/2) pounds is expressed in mass units of 'lb-s²/in' to conform with assumed units. Damping, both external and internal, has been assumed negligible.

Figures (2-8) to (2-10) illustrate the element division schemes employed in the initial analyses. The fourth division type, illustrated in Figure (2-11), was tested after noting a dramatic jump in the frequency output from the third run as

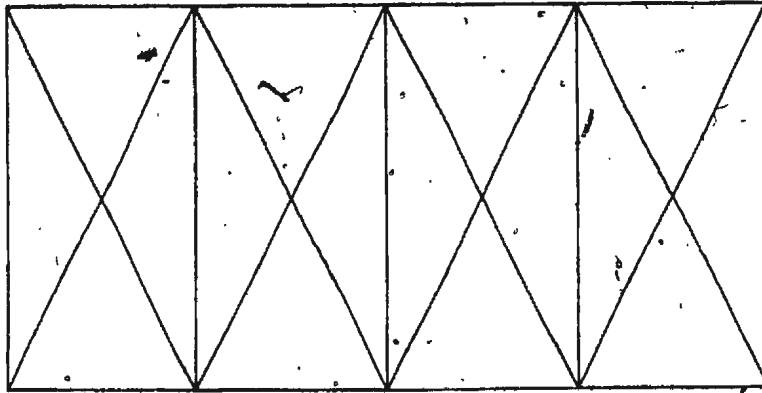


Figure 2-8: GTStrudl Plate Division #1

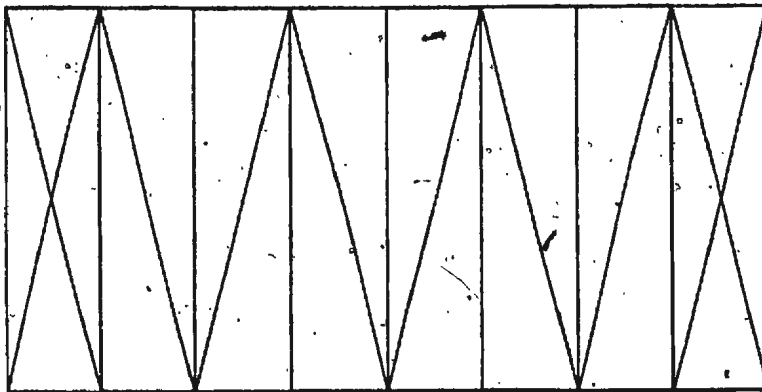


Figure 2-9: GTStrudl Plate Division #2

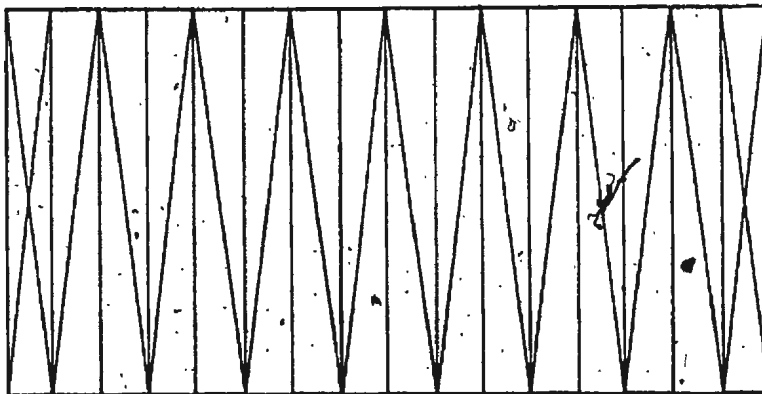


Figure 2-10: GTStrudl Plate Division #3

compared to the first two. An examination of literature pertaining to the algorithm, and discussions with other users revealed that there is a trend toward round-off error build-up as the triangular elements become more acute. The ideal

element is therefore an equilateral triangle, a division type not practical for a rectangular plate. Close approximations are the near half-squares of Figure (2-11). Here, the sash mass is distributed among the three end nodes, as $(2.5/3)$ pounds each.

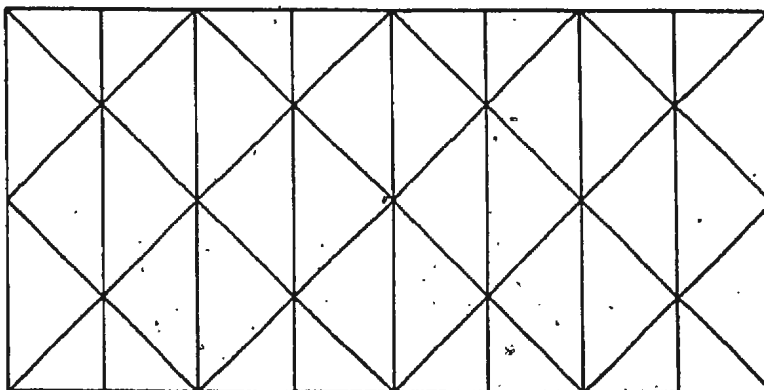


Figure 2-11: GTStrudl Plate Division #4

Table 2-1: Frequency Outputs from STRUDL Runs

Prog. #	# of Elements	# of Nodes	Freq (cyc/sec)	Freq (cyc/min)
A.2	16	14	4.116093	246.97
A.3	20	20	4.103624	246.22
A.4	44	44	4.407518	264.45
A.5	40	31	4.074682	244.48

Computer programs (A.2) to (A.5) show input commands and corresponding outputs for all four cases. The frequency results are listed in Table (2-1). All figures seem to validate the accuracy of the hand calculated value of 250.5

cycles/min. Although none hit this value exactly, and the trend may even be towards convergence in the other direction, all fall within the general region. For reasons of simplicity, a value of 250 cycles/min. will be used in the computer simulation program, and in all calculations to follow. As the actual sash mass is undetermined as mentioned, the analysis will be performed and conclusions drawn pertaining specifically to the kinematics, independent of the frequency of vibration, but applicable to all future stiffness conditions.

2.3. LOG FEED INCORPORATION

The computer program must generate data points representing the positions of the saw teeth tips relative to a fixed reference point on the log. Thus at any given time, the log feed effect is included as a simple subtraction from the curve data points generated as described in Section (2.1). While the feed is expressed in units of distance per time, the amount subtracted is a distance, which is the net horizontal amount the log has travelled at time 'T'. The subtraction is for convenience; the log moving to the right causes the relative position of the blade to shift to the left, or in the negative direction. The distance is simply the integral of the feed function from $t = 0$ to $t = T$. The log velocity is expressed in generalized terms as:

$$V_f = A + R \sin(\omega t + \theta) \quad (2.25)$$

thus:

$$S_f = AT + \frac{R}{\omega} \cos(\omega T + \theta) + \frac{R}{\omega} \cos \theta \quad (2.26)$$

where ' S_f ' is the net displacement at time 'T'. The values of the feed parameters 'A', 'R', and ' θ ' are input during the program run.

2.4. SAW BLADE AND MOUNTING GEOMETRY

The blade geometry comes into play only in the positioning of the traces of teeth in relation to the centre tooth, ie; that one which begins its cut at the top of a six inch deep log and ends its stroke at the bottom face. As the tooth tips lie along a straight line, the only important geometrical consideration is the tooth pitch 'P', or the spacing between adjacent tips. The mounting specification to be considered is the angle of inclination ' β ' of the blade from the vertical, normally referred to as 'overhang'. Both 'P' and ' β ' will be shown to have important influences on the efficiency of the system operation.

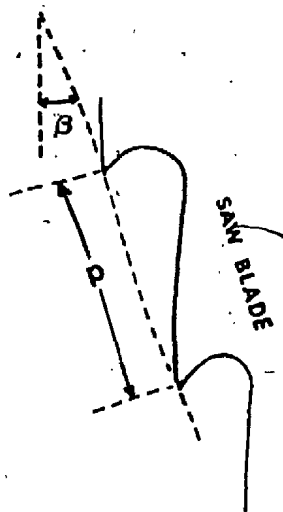


Figure 2-12: Saw Blade Overhang and Pitch

The two factors indicated in Figure (2-12) determine unit offsets in horizontal and vertical positioning for a tooth immediately adjacent to the centre reference tooth. These will be quantified in a later section.

All factors involved in the generation of the simulated tooth traces have now been discussed. The resulting computer program is shown in the appendix as

(A.1). A discussion of its internal logic is not to be included here; its comprehension is best left as the responsibility of the investigator. It should be noted that the program was developed through and used on the Digital PDP 11/60 system, and thus the inclusion of both data generation and plotting commands in a single program was possible. Some resulting tooth trace plots are shown and discussed in the following chapter.

Chapter 3

SAWING OPTIMIZATION

In this section it is intended to determine values of the system parameters for which the operation of the sash saw is most efficient. This will be accomplished through the separate analysis of various portions of the overall relative motion, and the assumption of specific objectives for each portion.

3.1. EQUATION GENERATION

To modify the relative sash motion by varying the system parameters, it is first necessary to develop the actual equations of motion. By means of the computer simulation program described in the previous section, data for plate end deflection, in both horizontal and vertical directions, were generated through the numerical integration of the integral curve equation of the deflected plate. To obtain a useable equation relating horizontal displacement to vertical deflection, that same data is used here in a curve fitting program to determine the coefficients in an arbitrary equation of selected order.

Data for one single 'sweep', as described above, is used. Trials with least squares fits for polynomial approximations yielded very unsatisfactory results, for any order of equation. However the seemingly periodic nature of the curve indicated that a Fourier fit may be more appropriate. In a Fourier series

approximation, the trigonometric form of a function $f(v)$ defined in the interval $(-l$ to $l)$ is given as⁷:

$$f(v) = \frac{a_0}{2} + \sum_{n=1}^{\infty} a_n \cos \frac{n\pi v}{l} + \sum_{n=1}^{\infty} b_n \sin \frac{n\pi v}{l} \quad (3.1)$$

where a_0 is an offset constant, while a_n and b_n are the Fourier constants to be determined.

The curve to be fit is of the shape shown in Figure (3-1) below. Its symmetry about the x-axis suggested that it might be best represented by an 'even' function, consisting of cosine terms only. To simplify the calculations, the data was normalized, or 'x' set to zero at the endpoints to eliminate the offset. The included computer program (A.6) uses a matrix formulation to determine the required Fourier coefficients, solving simultaneous equations equal in number to the data points input, the coefficients being the variables. All manageable series orders, up to $n = 10$, were explored. The sums of the squares of the deviances of the Fourier approximated values from input values were compiled for each set of output coefficients, and are listed in Table (3-1).

A comparison of total error for all cases showed that no significant reduction occurred as the number of terms increased even dramatically, with no convergence imminent. Thus greater complexity was in no way justified by greater accuracy. This indicated that a series with just four terms would prove both sufficiently accurate and easily manageable for future work. The plot of

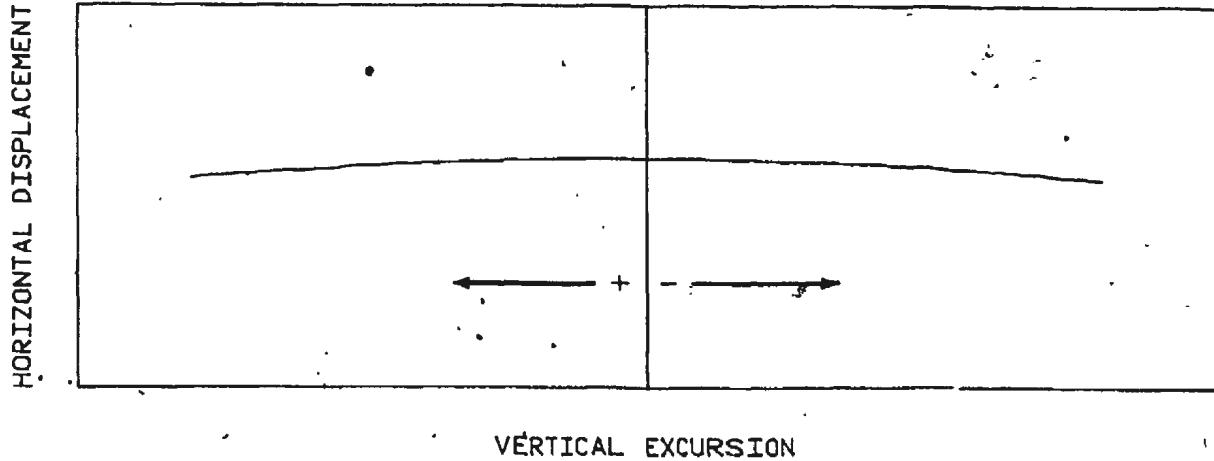


Figure 3-1: Plate End Deflection - Curve Shape

Table 3-1: Fourier Order vs. Compiled Error

Order (n)	Error ($\sum e^2$)
1	0.19570000
2	0.00094082
3	0.00006145
4	0.00006057
5	0.00006058
6	0.00006145
7	0.00006045
8	0.00006050
9	0.00006029
10	0.00006009

Figure (3-2) shows a comparison between the actual (numerical integration) data and that output by the final Fourier equation:

$$\begin{aligned}
 x(v) = & -0.08232 \cos\left(\frac{\pi v}{12}\right) + 0.30243 \cos\left(\frac{2\pi v}{12}\right) \\
 & - 0.09804 \cos\left(\frac{3\pi v}{12}\right) + 0.01173 \cos\left(\frac{4\pi v}{12}\right)
 \end{aligned}
 \quad (3.2)$$

The overall tooth position is thus described by a combination of the above, and terms representing the results of log feed and tooth and blade angle offsets. Again, all positions are relative to an arbitrary log reference point.

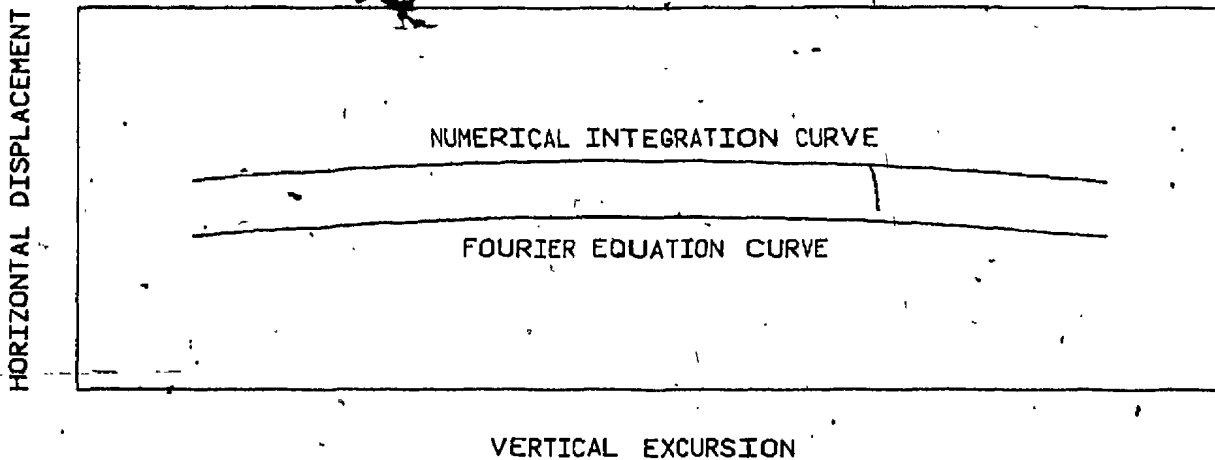


Figure 3-2: Fourier Curve vs. Original Curve

In the following sections, attention is focused separately on the two modes of motion of the blade:

1. The downward, or cutting stroke, for which the objective is to determine appropriate values for the feed and blade set-up parameters which will allow sawing at maximum capacity;
2. The upward, or return stroke, for which the objective is to bring the blade to a point at the top of its stroke from which the most effective cutting stroke can begin. At the same time, it is desired that the backsides of the teeth not be driven into the advancing log face.

From analysis of these, and examinations of generated tooth trace plots, the system parameters will be established and the governing equations developed.

3.2. EXPERIMENTAL EXAMINATION

As a means of validating assumptions to be made concerning the areas of material removed during the cutting stroke, and shapes remaining after the return stroke, a full-scale, two-dimensional test device was constructed. Depicted in the photograph of Figure (3-3), the device incorporates 40 inch long wooden strip 'springs', with the appropriate end mountings required to reproduce the plate deflection shape in the actual machine. Connected to the springs' 'free' ends is a relatively rigid end member, representing the sash frame. The hand-operated crank drive consists of a disc and connecting rod, with the correct full-scale dimensions. Finally, a section of the band saw blade type employed in the existing mechanism is mounted on the vertical end member, by connections which allow it to be inclined with respect to the vertical at a pre-selected angle.

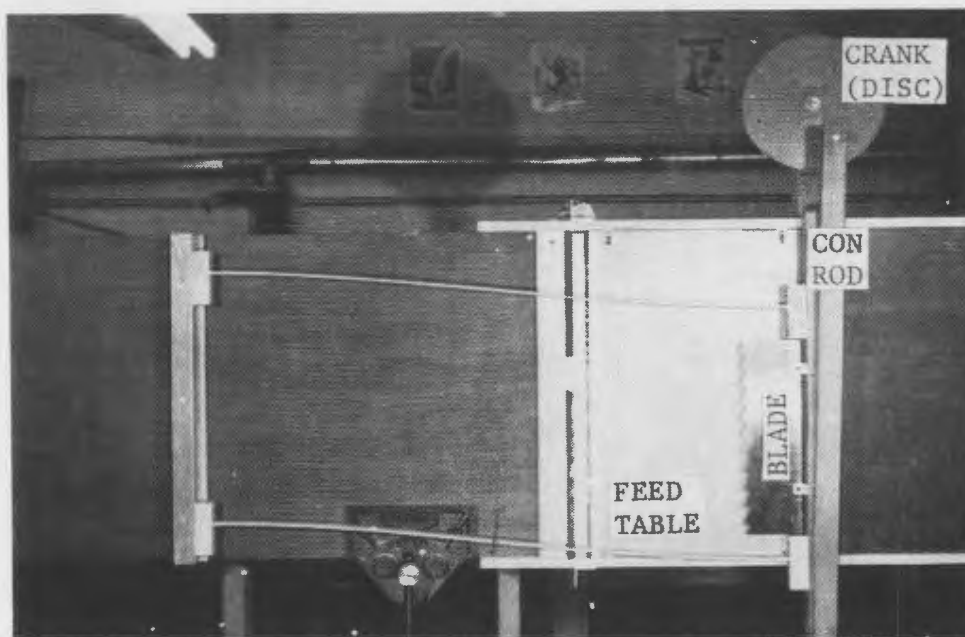


Figure 3-3: Experimental Set-Up

To facilitate viewing of the motions of the saw teeth relative to the work

material, a provision impossible when cutting inside a solid, opaque wooden log, a special 'sandwich' board was prepared. Dyed, molten wax was injected between a layer of clear, fairly rigid plexiglass and an arborite-surfaced backing board, spaced apart by sheet metal sections to produce a wax section of a thickness equivalent to that of the saw blade. The resulting dark rectangle, shown in Figure (3-4) is 6 inches in height, the maximum log depth assumed, and 2 inches wide, to allow for a number of cutting passes for a single mold. In operation, the saw blade section slides snugly between the plexiglass and backing surface, and during feeding removes slices and/or chips of wax of area and shape representing that wood which would be removed during sawing.

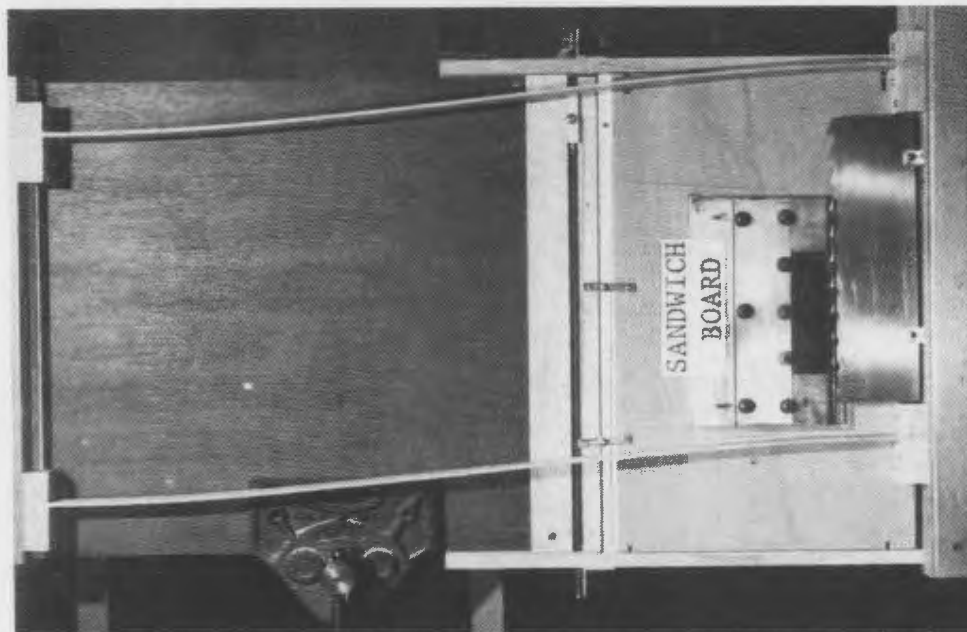


Figure 3-4: Wax Sandwich Board Mounted on Feed Table

To provide for the feeding into the saw blade, the entire sandwich board is mounted on a travelling feed table as shown, supported on spring-mounted rollers moving in upper and lower grooved tracks. A main cable simultaneously winds

and unwinds from the shaft of the drive disc, and in passing through a series of pulleys moves a sliding block and roller down along an inclined surface (of adjustable slope) bolted to the trailing edge of the feed board. Six complete revolutions of the drive disc (or six cutting/return strokes) moves the sliding block along the entire vertical depth of the incline, advancing the travelling board and sandwich a distance governed by the slope of the incline. Thus a feed per cutting stroke or, assuming a set frequency for the existing mechanism, a feed speed can be determined or input for a specific test run.

A series of photographs were taken at various points in both cutting and return strokes, for various arbitrary feed rates. Pictures were selected and included where appropriate in the sections to follow to justify assumptions made concerning the relative motions of the saw teeth.

3.3. DOWNWARD STROKE ANALYSIS

The important considerations in the analysis of the cutting stroke will be:

1. Tooth gullet capacity, ie; the volume of sawdust and/or wood chips which can efficiently be gathered 'inside' the tooth during the cutting cycle, and dumped out after the tooth has exited the log;
2. The wood expansion in passing from solid to waste material, expressed as an expansion factor 'EF', the ratio of produced sawdust/chip volume to original solid wood volume.

The complicated geometry of the gullet, and associated identifying terms, are shown in the illustrations of Figure (3-5)¹. The possibility of a simple mathematical solution to the projected area of any gullet was ruled out for obvious reasons. This value was determined manually, through the use of line

graph paper. In the second illustration, representing the existing gullet, fully included squares counted as whole units, while those cut by the curve were counted as half units. For the gullet shown the area was determined to be approximately 180 mm².

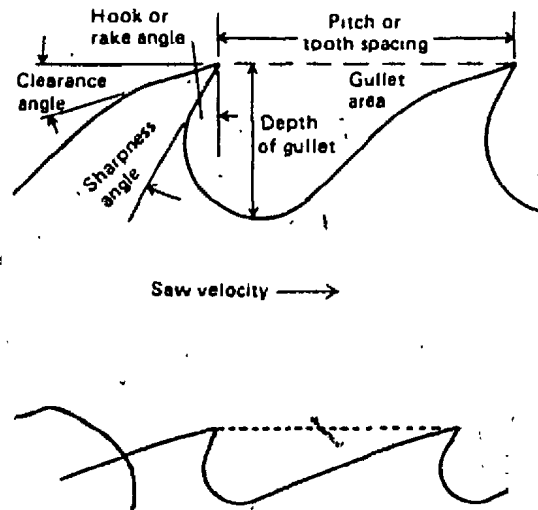


Figure 3-5: Gullet Nomenclature and Area Determination

Wood expansion factors were listed in the reviewed literature as anywhere in the 1.5 to 3.0 range. Williston, in a gullet loading discussion, quotes 70%, or an 'EF' of 1.43, as a rule of thumb¹⁰. The appropriate value for any given situation depends upon specific wood characteristics such as density and moisture content, and on the sawing operation, which determines the relative amounts of sawdust and chip material produced. A value to be used in this analysis will be selected later, as other factors come into play which have not as yet been considered.

A secondary consideration is the relation between the clearance angle of the tooth, as shown in Figure (3-5), and the blade inclination ' β '. It is obvious that inclines which approach the clearance value would severely restrict the tooth's ability to cut into the wood face. Upon calculation of ' β ' values, this aspect will be reconsidered if necessary.

3.3.1. Area calculation

A representative tooth trace, as produced by the computer simulation program described in the previous section, is shown in Figure (3-6). It serves to illustrate the mechanics of cutting for a near ideal situation, for log feed values which may represent a desirable production rate. As a diagnostic tool it is invaluable, as it shows the actual wood 'slices' cut out by the individual teeth, the wood profile left after a cutting stroke (superimposed), and the amount and points of interference to be expected on the return stroke. On the plot, the horizontal axis gauges the plate end vertical deflection, ie; the excursion of the entire saw blade (the centre tooth travels between the limits +3.0 and -3.0 inches). The trace of the adjacent lower tooth, that one which immediately precedes the centre tooth in the cutting sequence, is shown with the appropriate offsets in both horizontal and vertical directions (to be discussed). Both traces cover two complete cycles; two cutting and return strokes. They will prove to be sufficient in the development of the system equations.

The single hatched area represents the profile of the kerf remaining at the end of a cutting stroke, assuming that the wood retains the shapes of the paths of the individual teeth after their retractions. Note that rather than a continuous

FEED SPEED = $50.8 + 50.8 * \cos(wt)$ mm/sec

= $2.00 + 2.00 * \cos(wt)$ ips

BLADE OVERHANG ANGLE = 5.000 degrees

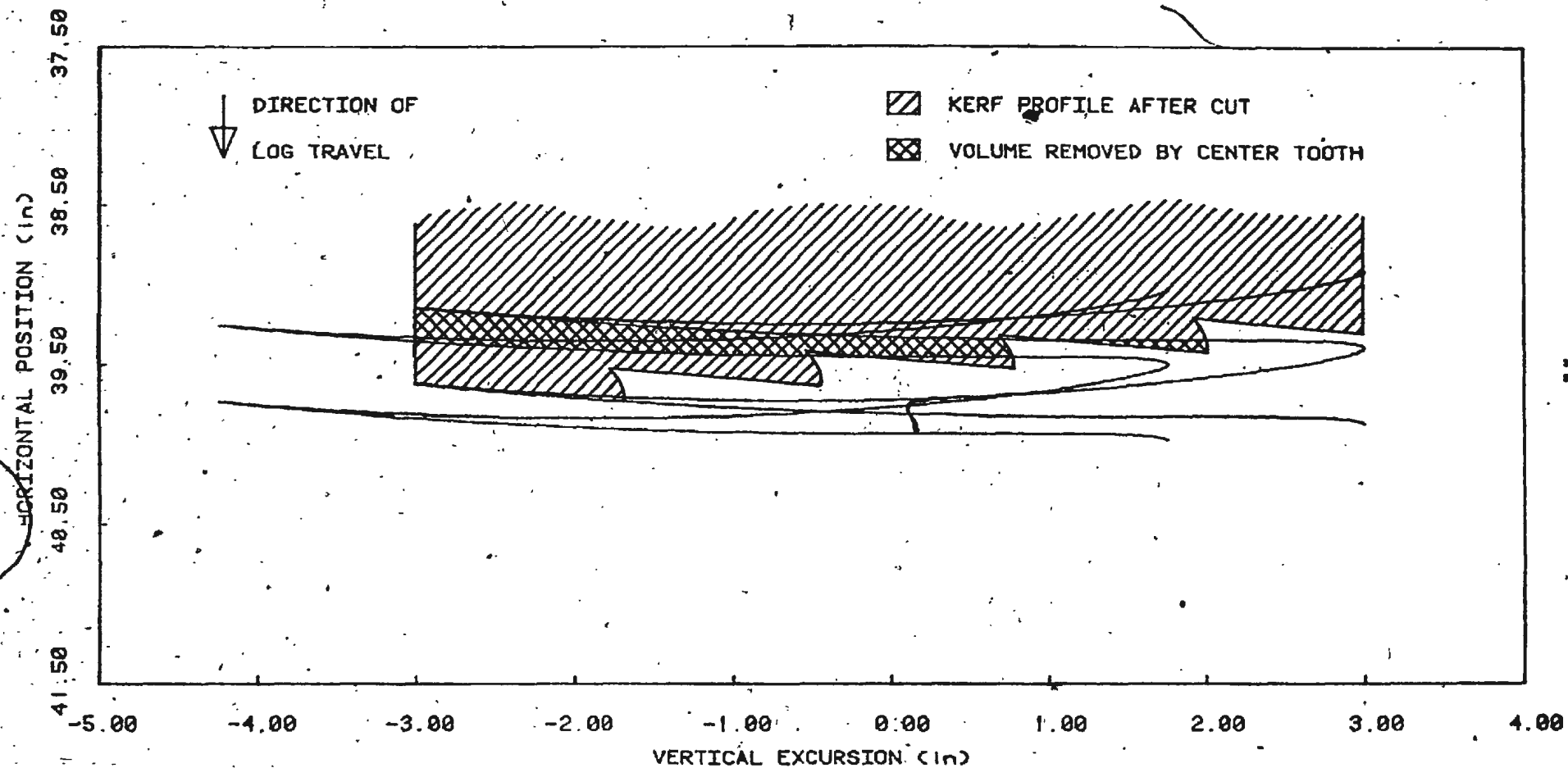


FIG. 3.6 Example Tooth Trace

curved surface, the kerf is of a shape similar to inverted saw teeth, with the bottom of the stroke of each tooth corresponding to a notch corner. From the experimental set-up described above, the photograph of Figure (3-7) was taken. The obvious notched shape in the wax at the bottom of the cutting stroke verifies this assumption.

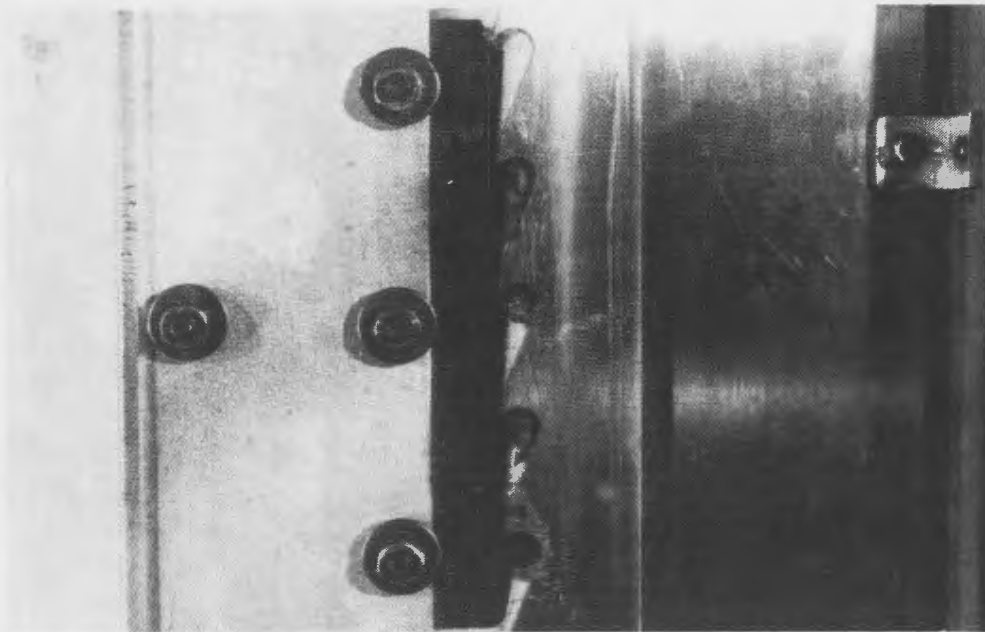


Figure 3-7: Kerf Profile After Cutting Stroke

The cross-hatched region, superimposed on the trace, represents that 'area' (or 'volume', divided by the blade thickness) cut out by the centre tooth, which is the only one to engage a six-inch log throughout its entire depth. This is the rate determining tooth, as it is safely assumed that each of the other teeth cuts out an area progressively less, depending on its position relative to the centre. This is justified by the photograph of Figure (3-7), which clearly shows that the lowermost tooth is considerably more packed with cut material than all those

above. Note that the cross-hatched area on the plot is bordered on the right by the trace of the lower tooth, which has just previously made its cut, and on the left by the trace of the centre tooth as it cuts through individual 'ledges' of the jagged kerf profile. The area thus consists not of one continuous strip, but rather of one thin wedge-shaped portion, resulting from the truncation of the first ledge encountered by the tooth, and a lower, nearly continuous portion (less one thin notch).

Since a six-inch long strip is not cut out by any one tooth, the area determination will not consider the total space between two adjacent tooth traces. Rather, the area will be obtained by integrations of the the two curves over an adjusted, shorter section. This section will represent the combination of the two areas described in the preceding paragraph. Assuming that the thin wedge just fills in the missing notch of the lower shaded strip, the limits will be taken as the vertical boundaries of that strip, ie; -3.0 to +1.0 inches.

In cases involving different parameters, for instance greater blade angles ' β ', the starting points of cutting may occur at less favourable positions. The example trace only indicates the type of cut desired, beginning at the highest possible point. Once values have actually been determined and assigned to these variables, new traces will be generated and the cutting geometry re-evaluated.

3.3.2. Integration of centre tooth trace equation

Equation (3.2) expresses the horizontal displacement of the 'free' end of the distorted plate. Combined with the type of feed discussed, as expressed in Equation (2.25), the equation of relative position for the centre tooth is given as:

$$\begin{aligned}
 x_c(v,t) = & - 0.08232 \cos\left(\frac{\pi v}{12}\right) + 0.30243 \cos\left(\frac{\pi v}{6}\right) \\
 & - 0.09804 \cos\left(\frac{\pi v}{4}\right) + 0.01173 \cos\left(\frac{\pi v}{3}\right) \\
 & - \int_0^T [A + R \sin(\omega t + \theta)] dt
 \end{aligned} \tag{3.3}$$

The integral term represents the displacement at the time in question due to the forward motion of the log. Its sign is negative, as discussed.

The first integration of the feed terms gives the feed net displacement function, as before:

$$\begin{aligned}
 \int_0^t [A + R \sin(\omega t + \theta)] dt &= At - \frac{R}{\omega} \cos(\omega t + \theta) \Big|_0^t \\
 &= At - \frac{R}{\omega} \cos(\omega t + \theta) + \frac{R}{\omega} \cos \theta
 \end{aligned} \tag{3.4}$$

Integrating the first four terms of Equation (3.3):

$$\begin{aligned}
& \left| -\frac{12}{\pi} (0.08232) \sin\left(\frac{\pi v}{12}\right) + \frac{6}{\pi} (0.30243) \sin\left(\frac{\pi v}{6}\right) \right. \\
& \quad \left. - \frac{4}{\pi} (0.09804) \sin\left(\frac{\pi v}{4}\right) + \frac{3}{\pi} (0.01173) \sin\left(\frac{\pi v}{3}\right) \right|_{-3.0}^{1.0} \\
& = 0.39586 \text{ in}^2
\end{aligned}$$

This area represents the space between the curve described by Equation (3.2) and the vertical axis, between the prescribed limits. The area under the curve of Equation (3.3) will be a combination of this area and that under the curve of Equation (3.4), the log feed net displacement, since the two are superimposed.

While the feed terms represent an absolute displacement at any time 't' in inch units, the variable unit involved is still seconds, rather than inches of vertical displacement. The integration would thus yield an answer in units of in-sec, rather than in² as desired. To rectify the situation, the relation between vertical displacement and time will be assumed to be (ignoring motor-crank induced error):

$$v = 3.0 \cos(\omega t)$$

or:

$$t = \frac{1}{\omega} \cos^{-1}\left(\frac{v}{3}\right) \quad (3.5)$$

Using the trigonometric relation for $\cos(A+B)$, the feed terms expand to become:

$$-At + \frac{R}{\omega} [\cos \theta \cos(\omega t) - \sin \theta \sin(\omega t)] - \frac{R \cos \theta}{\omega} \quad (3.6)$$

Introducing equation (3.5), the area under the feed curve becomes:

$$A_{fc} = -\frac{A}{\omega} \int_{-3.0}^{1.0} \cos^{-1}\left(\frac{v}{3}\right) dv + \frac{R \cos \theta}{\omega} \int_{-3.0}^{1.0} \left(\frac{v}{3} - 1\right) dv - \frac{R \sin \theta}{\omega} \int_{-3.0}^{1.0} \sqrt{1 - v^2/9} dv \quad (3.7)$$

$$(\cos \omega t = v/3 ; \sin \omega t = \sqrt{1 - \cos^2 \omega t} = \sqrt{1 - (v/3)^2})$$

Integrating and solving:

$$\begin{aligned} A_{fc} &= \left[-\frac{A}{\omega} \left[v \cos^{-1}\left(\frac{v}{3}\right) - 3\sqrt{1 - v^2/9} \right] + \frac{R \cos \theta}{\omega} \left(\frac{v^2}{6} - v \right) \right. \\ &\quad \left. - \frac{R \sin \theta}{\omega} \left[\frac{v}{6} \sqrt{1 - v^2/9} + \frac{\sin^{-1}(v/3)}{2} \right] \right] \Big|_{-3.0}^{1.0} \\ &= -\frac{A}{\omega} (7.8273) - \frac{R \cos \theta}{\omega} (5.3333) - \frac{R \sin \theta}{\omega} (1.1125) \quad (3.8) \end{aligned}$$

Thus, the total area under the curve $x_c(v)$ between the assumed limits, for $\omega = 26.18$ rad/sec as calculated, is:

$$A_c = 0.3959 - 0.2990 A - 0.2037 R \cos \theta - 0.0425 R \sin \theta \quad (3.9)$$

3.3.3. Integration of adjacent tooth trace equation

Equation (3.2) again gives the basic horizontal displacement of the beam end due to its vertical displacement. In addition, the tooth being considered here is offset in both the horizontal and vertical directions, due to the tooth pitch ' p ' and blade angle ' β ', as illustrated in Figure (2-12). The offsets are as illustrated in Figure (3-8) below, where ' T_c ' and ' T_a ' represent the tips of the centre and adjacent teeth respectively.

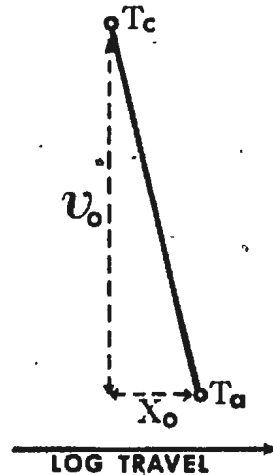


Figure 3-8: Tooth Vertical and Horizontal Offsets

The x -offset may be introduced directly into the equation for $x_a(v)$ simply as an addition to Equation (3.2). The v -offset however is dealt with as a change in the limits of integration, as a different portion of the curve described by Equation (3.2) is being considered. The feed factors will retain the same time limits as above, as the amount of horizontal advance due to log feed is the same for both simultaneously cutting teeth.

At this point it is observed that five independent variables have surfaced;

the three feed components 'A', 'R', and 'θ', and the two blade parameters 'p' and 'β'. To obtain definite values for all would require the solving of five independent equations simultaneously. However, the present situation does not lend itself to producing five equations; from exhaustive tooth trace and cutting mechanics examinations it appears that only three equations can be derived.

Based on existing conditions, it will be assumed that 'p' has a value of 1.25 inches. At a later point in this analysis a value will be assigned to 'θ', directly from empirical examination. For future cases, where a different pitch may be determined to be more desirable (or more readily available in standard blade stock) the analysis can be altered where appropriate to determine new system parameters. The gullet area determined from Figure (3-5) will thus remain valid. The offsets of Figure (3-8) now become:

$$\begin{aligned} x_0 &= 1.25 \sin \beta \\ &= 1.25 \beta \quad (\text{for small } \beta) \\ v_0 &= 1.25 \cos \beta \\ &= 1.25 \quad (\text{for small } \beta) \end{aligned} \tag{3.10}$$

The overall horizontal position of the second tooth is thus:

$$\begin{aligned} x_a(v', t) &= -0.08232 \cos\left(\frac{\pi v'}{12}\right) + 0.30243 \cos\left(\frac{\pi v'}{6}\right) \\ &\quad - 0.09804 \cos\left(\frac{\pi v'}{4}\right) + 0.01173 \cos\left(\frac{\pi v'}{3}\right) \\ &\quad + 1.25\beta + \left[-At + \frac{R}{\omega} \cos(\omega t + \theta) - \frac{R}{\omega} \cos \theta\right] \end{aligned} \tag{3.11}$$

(where $v' = v + v_0 = v + 1.25$)

The new limits of integration are therefore:

$$\text{at } v = 1.0; \quad v' = 2.25$$

$$\text{at } v = -3.0; \quad v' = -1.75$$

Integrating the first five terms of Equation (3.11):

$$\begin{aligned} & \int_{-1.75}^{2.25} \left[-0.08232 \cos\left(\frac{\pi v'}{12}\right) + 0.30243 \cos\left(\frac{\pi v'}{6}\right) \right. \\ & \quad \left. - 0.09804 \cos\left(\frac{\pi v'}{4}\right) + 0.01173 \cos\left(\frac{\pi v'}{3}\right) + 1.25\beta \right] dv' \\ & = (0.24444) - (-0.20757) + 5\beta \\ & = 0.45201 + 5\beta \end{aligned}$$

The feed components will be integrated in the same manner as above. However, the relation given in Equation (3.5) is valid only after the incorporation of the offset factor ' v_0 ', ie;

$$\begin{aligned} v &= 3.0 \cos(\omega t) - v_0 \\ &= 3.0 \cos(\omega t) - 1.25 \end{aligned}$$

or:

(3.12)

$$t = \frac{1}{\omega} \cos^{-1} \left(\frac{v + 1.25}{3} \right)$$

$$= \frac{1}{\omega} \cos^{-1} \left(\frac{v'}{3} \right)$$

Thus, the form is the same as shown in Equation (3.7), with v' replacing v , and limits as above.

The area under the feed curve for the second tooth is calculated to be:

$$A_{fa} = - \frac{A}{\omega} (5.9174) - \frac{R \cos \theta}{\omega} (3.6667)$$

$$- \frac{R \sin \theta}{\omega} (1.2204) \quad (3.13)$$

Thus, the total area under the curve $x_a(v)$ between the assumed limits, for $\omega = 26.18$ rad/sec as calculated, is:

$$A_a = 0.45201 - 0.2260 A - 0.1401 R \cos \theta$$

$$- 0.0466 R \sin \theta + 5\beta \quad (3.14)$$

Therefore, the area between the two curves over the given area is a function of the blade angle, and the three feed parameters:

$$A_{tot} = \int_{-3.0}^{1.0} [x_a(v) - x_c(v)] dv$$

$$= 0.0562 + 5\beta + 0.0730 A + 0.0636 R \cos \theta$$

$$- 0.0041 R \sin \theta \quad (3.15)$$

Note that for effective sawing, ' A_{tot} ' must be somewhat less than the gullet capacity.

3.4. UPWARD STROKE ANALYSIS

The important considerations in the analysis of the return stroke will be:

1. The amount and points of interference of the back edges of the saw teeth with the kerf profile remaining after the cutting stroke;
2. The return of the blade to a point horizontally suitable for the teeth to begin an efficient cutting stroke.

In the previous section, an equation was derived in which the gullet capacity could be related to the amount of material cut out by a single tooth, expressed in terms of four system variables. In this analysis, also of the motion of a single tooth, two more equations are derived, which express system restraints in terms of the same four variables.

3.4.1. Interference assessment

As discussed above, the factor which most adversely effects the operation of conventional sash saw equipment seems to be 'back cutting'. An examination of the example tooth trace of Figure (3-6) reveals some interesting aspects pertaining to this subject.

As briefly touched upon, the kerf profile remaining after a cutting stroke is not a smooth curved edge. Instead, the multiple teeth leave a jagged, inverted-tooth shaped profile. An examination of any tooth's upward path (for the input parameters used) shows that it will interfere only with the most immediate ledge, and completely clear the remainder of the profile. This upper clearance is so great that it appears that this may be true for any case where the parameters are

in the range of those of the example trace. This will therefore be the basis for formulating equations expressing the interference as a function of the system variables. Again, once values are determined for the variables in question, new traces will be analysed to ensure the validity of these assumptions.

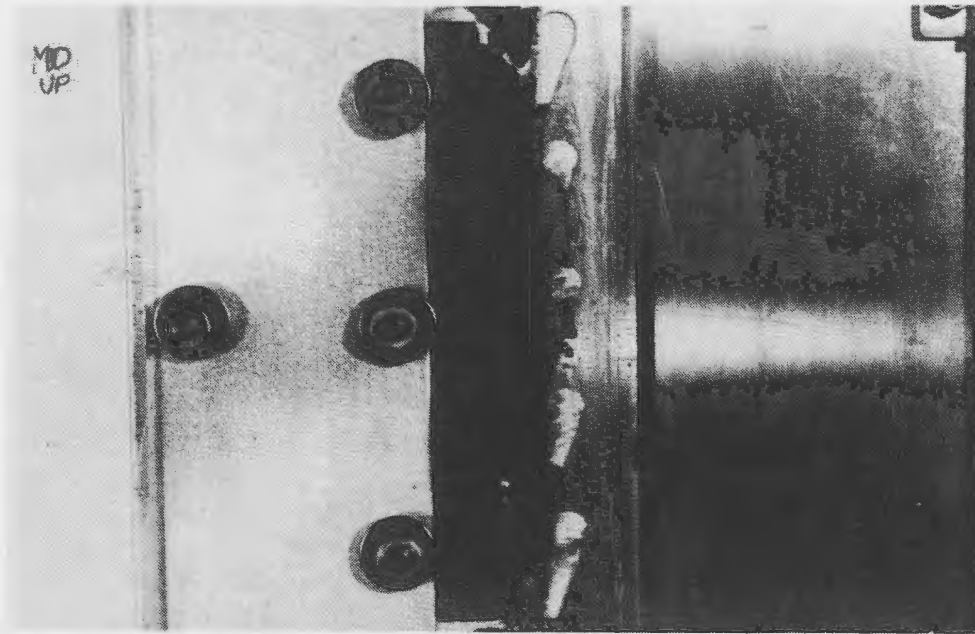


Figure 3-9: Interference Illustration - Wide View

The photographs of Figures (3-9) and (3-10) show the paths which the tooth backsides take with respect to the most immediate ledges, on their respective upstrokes. The feed conditions under which the pictures were taken were arbitrary, but not excessive. Note that each tooth is driven into the soft wax as the sandwich board advances under constant feed, despite a slight retraction of the blade due to the curved nature of its path. The amount of maximum interference, which occurs at the tip of a ledge, is expressed as a horizontal displacement, or the difference of two horizontal positions:

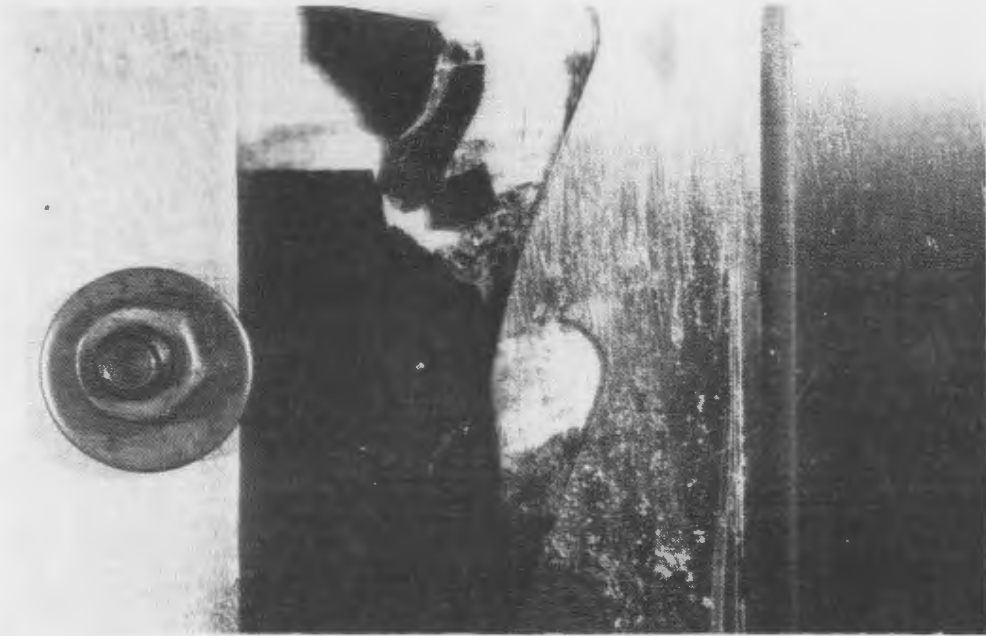



Figure 3-10: Interference Illustration - Isolation View

$$I = x_d(v) - x_u(v) \quad (3.16)$$

Here, ' $x_d(v)$ ' and ' $x_u(v)$ ' are the horizontal positions, where the tooth tip coincides vertically with the ledge tip, for the downward and upward strokes respectively. With the vertical position being the same for both, the effect of the curved path of the plate end is eliminated, leaving 'I' as a function of the feed factors only. It would be impossible therefore to set the interference to zero without an absolute pause or temporary reversal of the log feed, forcing the tooth tip to at least follow the same path during the initial period of the upstroke that it followed on the downstroke. Such characteristics are not overly desirable, as large vibrational forces would be induced in the case of massive logs. It will be sufficient here to derive an interference expression to be minimized, or set to some acceptable level.



Note also that this initial back-cutting could not be eliminated through blade overhang alone, which serves mainly to restrict interference with the remainder of the kerf profile.

The vertical position of the ledge tip 'v' is directly related to the tooth pitch 'p', as this is the distance separating adjacent ledges. The length of the ledge section (vertically) is however slightly longer than 'p' due to the notch geometry. A direct measurement from Figure (3-6) gives the distance as approximately 1 5/16 in, or 1.3125 inches. The vertical position is thus $(-3.0) + (1.3125) = -1.6875$ inches. Recalling Equation (3.5), the time value for this point in the downward stroke is:

$$t_d = \frac{1}{26.18} \cos^{-1} \left(\frac{-1.6875}{3} \right)$$

$$= 0.08282 \text{ sec}$$

The time for a complete downward (or upward) stroke (for $v = -3.0$ in.) is calculated to be:

$$T_s = \frac{1}{26.18} \cos^{-1} \left(\frac{-3.0}{3} \right)$$

$$= 0.12000 \text{ sec}$$

The time value for the point on the upward stroke is thus:

$$t_u = (0.12000) + (0.12000 - 0.08282)$$

$$= 0.15718 \text{ sec}$$

Recalling Equation (3.4), left in time mode for convenience, the interference is:

$$I = x(0.08282) - x(0.15718)$$

$$= -A(0.08282) + \frac{R}{\omega} \cos [(0.08282)\omega + \theta] \\ + A(0.15718) - \frac{R}{\omega} \cos [(0.15718)\omega + \theta]$$

For $\omega = 26.18$;

$$I = 0.07436 A - 0.06316 R \sin \theta \quad (3.17)$$

This therefore defines the distance that each tooth has been forced into the tip of the most immediate ledge, at the end of the assumed period of back-cutting.

At this point it is obvious that the phase angle ' θ ' will have a significant effect on the amount of interference to be expected. The purpose of including a phase lag at the start (or phase advance, depending on the point of view) was to allow for the provision of appropriate amounts of log travel during specific periods of the strokes. For this case, minimum 'I' will be realized when ' θ ' has a value of $\pi/2$; thus the periodic portion of the feed is a cosine function rather than a sine. This value will be kept for consideration during the final evaluation of the equations derived in this chapter.

3.4.2. Return stroke assessment

It is essential, for efficient cutting, that the points of the teeth return to positions from which the next cutting stroke as described above can begin. If the log does not advance enough during the return stroke, the teeth will miss the upper ledges and begin their cuts at points somewhat below the desired levels. More importantly, an opportunity for additional log advance is wasted. Conversely, excessive advance will cause the back edges of the teeth to be forced into the kerf face before the upstroke is complete.

An examination of the example tooth trace of Figure (3-6) shows that while fairly efficient cutting will occur for the given conditions, there is still room for improvement. The blade appears to be doing no cutting during the first 'p' distance of its downstroke, which will be the case regardless, due to the slope of the notches in the profile. There does however appear to be room for an increase in the travel of the log during the upstroke. The ideal situation would be to bring each tooth tip back to a point where it is just touching the kerf face at the respective uppermost ledge, and subsequently begin cutting into the ledge immediately below.

Points to be noted before continuing are:

1. The slope of a line drawn through the points of the ledges is equivalent to the slope, or angle of inclination of the blade, ' β '.
2. The 'loop' at the top of the trace indicates that the tooth advances horizontally a significant distance during the first instant of its downstroke, due to the sinusoidal nature of its vertical motion.
3. The pitch value of 1.25 inches does not divide evenly into the assumed maximum log depth of 8 inches. Thus, the top ledge is incomplete, and the tooth will not begin its descent from the tip of ledge.

The second consideration indicates that if the blade teeth are brought back to points at which they are just touching the kerf face at the tops of their strokes, they will be driven into the face slightly during the slow reversal of vertical motion. Conversely, the third consideration shows that if the return is based on a line passing through the points of the ledges, interference should not occur, as some space is available due to the incomplete top ledge.

The amount of horizontal advance allowable during the upstroke of the blade can be related to vertical position and blade angle as (from Fig. 3-6):

$$\begin{aligned} \text{Advance} &= (6.0 - 1.3125) \sin \beta \\ &= 4.6875\beta \quad (\text{for small } \beta) \end{aligned} \quad (3.18)$$

Note that the return starts at the point of maximum back-cutting interference, as discussed above, and ends at the top of the stroke. The difference in horizontal position between the two points is to be equated to the allowable advance, 4.6875β , to produce the third equation.

At the top of the stroke, from Equation (3.3):

$$t = 0.2400 \text{ sec}, \quad v = +3.0 \text{ in};$$

$$\begin{aligned}
 x(v,t) &= -0.08232 \cos\left(\frac{3\pi}{12}\right) + 0.30243 \cos\left(\frac{3\pi}{6}\right) \\
 &\quad - 0.09804 \cos\left(\frac{3\pi}{4}\right) + 0.01173 \cos\left(\frac{3\pi}{3}\right) \\
 &\quad - A(0.24) + \frac{R}{\omega} \cos[(0.24)\omega + \theta] - \frac{R}{\omega} \cos \theta \\
 &= \frac{R}{\omega} [\cos(2\pi)\cos \theta - \sin(2\pi)\sin \theta] \\
 &\quad - \frac{R}{\omega} \cos \theta - 0.24 A \\
 &= -0.24 A
 \end{aligned} \tag{3.10}$$

At the point of maximum interference:

$$t = 0.15718 \text{ sec}, \quad v = -1.6875 \text{ in};$$

$$\begin{aligned}
 x(v,t) &= -0.08232 \cos\left(\frac{-1.6875\pi}{12}\right) + 0.30243 \cos\left(\frac{-1.6875\pi}{6}\right) \\
 &\quad - 0.09804 \cos\left(\frac{-1.6875\pi}{4}\right) + 0.01173 \cos\left(\frac{-1.6875\pi}{3}\right) \\
 &\quad - A(0.15718) + \frac{R}{\omega} \cos[(0.15718)\omega + \theta] - \frac{R}{\omega} \cos \theta \\
 &= 0.09134 - 0.15718 A - 0.05968 R \cos \theta \\
 &\quad + 0.03158 R \sin \theta
 \end{aligned} \tag{3.20}$$

Equating the difference to the allowable advance gives the final equation:

$$\text{Adv} = 4.6875\beta$$

$$= 0.09134 + 0.08282 A - 0.05968 R \cos \theta$$

$$+ 0.03158 R \sin \theta$$

(3.21)

3.5. EQUATION SOLUTIONS - INITIAL

In summary, the three simultaneous equations derived are:

$$(3.15) \text{ Area} = 0.0562 + 5\beta + 0.0730 A + 0.0636 R \cos \theta - 0.0041 R \sin \theta$$

$$(3.17) \text{ Interference} = 0.07436 A - 0.06316 R \sin \theta$$

$$(3.21) \text{ Advance} = 0.09134 + 0.08282 A - 0.05968 R \cos \theta + 0.03158 R \sin \theta$$

Before solution is possible, it will be necessary to dispose of one variable, as it appears that the source of equations has been exhausted. As well, numerical values must be assigned to 'Area' and 'Interference' ('Advance' is assigned the value determined above).

3.5.1. Variable reduction

An examination of the mathematics of the three equations indicates that it would be most advantageous to dispose of ' θ ', to allow a solution through simple matrix algebra. However, the effects of this factor on the system characteristics must first be explored.

The value of ' θ ' has a major influence on the amount of interference occurring, as indicated in Equation (3.17) above. A value of $\pi/2$ will reduce 'I' to a minimum. To a lesser extent, ' θ ' influences the maximum average log feed speed possible, as shown in Equation (3.15) above. Reducing the last two factors of the equation to a minimum allows the value of 'A' to reach its maximum, ie;

$$0.0636 \cos \theta - 0.0041 \sin \theta = \min \quad (3.22)$$

A simple observation shows that the above will be minimized when ' θ ' is somewhere near ' π ', due to the weighting of the cosine term. At $\pi/2$, the value is quickly approaching zero (it reaches zero at 86.31 degrees).

The third equation gives the net horizontal displacement occurring as the blade returns to the top of its stroke. A value of $\pi/2$ for ' θ ' implies that minimum log velocity occurs precisely at the bottom of the downstroke, while the maximum occurs at the top of the upstroke, as shown in Figure (3-11). The log is thus accelerating through the return stroke, and decelerating through the cutting stroke. The latter would be desirable, as it may prevent the teeth from cutting into the wood at an improper angle. The former will be inconsequential, unless the blade tends to interfere with the upper portion of the kerf profile on the upstroke.

Since the minimization of interference may be the most important consideration in the optimization, and other factors will come into play through which the average feed speed may be increased, a value of $\pi/2$ for ' θ ' seems most appropriate. Of course, this assumption will be re-evaluated through the examination of new plots for values to be calculated.

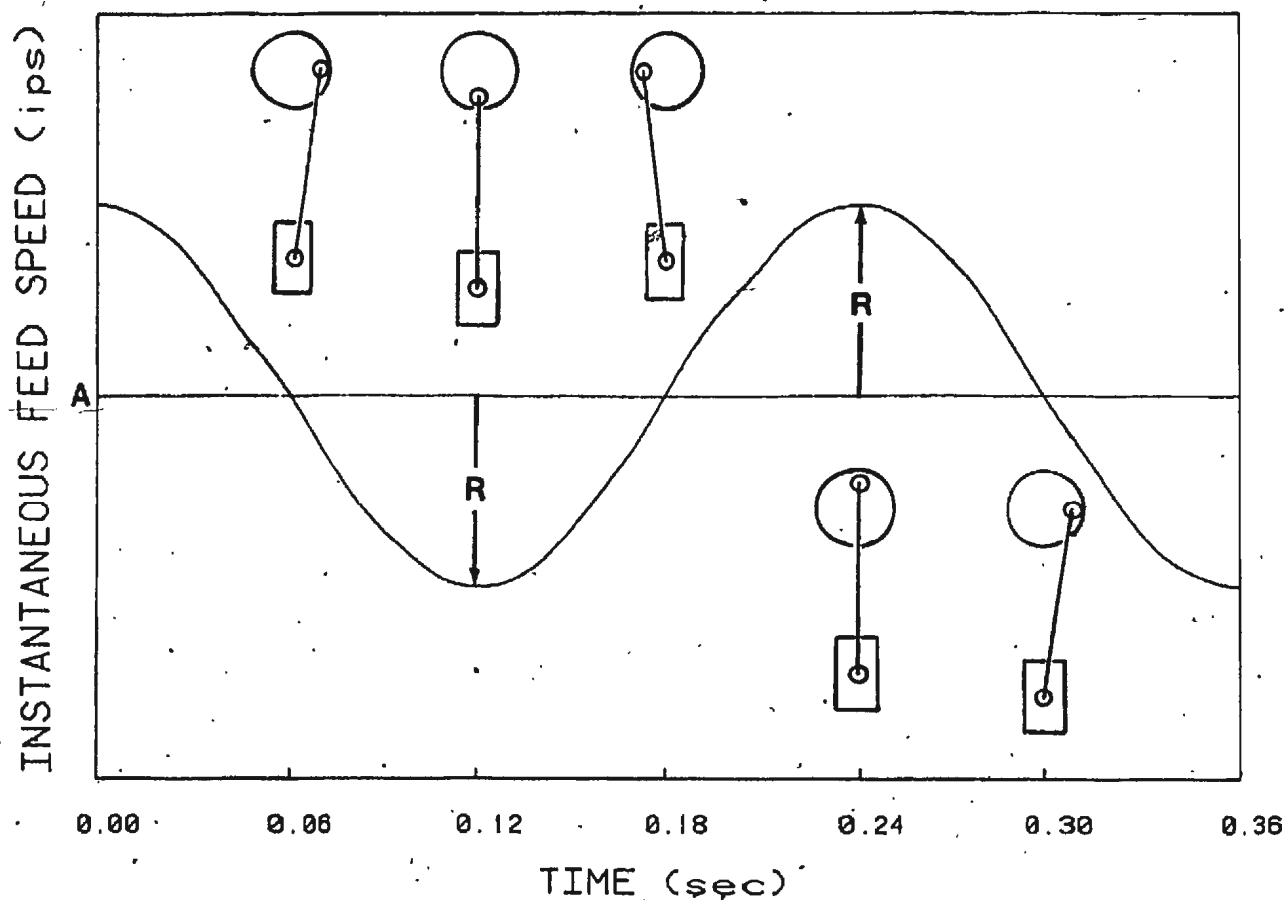


Figure 3-11: Log Velocity vs. Sash Position

3.5.2. Assignment of objective values

From Figure (3-5) the gullet area was approximated as 180 mm^2 , or 0.2790 in^2 . The appropriate expansion factor 'EF' can only be accurately determined through consideration of all factors involved in the cutting process, as discussed earlier. In deciding an 'EF' which would be applicable in the majority of cases, a number of considerations were taken into account:

1. Only one tooth makes a complete cutting path through the wood; all other teeth cut out a comparatively lesser amount of material.
2. The assumption of the volume of the cut, or more specifically the length of the cut, was slightly on the conservative side at the start.
3. Some 'squeezing out' of sawdust should occur, especially with any

amount of swaging of the teeth (to be discussed later), to possibly provide a greater effective gullet area.

4. All assumptions and calculations have been based on the maximum log depth of 6 inches.
5. For Newfoundland operations, sawing will involve mostly softwoods which, being less dense, should have expansion factors near the bottom of the aforementioned range.

On the negative side, part of a ledge occupies each gullet at the end of a cutting stroke of all but the centre tooth, which breaks through the wood at the end of its stroke. Since all other teeth are assumed to cut a lesser amount than that of the centre, this effect should be negligible. All other considerations indicate that the area analysis has been on the conservative side. For this reason, an 'EF' of 1.5 will be used in the formulation. Assigning the value of $\pi/2$ to ' θ ', Equation (3.15) becomes:

$$\frac{0.2790}{1.5} = 0.0561 + 5\beta + 0.0730 A - 0.0041 R \quad (3.23)$$

Again using $\theta = \frac{\pi}{2}$, Equation (3.21) becomes:

$$0.09134 = 4.6875\beta - 0.08282 A - 0.03158 R \quad (3.24)$$

Finally, Equation (3.17) becomes:

$$I = 0.07436 A - 0.06316 R \quad (3.25)$$

Solution now requires that a value be assigned to 'I'. Of course, zero interference

is most desirable, but this would require a temporary reversal of the forward motion of the log, as 'R' would exceed 'A'. Any fluctuation in the velocity of the log will create a vibrational force function in the horizontal plane, as mentioned. Conversely, with excessive interference, the teeth will tend to pull upward on the log at each ledge slope, increasing the sawing power required and causing undue wear on the blade. As the teeth are driven into the faces of the kerf profile, internal vibrations will be set up in the horizontal plane anyway, in this case in the form of a sharp jolt at the beginning of the return stroke rather than in a more gentle sinusoidal pattern. On the positive side, some compression of the wood should be possible, making some degree of interference tolerable. The amount will depend on the wood's mechanical properties and the sample condition at the time of sawing.

3.5.3. Matrix solution of equations

Computer program (A.7) solves the simultaneous equations through the Gauss-Jordan elimination method⁷. Table (3-2) below shows variable solutions for a range of assumed interference levels. In the last line of the table, 'R' is assumed zero (ie; constant velocity) and the interference is calculated rather than assumed.

Plots shown in Figures (3-12) and (3-13) are tooth traces for the calculated values indicated, illustrating minimum interference and constant velocity conditions respectively. The cross-hatched areas, assuming that initial assumptions concerning the specifics of the cutting action are correct, represent the wood 'volume' cut out by the centre tooth, as before.

Table 3-2: Parameter Solutions - Initial

I mm (in)	A mm/sec (ips)	R mm/sec (ips)	β deg	Plot #
0.000	4.204 (0.1655)	4.950* (0.1949)	1.359	(3-12)
0.127 (0.005)	4.509 (0.1775)	3.297 (0.1298)	1.346	
0.254 (0.010)	4.811 (0.1894)	1.643 (0.0647)	1.333	
0.381 (0.015)	5.113 (0.2013)	-0.013 (-0.0005)	1.320	
0.508 (0.020)	5.418 (0.2133)	-1.666 (-0.0656)	1.307	
*0.381 (0.0150)	5.113 (0.2013)	0.000	1.320	(3-13)

*calculated

Examinations of the calculated values and associated traces bring to light some important considerations:

1. Calculated ' β ' values are very low, which justifies assumptions made in the previous sections concerning offset values and efficient cutting angles.
2. The top of the return path of the first stroke clears the kerf profile by a slight margin, as predicted.
3. Calculated maximum allowable velocities are extremely low. At an average speed of 5.418 mm/sec (0.2133 in/sec) (the maximum above assuming a fairly high interference level) it would take more than six minutes to make a complete pass through a two meter long log.
4. The assumed allowable gullet area of 0.1860 in², after taking into consideration 'EF', is reduced initially by about one-third through the geometry of the two adjacent plate deflection curves, ie; integration of the curves between the assumed limits gives a value of 0.0582 in².
5. The available gullet area is further reduced substantially by the ' 5β ' term of Equation (3.23). For an angle of only 1.307 degrees (the minimum calculated above), the reduction is in the order of 0.1140 in². Therefore, considering both the blade and curve geometry, the gullet area remaining to be accounted for by the log feed is only 0.0158 in². In other words, most of the space available for removed material

would be eliminated even if the log remained stationary during the cutting stroke.

6. The range speed 'R' becomes negative as the interference passes that value listed on the last line of the table. This indicates that the phase angle ' θ ' has become -90° , with the maximum log velocity now occurring at the bottom of the stroke, and the minimum at the top. This, in conjunction with the previous observation, indicates that log feed is more plausible during the return stroke than during the cutting stroke for the present small gullet capacity.
7. Reducing ' θ ' to a very small value would not lead to any great advantage, as this would greatly restrict the amount of feeding allowable during the return stroke, to avoid interference with the kerf face at the top of the stroke.
8. The initial assumptions made concerning the sizes and shapes of the areas cut out, as shown in Figure (3-6), are proven invalid by the tooth traces. It appears that cutting does not begin at the first 'ledge', but rather at some lower point, depending on the feed values involved.
9. Although the equation expressing the area between the curves for the assumed limits is correct, it does not accurately reflect the area removed by the centre tooth. For the extremely low feed rates calculated, the area between the curves over the range of integration does not fall wholly within the area of the remaining kerf (single hatched area). Thus, the expression for enclosed area will include an amount of open space along with kerf profile space. Equating this to the tooth gullet area therefore induces a large degree of conservatism.

In light of these new observations, particularly the last two, new assumptions will be made regarding the area(s) of the centre tooth's cut. Equation (3.23) will be reassessed to better reflect the true situation, while Equations (3.24) and (3.25) remain valid.

FEED SPEED = $4.204 + 4.950 * \cos(wt)$ mm/sec

= $0.166 + 0.195 * \cos(wt)$ ips

BLADE OVERHANG ANGLE = 1.359 degrees

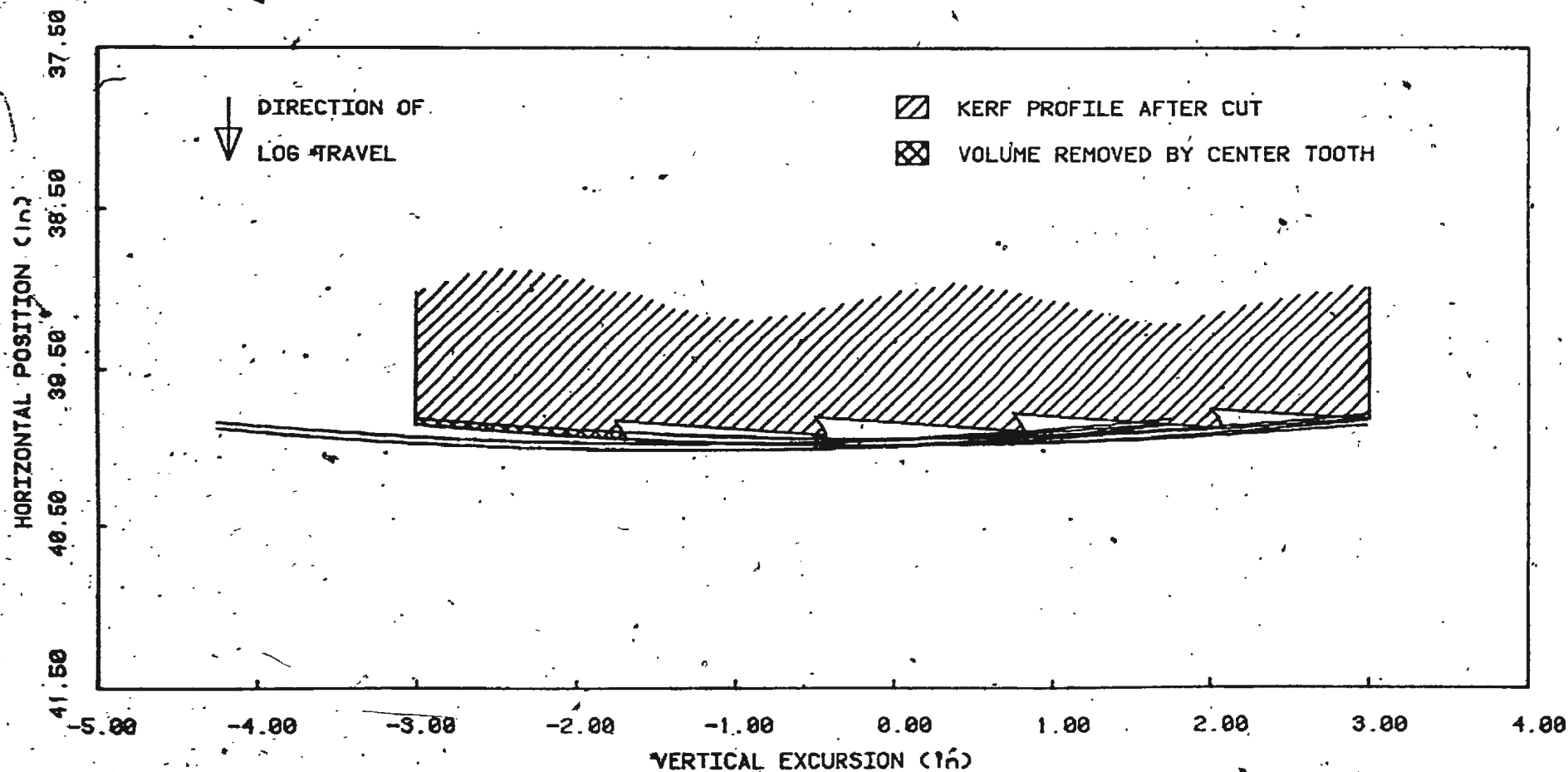


FIG. 3.12 Tooth Trace. - 0.000 in. Interference

FEED SPEED = $5.113 + 0.000 * \cos(wt)$ mm/sec

= $0.201 + 0.000 * \cos(wt)$ ips

BLADE OVERHANG ANGLE = 1.320 degrees

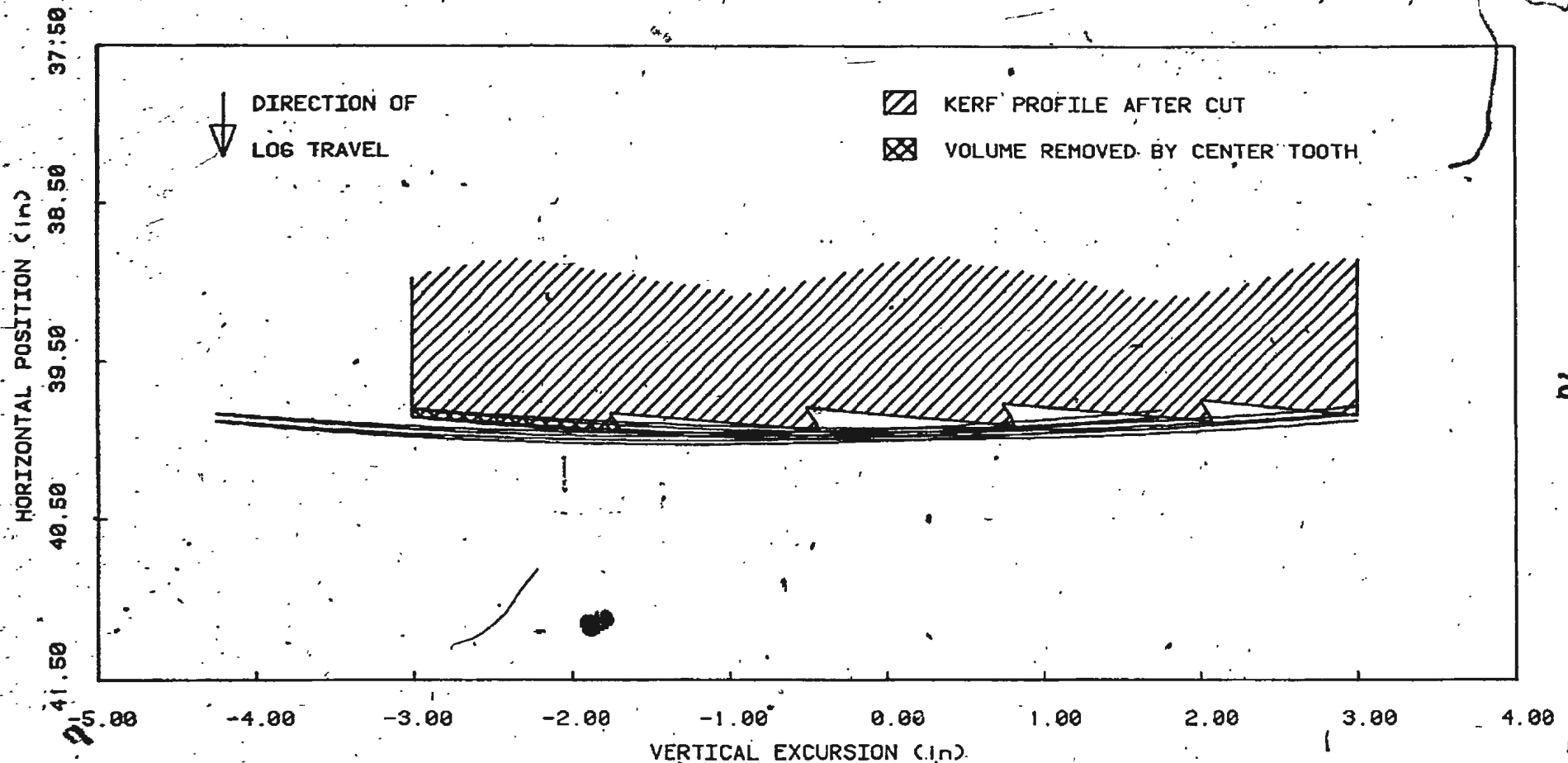


FIG. 3.13 Tooth Trace - Constant Log Feed Speed

3.8. EQUATION SOLUTIONS - RE-ITERATION

Equation forms developed in Section (3.3.1) will be used directly in this revised analysis, with simply the introduction of new limits of integration. Assuming that sawing begins at the next lowest ledge, and that once again a wedge-shaped portion and a solid strip less a wedge slice are cut, the upper limit becomes -0.5 in. The lower limit remains -3.0 in.

From Equation (3.3), the constant area under the stationary curve portion of $x_c(v,t)$ is 0.2007 in^2 . From Equation (3.7) the area under the feed curve is calculated to be (for $\theta = 90^\circ$):

$$A_{fc} = -\frac{A}{\omega}(5.5976) - \frac{R}{\omega}(0.6195) \quad (3.26)$$

The total area under the trace $x_c(v,t)$ between the new limits (for $\omega = 20.18 \text{ rad/sec}$) is now:

$$A_c = -0.2138 A - 0.02366 R + 0.2007 \quad (3.27)$$

The new limits of integration for $x_a(v,t)$, the adjacent tooth, are:

$$\begin{array}{ll} \text{at } v = -0.5; & v' = 0.75 \\ \text{at } v = -3.0; & v' = -1.75 \end{array}$$

The first five terms of Equation (3.11) give $0.3058 + 3.125\beta \text{ in}^2$ as the area under the stationary curve. From Equation (3.7) the area under the feed curve is:

$$A_{fa} = -\frac{A}{\omega}(4.3594) - \frac{R}{\omega}(0.7957) \quad (3.28)$$

The total area under the adjacent tooth trace is now;

$$A_a = -0.1663 A - 0.03039 R + 3.125\beta + 0.3058 \quad (3.29)$$

Finally, the area between the traces is:

$$A_{tot} = \int_{-3.00}^{0.5} [x_a(v,t) - x_c(v,t)] dv$$

$$= 0.1051 + 3.125\beta + 0.0475 A - 0.00673 R \quad (3.30)$$

New solutions based on the revised Equation (3.30) are generated as before, and are listed in Table (3-3).

Table 3-3: Parameter Solutions - Second Iteration

I mm (in)	A mm/sec (ips)	R mm/sec (ips)	β deg	Plot #
0.000	4.249 (0.1673)	5.004 (0.1970)	1.362	(3-14)
0.127 (0.005)	4.486 (0.1766)	3.277 (0.1290)	1.345	
0.254 (0.010)	4.732 (0.1863)	1.549 (0.0610)	1.329	
0.381 (0.015)	4.973 (0.1958)	-0.178 (-0.0070)	1.312	
0.508 (0.020)	5.212 (0.2052)	-1.905 (-0.0750)	1.295	
*0.368 (0.0145)	4.948 (0.1948)	0.000	1.3138	

*calculated

The plot shown in Figure (3-14) is a tooth trace for the selected values indicated. As before, the cross-hatched area represents the wood 'volume' cut out by the centre tooth.

Examinations of the equations, solutions and plot again bring to light some interesting features:

1. Calculated maximum allowable feed rates are still low - the improvement over the previous results is insignificant.
2. The area between the stationary curves over the new, shorter range has actually increased by almost double; from 0.0562 in² to 0.1051 in². This is due to the curved nature of their paths, creating a cross-over point above which the area is numerically negative. It is this negative region which is decreased when the range is shortened, thereby increasing the actual area value. This offsets much of the advantage gained through a lesser area accounted for by the blade inclination.
3. ' β ' values remain low enough to still justify earlier assumptions.
4. The profile is again cleared on the upstroke.
5. The range speed again becomes negative as interference values are allowed to increase.
6. Cutting still begins at a point below that assumed in the initial derivation of the equations.
7. Again, the cross-hatched area does not cover the entire area between the curves over the interval in question.

It is obvious that the maximum allowable feed rate is ultimately limited, regardless of the blade angle or integration range assumed. The general conclusion to be made therefore is that given the existing blade and system conditions, high log throughput rates are an impossibility. Improvement is thus possible only through a variation of one or more of the set parameters.

An increase in the oscillation frequency of the sash frame would lead to improved feed rates, as there is a direct linear relationship between the two. This does lie in the future of the machine, but since a calculation for the increase in

$$\text{FEED SPEED} = 4.732 + 1.549 * \cos(wt) \text{ mm/sec}$$

$$= 0.186 + 0.061 * \cos(wt) \text{ ips}$$

$$\text{BLADE OVERHANG ANGLE} = 1.329 \text{ degrees}$$

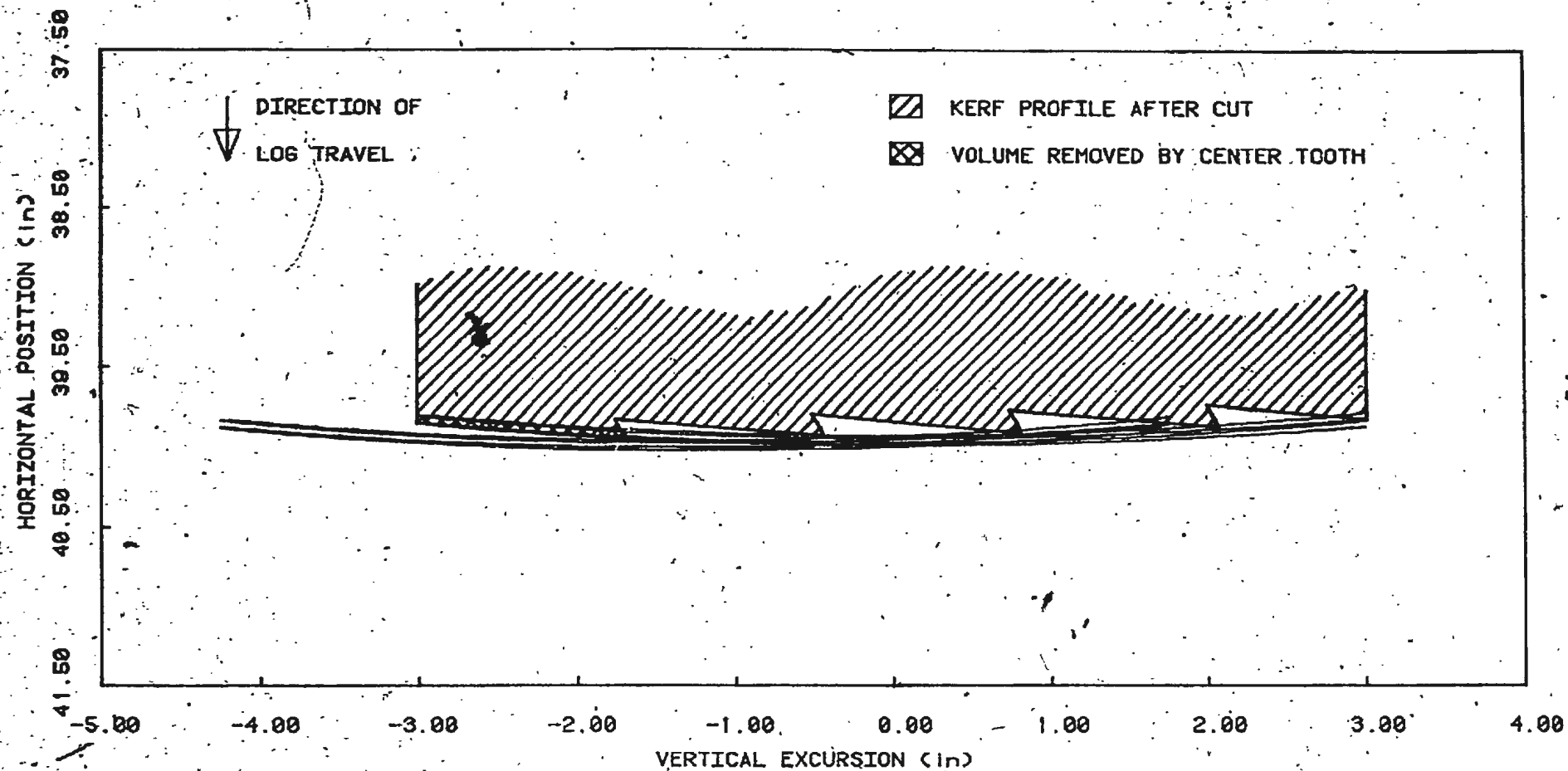


FIG. 3.14 Tooth Trace - Revised Integration Limits

feed rate for an associated frequency increase is not necessary, it will not be discussed further. Increased feed may also be realized through a reduction in the depth of log being sawn. As this would depend on the particular circumstances, it does not pertain to the calculations here. A change in the phase angle ' θ ' may provide a slight feed improvement, but would be accompanied by increased interference.

The remaining parameters to consider are the blade geometrical factors of pitch and gullet area. The first is directly incorporated into the derivations leading to the three governing equations, and thus an exploration of its effect on feed rates would involve considerable alterations. An initial empirical examination of standard tooth profiles shows that gullet area is somewhat related to pitch, and thus greater allowable feeds might realistically be expected with greater pitch values. However, an increased pitch would increase the horizontal offset between teeth (ie; the ' β ' factor), and thus negate a proportionate amount of the newly gained gullet area. A greater pitch would also raise the point of maximum interference, as described in Section (3.4.1), and thus increase interference by increasing the log advance during the initial period of upstroke. A lesser pitch would lessen the available gullet area, but also lessen the horizontal offset and the interference.

A more feasible approach at this time is the consideration of greater gullet areas for saw blades with pitch as assumed throughout the analysis. This is detailed in the following section. At a later time, extraneous to this study, the combined effects of smaller pitch values and deeper gullets will be examined.

3.7. EQUATION SOLUTIONS - DEEPER GULLETS

Gullet areas for five standard North American band saw blade teeth, as shown in Figure (3-15)¹⁰, are listed in the adjoining table (as estimated through the method described in Section (3.3) above). Solutions to the three simultaneous equations for each of the various gullet areas (divided by the assumed E.F. of 1.5) for a range of interferences are as listed in Table (3-5). Plots for selected values as indicated are shown in Figures (3-16) through (3-23).

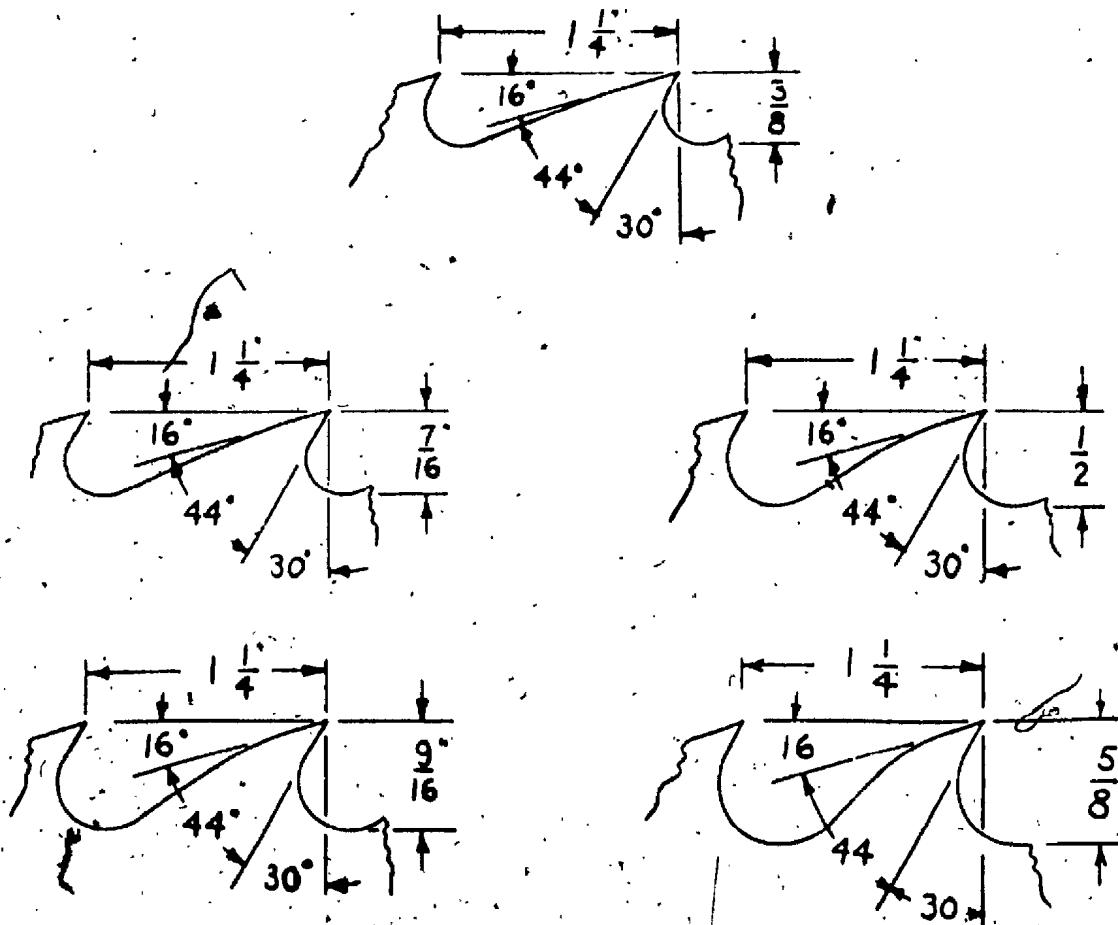


Figure 3-15: Standard North American Band Saw Blade Gullets

From examinations of the various solutions and plots, a few general observations are noted, and some conclusions drawn:

Table 3-4: Gullet Areas (est.) for 1.25 inch Pitch

Gullet Depth (in)	Gullet Area (mm ²)	Gullet Area (in ²)
0.3750	180	0.2790
0.4375	203	0.3147
0.5000	228	0.3534
0.5625	257	0.3984
0.6250	320	0.4960

1. As the gullet area has increased, so has the resulting ' β ' value, but not to a point where the original assumption has become invalid. Considering the maximum ' β ' listed of 3.137 degrees, or 0.0548 radians; $\sin(0.0548) = 0.0547$.
2. In all plots shown it appears that the entire kerf profile is cleared on the upstroke.
3. As gullet areas increase, 'R' has a tendency to become negative at a progressively higher rate of interference, and not at all for the deepest gullets.
4. As expected, there is a considerable increase in the maximum allowable log velocities calculated. Values for the first deeper gullet, 0.4375 in., are more than twice those determined for the initial gullet depth. Similarly, the velocities are about 3.5 times better for the 0.5000 in. gullet, about 5 times better for the 0.5625 in. gullet, and more than 8 times better for the deepest, 0.625 in. gullet.
5. As before, at a zero interference level, 'R' exceeds 'A', with the difference becoming much greater with the progression through the range of gullets.
6. To obtain a reasonable 'A/R' ratio, which was the factor in selecting

Table 3-5: Parameter Solutions - Deeper Gullets

Gullet (in)	I mm (in)	A mm/sec (ips)	R mm/sec (ips)	β deg
0.4375	*0.000	9.304 (0.366)	10.955 (0.431)	1.654
	0.127 (0.005)	9.545 (0.376)	9.228 (0.363)	1.637
	0.254 (0.010)	9.787 (0.385)	7.501 (0.295)	1.621
	0.381 (0.015)	10.028 (0.395)	5.773 (0.227)	1.604
	*0.508 (0.020)	10.269 (0.404)	4.046 (0.159)	1.587
	0.635 (0.025)	10.511 (0.414)	2.319 (0.091)	1.571
	0.762 (0.030)	10.749 (0.423)	0.592 (0.023)	1.554
	0.889 (0.035)	10.991 (0.433)	-1.135 (-0.045)	1.537
	0.805 (0.032)	10.833 (0.427)	0.0000	1.548
0.5000	*0.000	14.785 (0.582)	17.407 (0.685)	1.971
	0.254 (0.010)	15.268 (0.601)	13.952 (0.549)	1.937
	0.508 (0.020)	15.748 (0.620)	10.498 (0.413)	1.904
	*0.762 (0.030)	16.231 (0.639)	7.043 (0.277)	1.871
	1.106 (0.040)	16.713 (0.658)	3.589 (0.141)	1.837
	1.270 (0.050)	17.193 (0.677)	0.135 (0.005)	1.804
	1.280 (0.0504)	17.214 (0.678)	0.0000	1.803
0.5625	*0.000	21.158 (0.833)	24.910 (0.981)	2.339
	0.254 (0.010)	21.641 (0.852)	21.445 (0.845)	2.305
	0.508 (0.020)	22.121 (0.871)	18.001 (0.709)	2.272
	0.762 (0.030)	22.603 (0.890)	14.547 (0.573)	2.239
	*1.106 (0.040)	23.086 (0.909)	11.092 (0.437)	2.205
	1.270 (0.050)	23.566 (0.928)	7.638 (0.301)	2.172
	1.831 (0.0721)	24.633 (0.970)	0.0000	2.098
0.6250	*0.000	34.986 (1.377)	41.191 (1.622)	3.137
	0.254 (0.010)	35.469 (1.396)	37.737 (1.486)	3.104
	0.508 (0.020)	35.949 (1.415)	34.282 (1.350)	3.071
	0.762 (0.030)	36.431 (1.434)	30.828 (1.214)	3.037
	1.106 (0.040)	36.914 (1.453)	27.374 (1.078)	3.004
	*1.270 (0.050)	37.394 (1.472)	23.919 (0.942)	2.971
	3.028 (0.1192)	40.731 (1.604)	0.0000	2.740

*plotted

conditions to illustrate on the plots, a high interference level had to be assumed. When deciding on an appropriate gullet size, this might be an unacceptable situation, ruling out the deepest gullets as possibilities and effectively limiting the ultimate velocities.

Enough information has now been compiled concerning the influences of the many factors involved in the cutting to draw some solid conclusions, and make recommendations on the future development of the MUN sash saw. These are covered in the next and final chapter.

$$\text{FEED SPEED} = 9.304 + 10.955 * \cos(wt) \text{ mm/sec}$$

$$= 0.366 + 0.431 * \cos(wt) \text{ ips}$$

$$\text{BLADE OVERHANG ANGLE} = 1.654 \text{ degrees}$$

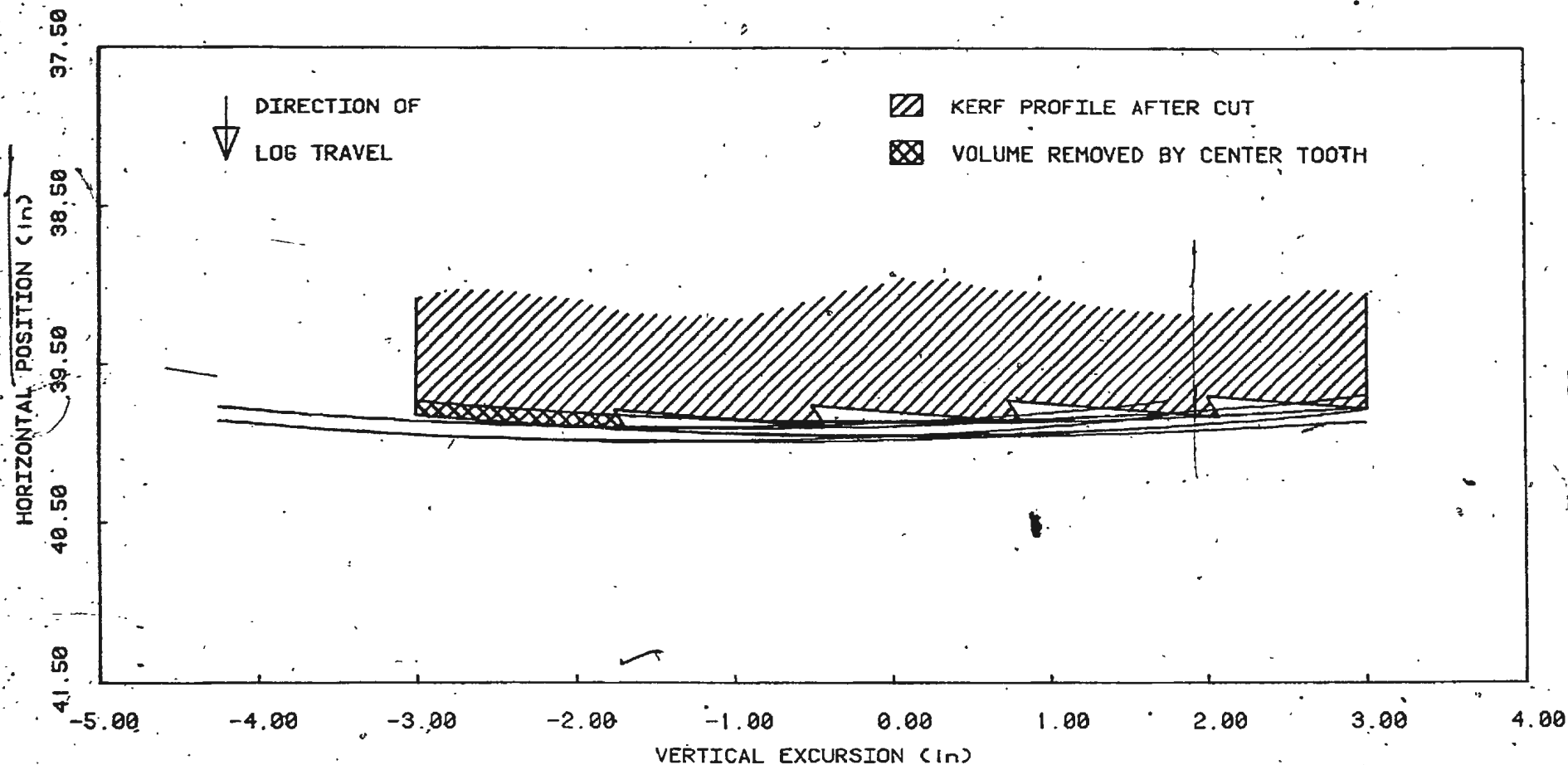


FIG. 3.16 0.4375 in. Gullet - .0000 in. Interference Trace

$$\text{FEED SPEED} = 10.269 + 4.046 * \cos(wt) \text{ mm/sec}$$

$$= 0.404 + 0.159 * \cos(wt) \text{ ips}$$

$$\text{BLADE OVERHANG ANGLE} = 1.587 \text{ degrees}$$

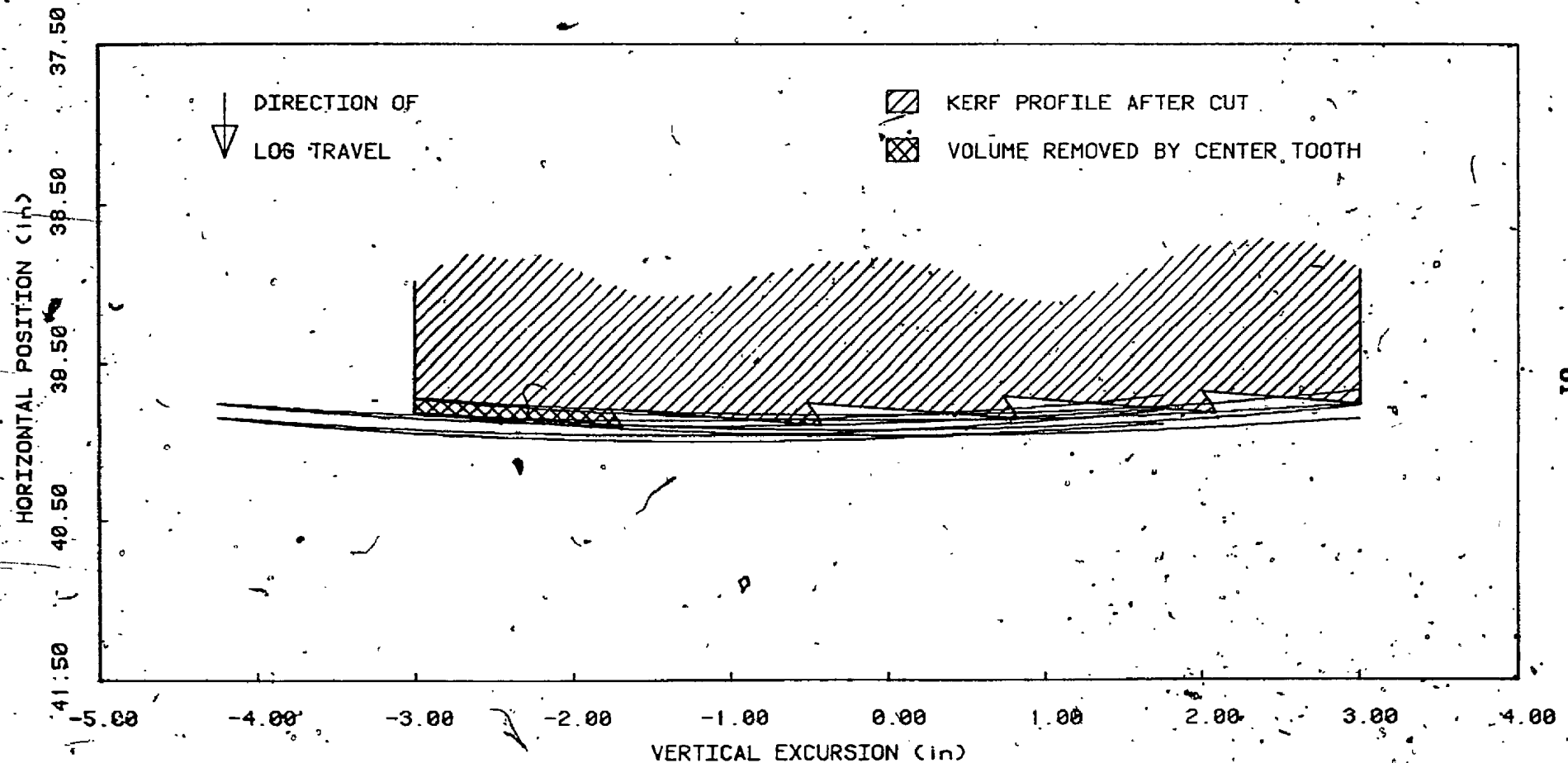


FIG. 3.17 0.4375 in. Gullet - 0.0200 in. Interference Trace

FEED SPEED = $14.785 + 17.407 * \cos(wt)$ mm/sec

= $0.582 + 0.685 * \cos(wt)$ ips

BLADE OVERHANG ANGLE = 1.971 degrees

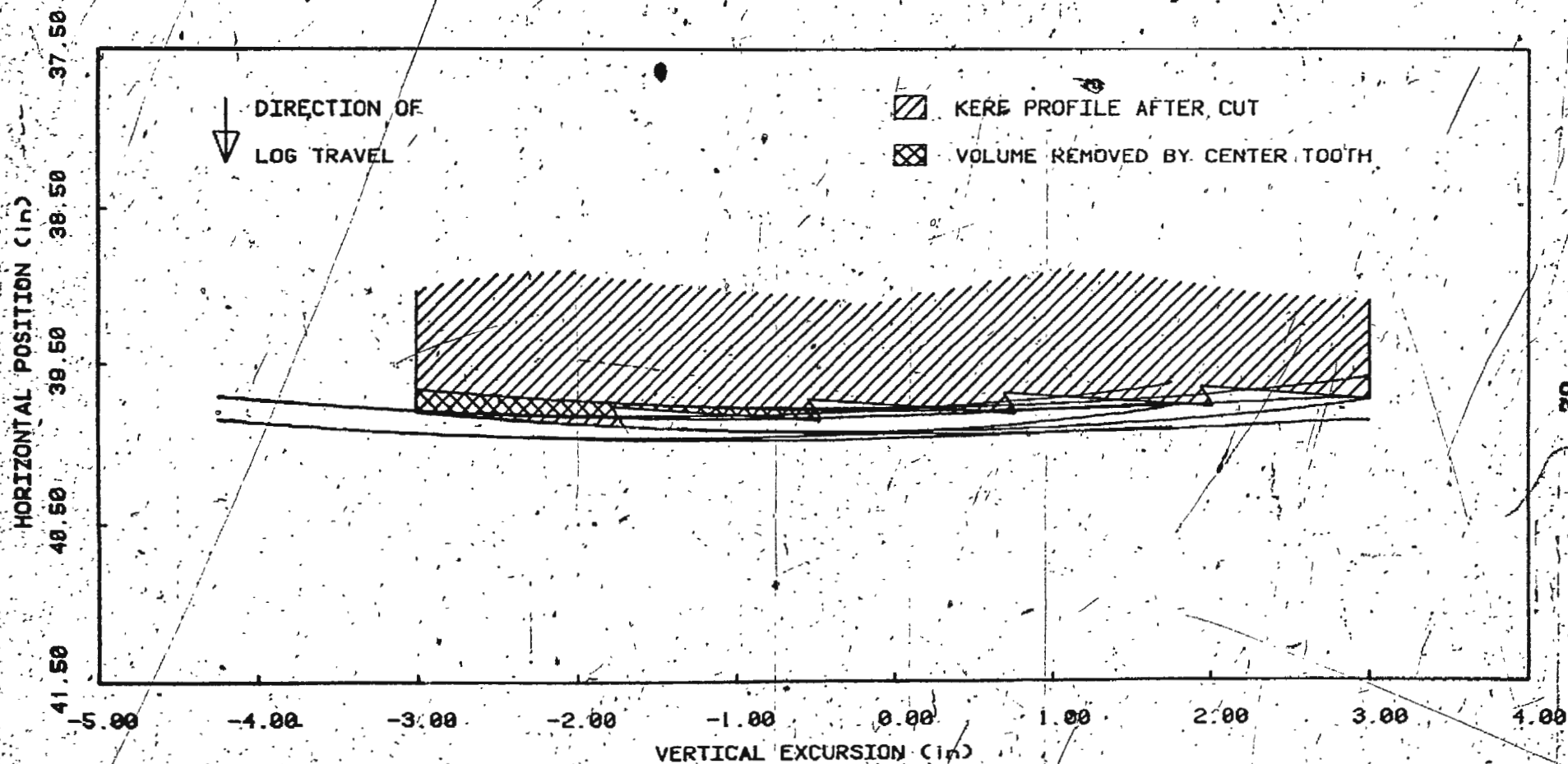


FIG. 3.18 0.5000 in. Gullet - 0.0000 in. Interference Trace

FEED SPEED = $16.231 + 7.043 * \cos(wt)$ mm/sec

= $0.582 + 0.685 * \cos(wt)$ ips

BLADE OVERHANG ANGLE = 1.871 degrees

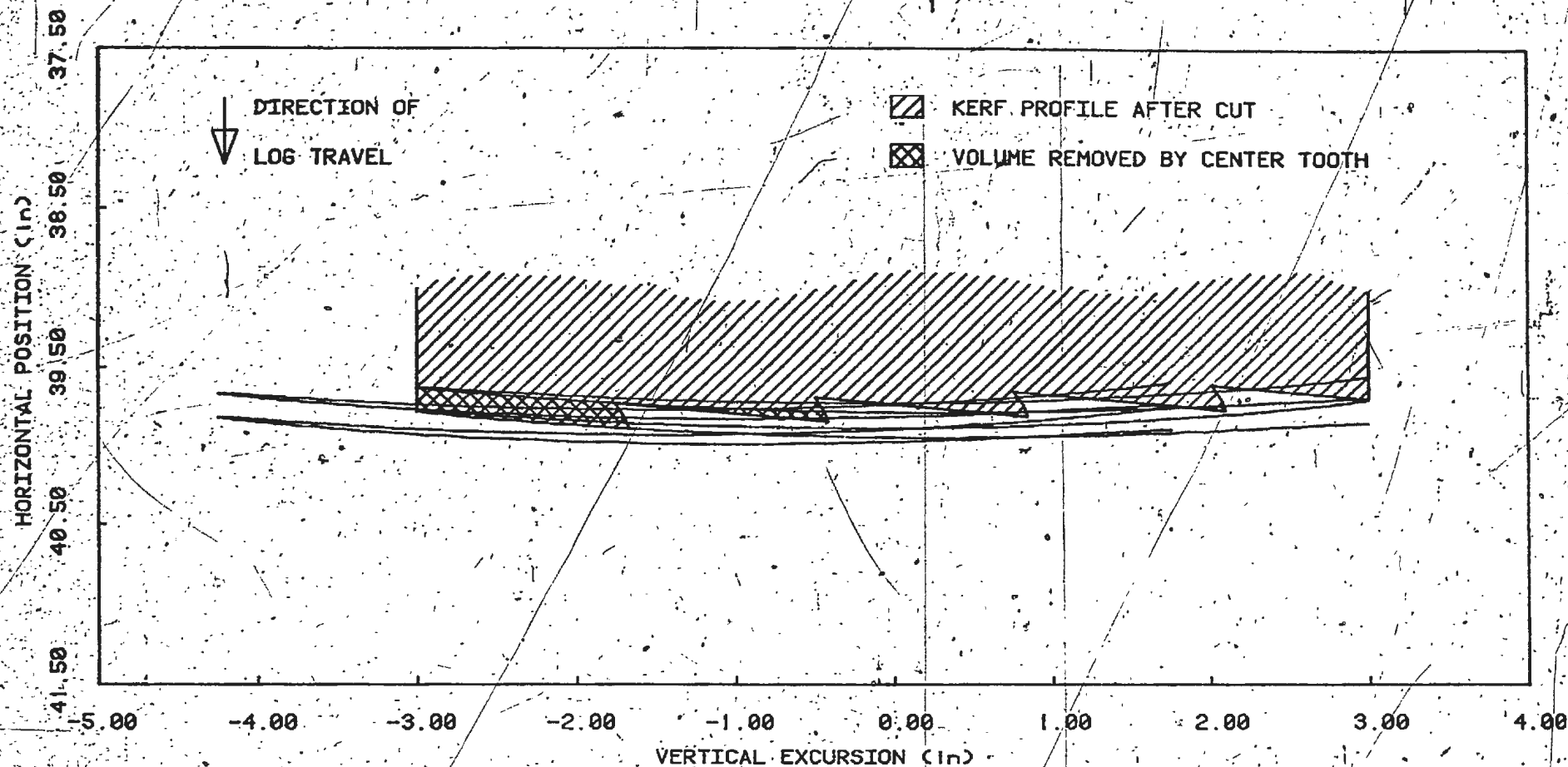


FIG. 3.19 0.5000 in. Gullet - 0.0300 in. Interference Trace

$$\text{FEED SPEED} = 21.158 + 24.910 * \cos(wt) \text{ mm/sec}$$

$$= 0.833 + 0.981 * \cos(wt) \text{ ips}$$

$$\text{BLADE OVERHANG ANGLE} = 2.339 \text{ degrees}$$

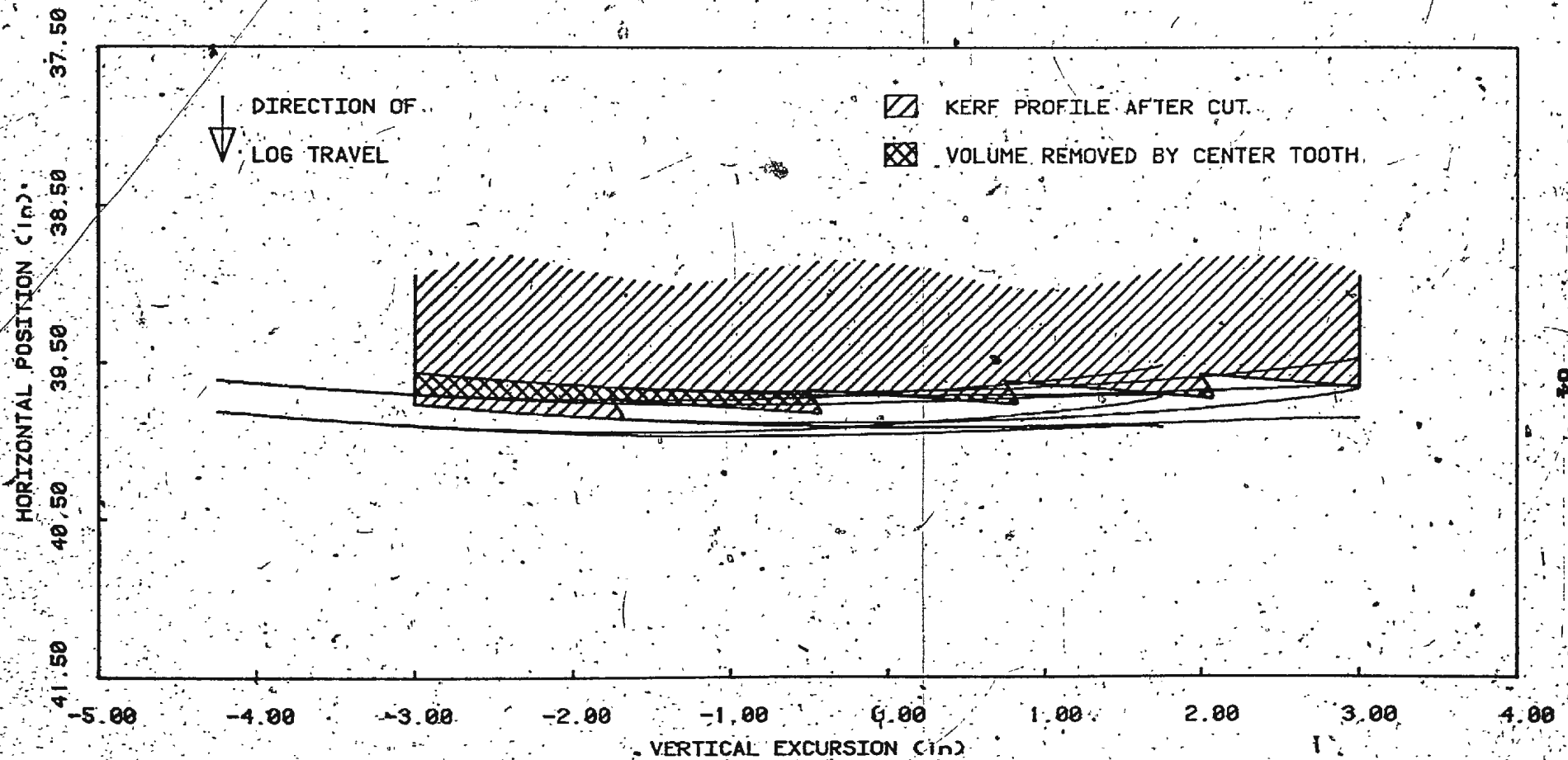


FIG. 3.20 0.5625 in. Gullet - 0.0000 in. Interference Trace

$$\text{FEED SPEED} = 24.915 + 11.092 * \cos(wt) \text{ mm/sec}$$

$$= 0.909 + 0.437 * \cos(wt) \text{ ips}$$

$$\text{BLADE OVERHANG ANGLE} = 2.205 \text{ degrees}$$

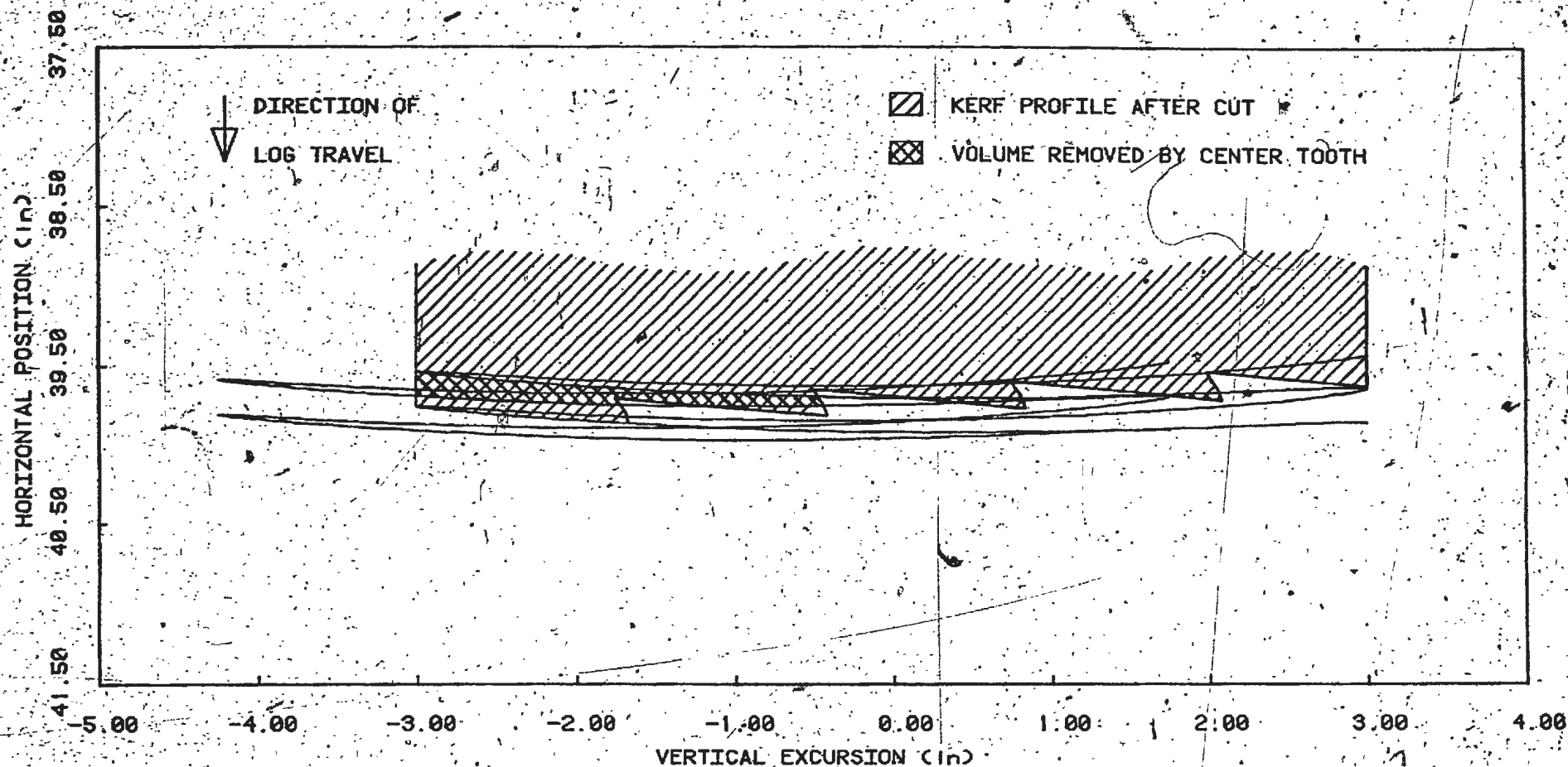


FIG. 3.21 0.5625 in. Gullet - 0.0400 in. Interference Trace

$$\text{FEED SPEED} = 34.986 + 41.191 * \cos(wt) \text{ mm/sec}$$

$$= 1.377 + 1.622 * \cos(wt) \text{ ips}$$

$$\text{BLADE OVERHANG ANGLE} = 3.137 \text{ degrees}$$

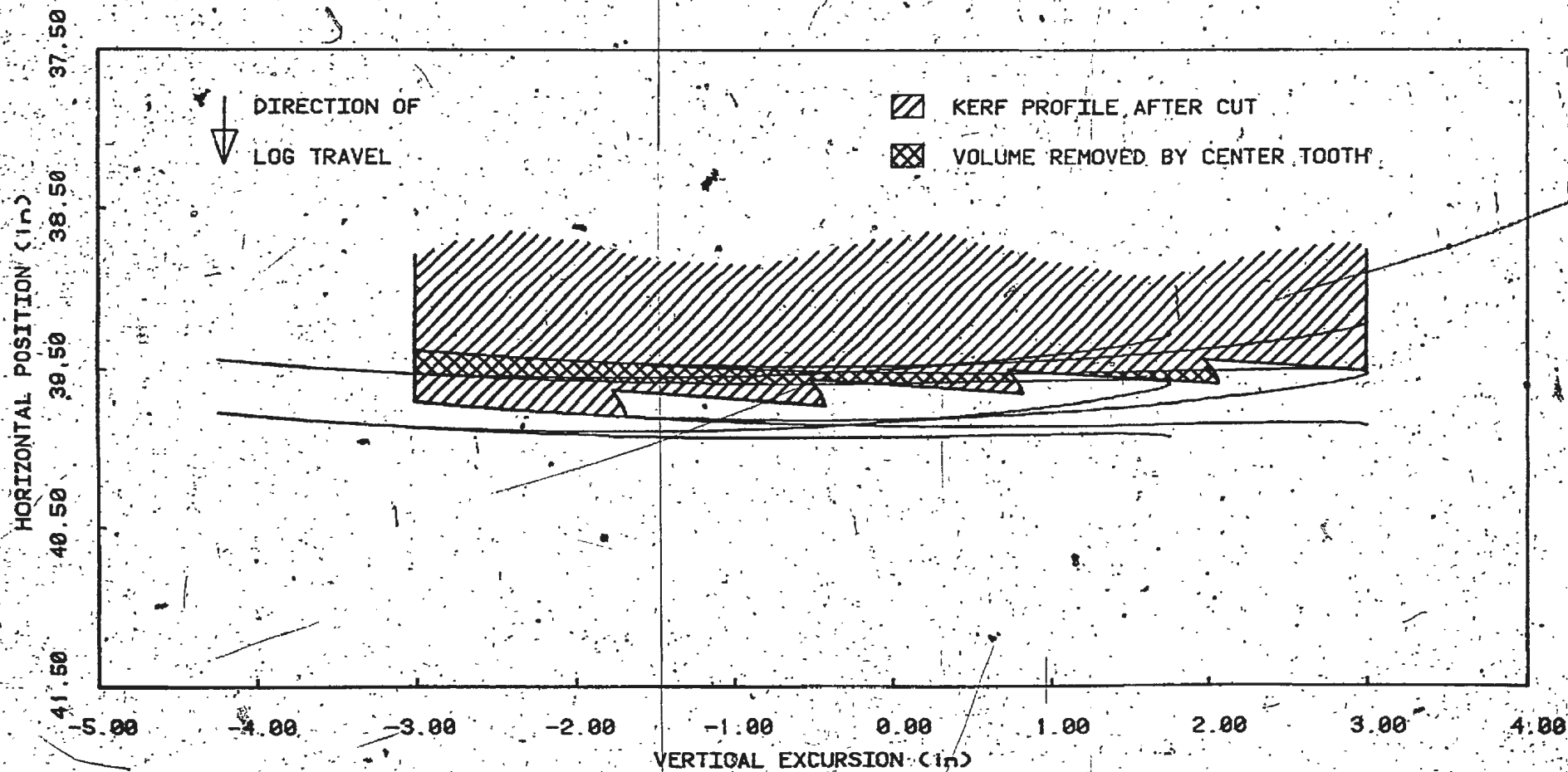


FIG. 3.22 0.6250 in. Gullet - 0000 in. Interference Trace

FEED SPEED = $37.394 + 23.919 * \cos(wt)$ mm/sec

= $1.472 + 0.942 * \cos(wt)$ ips

BLADE OVERHANG ANGLE = 2.971 degrees

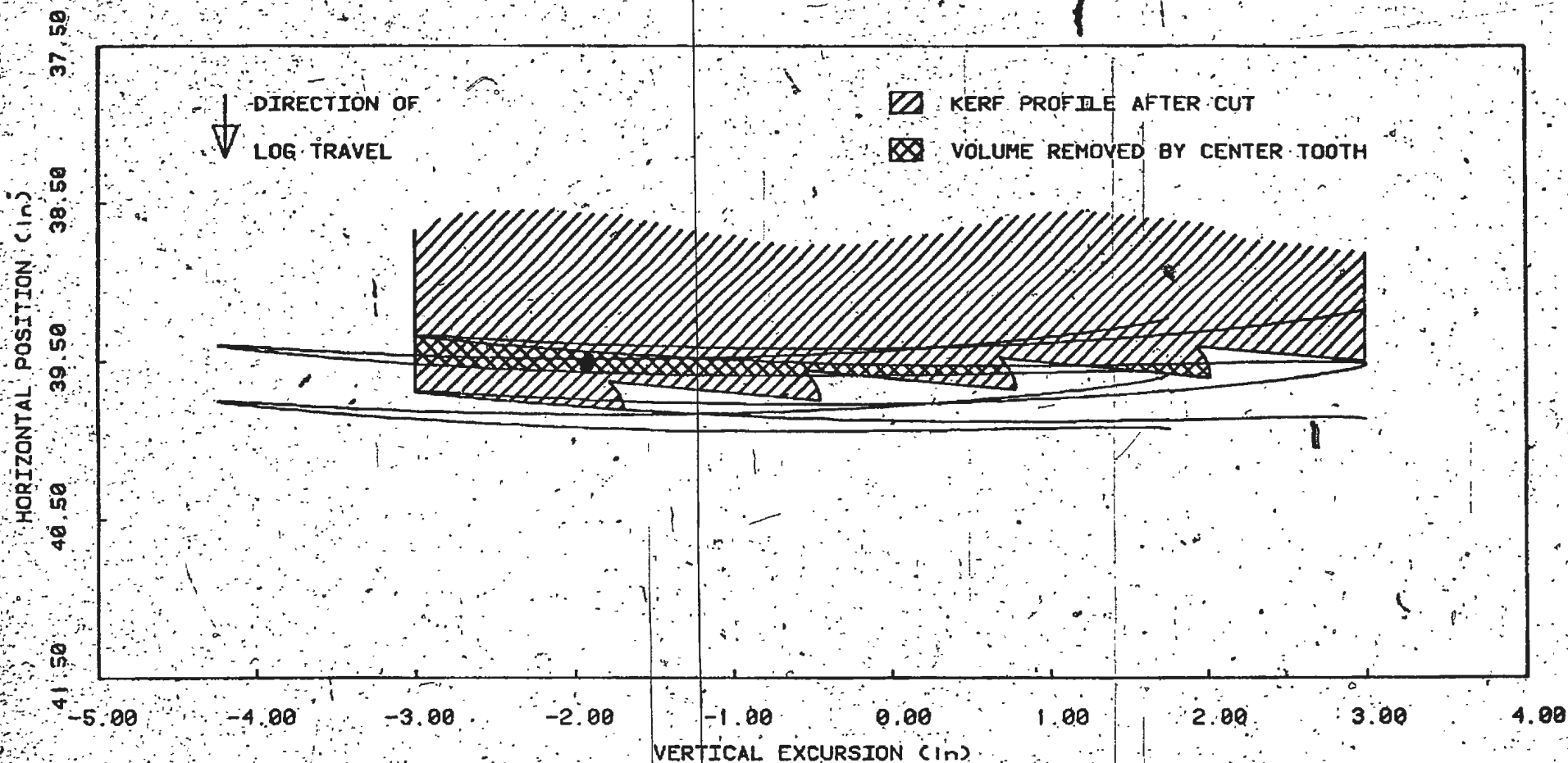


FIG 3.23 0.6250 in. Gullet - 0.0500 in. Interference Trace

Chapter 4

SUMMARY AND CONCLUSIONS

4.1. Results of study

In general, generated traces did validate the three major assumptions purported within the text of the analysis portion of this study. Manual measurements obtained from the generated traces indicated that interference levels at the appropriate points corresponded with those assumed in the calculations. Rough measurements also showed that where the integration limits assumed were valid, the areas between the adjacent traces approximated the gullet capacities assumed, although for the original gullet this area did not fall wholly within the kerf profile. Finally, in all cases the tooth returned to the correct horizontal position at the culmination of the return stroke.

Results indicate without doubt that with the present tooth pattern, feed rates and thus possible production rates are severely limited. The rate determining factor appears to be the present gullets' limited capacity to store cut material efficiently. The exceeding of the limit seems to be in a small part a consequence of the non-linear motion of the sash due to the deflection shape of the supporting plate springs. In the large part, the capacity is exceeded due to the necessity of inclining the blade from the vertical to limit back-cutting

interference. The corresponding horizontal offset between adjacent teeth multiplied by the length of the stroke produces a value which consumes a major portion of the available gullet area.

Some difficulty was experienced in deciding on the most appropriate limits for calculations of areas between adjacent tooth traces. However, in cases where the assumed limits did prove valid (ie, for the deeper gullets) reasonable feed rates resulted. These deeper gullets may appear at first glance to alleviate the feed restriction problem, but lateral strength complications may arise when the aspect ratio of the cantilevered tooth is increased. This however is not to be discussed here, as tooth deflections and any corresponding losses in sawing accuracy are a consequence of many combined influences. In conclusion it appears that for the assumed pitch value, an appropriate gullet depth, according to the method employed, may be 1/2 inch. This is a compromising value, midway in the range of standard depths, and the plots associated with this particular size agree very well with earlier assumptions. As a comparison, the use of a 0.50 inch gullet depth with a 0.75 inch pitch in typical Swedish frame saw designs proves successful, although a heavier gauge of blade is normally employed¹¹.

4.2. The future of the MUN Sash Saw

Feed rates calculated herein are expressed in units of distance per second, based upon a calculated rate of sash oscillation. The rates may be expressed absolutely in distance per stroke values, with the maximum constant portion feed rate of 40.73 mm/sec (1.604 ips) translating to 9.76 mm/stroke (0.385 in/stroke), for the assumed 250 cycles/sec oscillation rate. Thus a change in frequency

affects a directly proportionate change in the feed per second value. This is the first aim of the current sash saw related endeavour, initiated at the beginning of 1986. Frequency increases will be realized through a stiffening of the suspension, by either the addition of biasing springs at the plate ends, the selection of a more suitable plate material, or through a combination of both. Calculations as shown within will provide a guide for the determination of spring constant values appropriate for an objective frequency.

The second major area of development concerns the saw blade itself. Equations developed here lead the way in the selection of suitable blade and teeth geometrical parameters. A possible partial solution to the feed rate dilemma is the use of spring or swage set teeth, as illustrated in Figure (4-1) below¹. In the spring set case, teeth are alternately set to either side of the central plane of the blade, for the purpose of slicing a path through the log wider than the blade thickness. The wider cut provides clearance for the reduction of frictional forces and associated heat generation, while providing a possible storage area for waste material. In a typical Swedish frame saw, teeth with parameters as shown in Figure (3.15) are spring set 0.024 inches to either side, for a 15 or 16 gauge blade thickness (0.0625 or 0.0703 inch). Feed rates quoted are as high as 1.75 inches constant per stroke, but for 34 inch-high frames (and associated large stroke lengths), and cants less than 6 inches deep. The allowable feed is cut to about one-third for an 8 to 10 inch cant, for the same stroke length¹¹. However, as discussed earlier, this brute force method of sawing involves high energy consumption with only a moderate reduction in material wastage (the cut width becomes about 1/8 inch with the combined heavier gauge and spring setting).

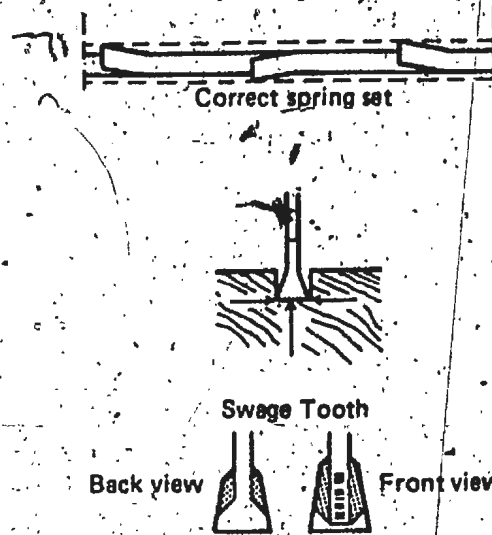


Figure 4-1: Saw Tooth Spring and Swage Sets

Another solution may be the incorporation of tooth swage setting, in which the tip of each tooth is initially widened through simple cold working between an anvil and die, and then shaped and sharpened to the most efficient profile. Each tooth then cuts a path normally twice as wide as the blade thickness, when shaped to the appropriate half gauge to either side of centre. In the present case the cut width would become about $1/16$ inch. An effective doubling of the gullet capacity may also be realized, except that twice the material is now being removed, and must be stored while the tooth is inside the cut. The nature of the tooth shape however may allow more material to be squeezed out between the sides of the blade and the wood faces.

Finally, a feed mechanism must be incorporated to provide a feed function with the inherent ability to reduce or eliminate back-cutting interference. The combined constant/sinusoidal function solution assumed was intended to provide for this without the introduction of an unreasonable horizontal shaking force.

The level of this force is dependent upon the actual log mass and the accelerations it experiences during speed transitions. Instantaneous stopping and starting, which would be the case with a hesitating feed are undesirable. However any feed function in which no net log movement is experienced during the bottom portion of the cutting stroke, and an equidistant portion of the upstroke would eliminate the interference problem. If this can be attained through gentle transitions, then it may prove to be a more viable solution. The mathematical analysis method employed within could then be used to evaluate the optimum velocities given the new feed function pattern.

Through the use of the analysis techniques developed, and the incorporation of the tooth modifications presented here, it is envisioned that a new efficient sash saw design and subsequent prototype will be realized in the near future.

REFERENCES

1. E. M. Williston, *Lumber Manufacturing: The Design and Operation of Sawmills and Planer Mills*, Miller Freeman Publishing, San Francisco, 1978.
2. P. Koch, *Wood Machining Processes*, Ronald Press Co., New York, 1964.
3. J. W. Church et al, "Sawmill Research And Development Programme: Progress Report", Tech. report, Faculty of Engineering and Applied Science, Memorial University of Newfoundland, March 1977.
4. Unknown, "The Frame Saw Manual", Tech. report. 39, Food and Agriculture Organization, 1982.
5. "The 8-Frame Built for Reducers", A Kokums Industri AB Trade Publication.
6. "Vollgater Gang Saw Type HDSN", A Esterer AG Trade Publication.
7. M. L. James et al, *Applied Numerical Methods for Digital Computation*, 2ed, Harper & Row, New York, 1977.
8. R. W. Clough et al, *Dynamics of Structures*, McGraw Hill Inc., New York, 1975.
9. *Georgia Tech. Strudl Users Manual*, 3rd, Rev. E ed., GTICES Systems Laboratory, School of Civil Engineering, Georgia Institute of Technology, Atlanta, Georgia, 1981.
10. E. M. Williston, *Saws: Design, Selection, Operation, and Maintenance*, Miller Freeman Publishing, San Francisco, 1978.
11. D. S. Jones, "Swedish Frame Saws", *Australian Timber Journal*, June 1956, pp. 484-498.

Appendix
COMPUTER PROGRAM LISTINGS

A.1. Tooth Trace Simulation Program

```

*****
*   PROGRAM #1 - COMPUTER SIMULATION OF THE RELATIVE
*   MOTION OF SASH SAW BLADE TEETH DURING THE SAWING
*   OF A CANT LOG
*****

```

```

DIMENSION DEFL(250),XDISPL(250)
DIMENSION X(501),Y(501),XX(501),YY(501)
DIMENSION H(501),V(501)
REAL AD,ADV,ANGLE,BLDANG,PITCH,MAXINT
INTEGER OPTION,FIG
LOGICAL*4 T1(7)
LOGICAL*4 T2(4)
LOGICAL*4 T3(7)
LOGICAL*4 T4(7)
LOGICAL*4 T5(7)
LOGICAL*4 T6(6)
LOGICAL*4 T7(6)
PI=4.0*ATAN(1.0)
TYPE*, 'WHAT IS DELTA XELL?'
TYPE*, '(TRY 0.000005)'
ACCEPT*,DXELL
TYPE*, 'WHAT IS XELL CHECK VALUE (EPSI)?'
TYPE*, '(TRY 0.00002)'
ACCEPT*,EPSI
EPSI=1/EPSI
TYPE*, 'HOW MANY INTERVALS FOR SIMPSONS (EVEN)?'
TYPE*, '(TRY 50)'
ACCEPT*,N
TYPE*, 'WHAT IS INITIAL END DISPLACEMENT VALUE (POS) IN INCHES?'
TYPE*, '(NORMALLY 3 in)'
ACCEPT*,VI
P=128
TYPE*, 'WHAT IS CRANK ARM LENGTH (in) PLEASE?'
TYPE*, '(PRESENTLY 36.469 in)'
ACCEPT*,CL
Q=P+1
DO13I=1,Q,1
T=(0.12)*(I-1)/P
TH=25.*PI*T/3
DEFL(I)=(VI*COS(TH)+CL*(1-SQRT(1-(VI**2)*(SIN(TH)**2/(CL**2)))))*0.025
* CONTINUE
13
C
C
C
A SET OF DEFLECTION POINTS FOR THE PLATE END HAVE NOW BEEN GENERATED
XELL=39.860/40.0
DO18I=1,Q
FAC=500.
25 VEE=DEFL(I)
2 CALL NUMINT(XELL,VEE,N,ELL)
2 IF(INT(CELL,-1)*EPSI)3,4,5
3 XELL=XELL+DXELL*FAC
GO TO 2
5 XELL=XELL-DXELL*FAC
FAC=FAC/2.
GO TO 3
4 DEFL(I)=40.*VEE
XDISPL(I)=40.*XELL
WRITE(6,9)DEFL(I),XDISPL(I)
18 CONTINUE

```

```

C
C
C
1      DO35I=1,Q
      X(I)=DEFL(I)
      Y(I)=XDISPL(I)
35     CONTINUE
      DO14I=1,Q,1
      J=I+P
      K=I+2*P
      L=I+3*P
      X(J)=-X(I)
      X(K)=X(I)
      X(L)=-X(I)
      Y(J)=Y(I)
      Y(K)=Y(I)
      Y(L)=Y(I)
14     CONTINUE
C
C      DATA FOR DEFLECTED PLATE HORIZONTAL SPAN vs. DEFLECTION
C      FOR TWO COMPLETE CYCLES HAS NOW BEEN STORED:
C      TO THE DATA WILL NOW BE ADDED QUANTITIES REFLECTING THE NET
C      HORIZONTAL DISPLACEMENT DUE TO LOG FEED
C
8      FORMAT(F7.3,10X,F8.4)
      TYPE*, 'WHAT IS MEAN VALUE (AVERAGE) OF FEED SPEED (in in/sec)?'
      ACCEPT*, A
      TYPE*, 'WHAT IS AMPLITUDE (RANGE) OF FEED FUNCTION (in in/sec)?'
      ACCEPT*, R
      MAXINT=0.07436*A-0.06316*R
      TYPE*, 'WHAT IS PHASE ADVANCE OF FEED SINE FUNCTION (degrees)?'
      ACCEPT*, ADV
      TYPE*, 'WHAT IS FIGURE NUMBER AND GULLET DEPTH?'
      ACCEPT*, IFIG, GUL
      AD=ADV*PI/180.
      W=25.*PI/3.
      DO7I=1,L,1
      T=(0.12)*(I-1)/P
      WT=W*T
      Y(I)=Y(I)-(R/W)*(COS(AD)-COS(AD)+COS(WT)+SIN(AD)*SIN(WT))
      Y(I)=Y(I)-A*T
7      CONTINUE
      N=L
      DO18I=1,N
      H(I)=X(I)
      V(I)=Y(I)
18     CONTINUE
      CALL PLOTS
      CALL AXIS(1.0,1.6, ' ', -1., 0., 0., -5.0, 1.0)
      CALL AXIS(1.0,1.6, ' ', 1., 4., 90., 41.5, -1.0)
      CALL DUMP
      DATA T6/'VERT', 'ICAL', ' DEF', 'LECT', 'ION ', '(in)'/
      DATA T7/'HORI', 'ZONT', 'AL S', 'PAN ', '(in)'/
      CALL SYMBOL(4.5,1.1,0.14,T6,0.0,24)
      CALL SYMBOL(0.67,2.72,0.14,T7,90.0,20)
      CALL DUMP
      CONTINUE
      X(N+1)=-5.0
      Y(N+1)=41.5
      X(N+2)=1.0
      Y(N+2)=-1.0

```

```

DATA Y1/'FEED', 'SPE', 'ED =', '
CALL SYMBOL(1.8,6.4,0.21,T1,0.0,28)
CALL DUMP
DATA T2/'CO', 'S(vt', ' ) in', '/sec'/
CALL SYMBOL(5.76,6.4,0.21,T2,0.0,16)
CALL DUMP
CALL NUMBER(3.55,6.4,0.21,0.0,A,'(F6.4)',6)
CALL DUMP
CALL NUMBER(4.88,6.4,0.21,0.0,R,'(F6.4)',6)
CALL DUMP
DATA T4/'FIG', 'A', ' ' in', 'Ga', 'ilet'/
CALL SYMBOL(1.75,0.5,0.21,T4,0.0,28)
CALL DUMP
DATA T5/' ' in', 'Inte', 'rfer', 'ance'/
CALL SYMBOL(6.39,0.5,0.21,T5,0.0,28)
CALL DUMP
CALL XYPL0T(1.75,0.45,3)
CALL XYPL0T(2.00,0.45,2)
CALL XYPL0T(1.75,0.45,2)
CALL NUMBER(2.66,0.5,0.21,0.0,2,0,'(I2)',IFIG)
CALL DUMP
CALL NUMBER(3.18,0.5,0.21,0.0,GUL,'(F6.4)',6)
CALL DUMP
CALL NUMBER(6.04,0.5,0.21,0.0,MAXINT,'(F6.4)',6)
CALL DUMP
TYPE*, 'CHANGE TO THIN PEN AND HIT 1 TO CONTINUE'
ACCEPT*, OPTION
IF(OPTION.NE.1)GO TO 400
CONTINUE
CALL LINE(X,Y,N,1.0,0.0,14)
CALL DUMP

C
C
C
C
THIS SECTION PROVIDES FOR THE PLOTTING OF ADDITIONAL BLADE
TEETH THROUGH INCLUSION OF VERTICAL AND HORIZONTAL OFFSETS

TYPE*, 'WHAT IS SAW BLADE ANGLE (+ve CCW from vert) IN DEGREES?'
ACCEPT*, BLDANG
ANGLE=BLDANG*PI/180.
TYPE*, 'WHAT IS SAW TOOTH PITCH (inches)?'
ACCEPT*, PITCH
150 TYPE*, 'WHICH TOOTH (1,2,4, or 5) DO YOU WISH PLOTTED?'
ACCEPT*, NBLD
IF(NBLD.EQ.3)GO TO 300
IF(NBLD.LT.1)GO TO 300
IF(NBLD.GT.5)GO TO 300
CALL BLADE(H,V,NBLD,PITCH,ANGLE,N,XX,YY)
XX(N+1)=-5.0
YY(N+1)=41.5
XX(N+2)=1.0
YY(N+2)=-1.0
CALL LINE(XX,YY,N,1.0,0.0,14)
CALL DUMP
GO TO 150
300 CONTINUE
DATA T3/'BLAD', 'E', 'AN', 'GLE', ' ' in', 'degr', 'ees'/
CALL SYMBOL(1.8,6.0,0.21,T3,0.0,28)
CALL DUMP
CALL NUMBER(3.65,6.0,0.21,0.0,BLDANG,'(F5.3)',5)
CALL DUMP
CALL PLEXIT
TYPE*, 'TO PLOT FOR OTHER PARAMETERS, TYPE 1'

```

```

ACCEPT*,OPT
IF(OPT.NE.1)GO TO 500
GO TO 1
500  STOP
      END

C
C  BEGINNING OF SUBROUTINE TO DETERMINE VERTICAL AND
C  HORIZONTAL OFFSETS FOR THE ADDITIONAL TEETH DUE TO
C  THE BLADE INCLINATION AND TOOTH PITCH
C
SUBROUTINE BLADE(H,V,NBLD,PITCH,ANGLE,N,XX,YY)
DIMENSION XX(501),YY(501)
DIMENSION H(501),V(501)
DO200I=1,N,1
XX(I)=H(I)-(3-NBLD)*PITCH*COS(ANGLE)
YY(I)=V(I)+(3-NBLD)*PITCH*SIN(ANGLE)
200  CONTINUE
      RETURN
      END

C
C  BEGINNING OF RUNGE-KUTTA NUMERICAL INTEGRATION SUBROUTINE
C  TO DETERMINE (APPROXIMATELY) THE HORIZONTAL SPAN OF THE
C  DEFLECTED PLATE
C
SUBROUTINE NUMINT(XELL,VEE,N,ELL)
DIMENSION Y(400),X(400)
H=XELL/N
J=1
N=N+1
SUM=0.0
10   X(J)=0.0*(J-1)*H
      Y(J)=SQRT(1.+(36.*VEE**2))*(X(J)**4-2.*X(J)**3+X(J)**2)
      IF(J.EQ.1)GO TO 20
      IF(J.EQ.N)GO TO 20
      IF(INT(J/2.)-J/2.)30,40,40
20   ADD=Y(J)*H/3.0
      GO TO 50
30   ADD=Y(J)*2.*H/3.0
      GO TO 50
40   ADD=Y(J)*4.*H/3.0
      GO TO 50
50   SUM=SUM+ADD
      IF(J.GE.N)GO TO 60
      J=J+1
      GO TO 10
60   ELL=SUM
      RETURN
      END

```


A.2. Strudl Analysis - Approach #1

```

*****
* STRUDL 'PLATE' 'PLATE DYNAMIC ANALYSIS - 1ST APPROACH' *
* 14 NODES - 16 ELEMENTS *
*****

```

```

*TITLE 'PLATE ANALYSIS'
**** ACTIVE UNITS - LENGTH WEIGHT ANGLE TEMPERATURE TIME
**** ASSUMED TO BE INCH POUND Radian FAHRENHEIT SECOND
TYPE PLATE
JOINT COORDINATES
1 0 0 0 SUPPORT
2 0 0 19 SUPPORT
3 5 0 9.5
4 10 0 0
5 10 0 19
6 15 0 9.5
7 20 0 0
8 20 0 19
9 25 0 9.5
10 30 0 0
11 30 0 19
12 35 0 9.5
13 40 0 0 SUPPORT
14 40 0 19 SUPPORT
JOINT RELEASES
13 14 FORCE X FORCE Y
ELEMENT INCIDENCES
1 1 2 3
2 1 3 4
3 2 3 5
4 3 4 5
5 4 5 6
6 4 6 7
7 5 6 8
8 6 7 8
9 7 8 9
10 7 9 10
11 8 9 11
12 9 10 11
13 10 11 12
14 10 12 13
15 11 12 14
16 12 13 14
ELEMENT PROPERTIES
1 TO 16 TYPE 'SBHT6' THICKNESS 0.5
CONSTANTS
DENSITY 0.0813 ALL & IN LB/IN3
E 4.1E+05 ALL
POISSON 0.35 ALL
INERTIA OF JOINTS LUMPED
INERTIA OF JOINTS 13 14 ADD LINEAR X 3.235E-3 Y 3.235E-3
EIGENPROBLEM PARAMETERS
SOLVE USING SUBSPACE
NUMBER OF MODES 1
END
DYNAMIC ANALYSIS MODAL

```

MODE	EIGENVALUE (RAD/SEC) ²	FREQUENCY (RAD/SEC)	FREQUENCY (CYC/SEC)	PERIOD (SEC/CYC)
1	6.888623D+02	2.58218D+01	4.116093D+00	2.429488D-01

A.3. Strudl Analysis - Approach #2

 * STRUDL 'PLATE' 'PLATE DYNAMIC ANALYSIS - 2ND APPROACH' *
 * 20 NODES - 20 ELEMENTS *

*TITLE 'PLATE ANALYSIS'

**** ACTIVE UNITS - LENGTH WEIGHT ANGLE TEMPERATURE TIME
 **** ASSUMED TO BE INCH POUND RADIAN FAHRENHEIT SECOND

TYPE PLATE

JOINT COORDINATES

1 0 0 0 SUPPORT

2 0 0 19 SUPPORT

3 2.5 0 9.5

4 5 0 0

5 5 0 19

6 10 0 19

7 10 0 0

8 15 0 0

9 15 0 19

10 20 0 19

11 20 0 0

12 25 0 0

13 25 0 19

14 30 0 19

15 30 0 0

16 35 0 0

17 35 0 19

18 37.5 0 9.5

19 40 0 0 SUPPORT

20 40 0 19 SUPPORT

JOINT RELEASES

19 20 FORCE X FORCE Y

ELEMENT INCIDENCES

1 1 2 3

2 1 3 4

3 2 3 5

4 3 4 5

5 4 5 6

6 4 6 7

7 6 7 8

8 6 8 9

9 8 9 10

10 8 10 11

11 10 11 12

12 10 12 13 13 12 13 14

14 12 14 15

15 14 15 16

16 14 16 17

17 16 17 18

18 16 18 19

19 17 19 20

20 18 19 20

ELEMENT PROPERTIES

1 TO 20 TYPE 'SDHT6' THICKNESS 0.5

CONSTANTS

DENSITY 0.0513 ALL 8 IN LB/IN3

E 4.1E+06 ALL
 POISSON 0.35 ALL
 INERTIA OF JOINTS LUMPED
 INERTIA OF JOINTS 19 20 ADD LINEAR X 3.235E-3 Y 3.235E-3
 EIGENPROBLEM PARAMETERS
 SOLVE USING SUBSPACE
 NUMBER OF MODES 1
 END
 DYNAMIC ANALYSIS MODAL

MODE	EIGENVALUE ($(\text{RAD/SEC})^2$)	FREQUENCY (RAD/SEC)	FREQUENCY (CYC/SEC)	PERIOD (SEC/CYC)
1	6.848059D+02	2.578383D+01	4.103824D+00	2.436870D-01

A.4. Strudl Analysis - Approach #3

```

*****
*   STRUDL 'PLATE' 'PLATE DYNAMIC ANALYSIS - 3RD APPROACH'   *
*   44 NODES - 44 ELEMENTS                                   *
*****

```

```

*TITLE 'PLATE ANALYSIS'
**** ACTIVE UNIT:  LENGTH  WEIGHT  ANGLE  TEMPERATURE  TIME
**** ASSUMED TO BE  INCH    POUND   RADIAN  FAHRENHEIT  SECOND
TYPE PLATE
JOINT COORDINATES
1 0 0 0 SUPPORT
2 0 0 19 SUPPORT
3 1 0 0.5
4 2 0 0
5 2 0 19
6 4 0 0
7 4 0 19
8 6 0 0
9 6 0 19
10 8 0 0
11 8 0 19
12 10 0 0
13 10 0 19
14 12 0 0
15 12 0 19
16 14 0 0
17 14 0 19
18 16 0 0
19 16 0 19
20 18 0 0
21 18 0 19
22 20 0 0
23 20 0 19
24 22 0 0
25 22 0 19
26 24 0 0
27 24 0 19
28 26 0 0
29 26 0 19
30 28 0 0
31 28 0 19
32 30 0 0
33 30 0 19
34 32 0 0
35 32 0 19
36 34 0 0
37 34 0 19
38 36 0 0
39 36 0 19
40 38 0 0
41 38 0 19
42 39 0 0.5
43 40 0 0 SUPPORT
44 40 0 19 SUPPORT
JOINT RELEASES
43 44 FORCE X FORCE Y

```

ELEMENT INCIDENCES

1 1 2 3
 2 1 3 4
 3 2 3 5
 4 3 4 6
 5 4 5 7
 6 4 6 7
 7 6 7 8
 8 7 8 9
 9 8 9 11
 10 9 10 11
 11 10 11 12
 12 11 12 13
 13 12 13 15
 14 12 14 15
 15 14 15 16
 16 15 16 17
 17 16 17 19
 18 16 18 19
 19 18 19 20
 20 19 20 21
 21 20 21 23
 22 20 22 23
 23 22 23 24
 24 23 24 25
 25 24 25 27
 26 24 26 27
 27 26 27 28
 28 27 28 29
 29 28 29 31
 30 28 30 31
 31 30 31 32
 32 31 32 33
 33 32 33 35
 34 32 34 35
 35 34 35 36
 36 35 36 37
 37 36 37 39
 38 36 38 39
 39 38 39 40
 40 39 40 41
 41 40 41 42
 42 40 42 43
 43 41 42 44
 44 42 43 44

ELEMENT PROPERTIES

1 TO 44 TYPE 'SBHT6' THICKNESS 0.6

CONSTANTS

DENSITY 0.0613 ALL & IN LB/IN3

E 4.1E+06 ALL

POISSON 0.35 ALL

INERTIA OF JOINTS LUMPED

INERTIA OF JOINTS 44 ADD LINEAR X 3.235E-3 Y 3.235E-3

EIGENPROBLEM PARAMETERS

SOLVE USING SUBSPACE

NUMBER OF NODES 1

END

DYNAMIC ANALYSIS MODAL

NODE	EIGENVALUE (RAD/SEC)**2	FREQUENCY (RAD/SEC)	FREQUENCY (CYC/SEC)	PERIOD (SEC/CYC)
1	7.889162D+02	2.769325D+01	4.407518D+00	2.269851D-01

A.5. Strudl Analysis - Approach #4

```

*****
*   STRUDL 'PLATE' 'PLATE DYNAMIC ANALYSIS - 4th APPROACH'   *
*   31 NODES - 40 ELEMENTS                                   *
*****

```

TITLE 'PLATE ANALYSIS'

```

**** ACTIVE UNITS - LENGTH WEIGHT ANGLE TEMPERATURE TIME
**** ASSUMED TO BE INCH POUND Radian FAHRENHEIT SECOND

```

TYPE PLATE

JOINT COORDINATES

1 0 0 19 SUPPORT

2 0 0 9.5 SUPPORT

3 0 0 0 SUPPORT

4 5 0 0

5 5 0 4.75

6 5 0 14.25

7 5 0 19

8 10 0 19

9 10 0 9.5

10 10 0 0

11 15 0 0

12 15 0 4.75

13 15 0 14.25

14 15 0 19

15 20 0 19

16 20 0 9.5

17 20 0 0

18 25 0 0

19 25 0 4.75

20 25 0 14.25

21 25 0 19

22 30 0 19

23 30 0 9.5

24 30 0 0

25 35 0 0

26 35 0 4.75

27 35 0 14.25

28 35 0 19

29 40 0 19 SUPPORT

30 40 0 9.5 SUPPORT

31 40 0 0 SUPPORT

JOINT RELEASES

29 30 31 FORCE X FORCE Y

ELEMENT INCIDENCES

1 1 6 7

2 1 2 8

3 2 5 6

4 2 3 2

5 3 4 5

6 4 5 10

7 5 9 10

8 5 6 9

9 6 6 9

10 6 7 8

11 8 13 14

12 8 9 13

13 9 12 13
 14 9 10 12
 15 10 11 12
 16 11 12 17
 17 12 16 17
 18 12 13 16
 19 13 15 16
 20 13 14 15
 21 15 20 21
 22 15 16 20
 23 16 19 20
 24 16 17 19
 25 17 18 19
 26 18 19 24
 27 19 23 24
 28 19 20 23
 29 20 22 23
 30 20 21 22
 31 22 27 28
 32 22 23 27
 33 23 26 27
 34 23 24 28
 35 24 25 26
 36 25 26 31
 37 26 30 31
 38 26 27 30
 39 27 29 30
 40 27 28 29

ELEMENT PROPERTIES

1 TO 40 TYPE 'SBHT6' THICKNESS 0.5

CONSTANTS

DENSITY 0.0513 ALL $\frac{1}{2}$ IN LB/IN³

E 4.1E+06 ALL

POISSON 0.35 ALL

INERTIA OF JOINTS LUMPED

INERTIA OF JOINTS 29 30 31 ADD LINEAR X 2.157E-3 Y 2.157E-3

EIGENPROBLEM PARAMETERS

SOLVE USING SUBSPACE

NUMBER OF MODES 1

END

DYNAMIC ANALYSIS MODAL

MODE	EIGENVALUE (RAD/SEC)**2	FREQUENCY (RAD/SEC)	FREQUENCY (CYC/SEC)	PERIOD (SEC/CYC)
1	6.554613D+02	2.560198D+01	4.074682D+00	2.454180D-01

A.6. Fourier Series Fitting Program.

```

*****
* SOLUTION OF SIMULTANEOUS EQUATIONS FOR THE PURPOSE *
* OF FITTING A FOURIER SERIES EQUATION THROUGH THE *
* PLATE END DEFLECTION DATA IN QUESTION *
*****

```

```

10  DIMENSION A(126,126),B(127,126),AT(126,126),C(127,127)
    DIMENSION X(126),Y(126),YFIT(126)
    BYTE FILE(16)
    TYPE*, 'ENTER DATA FILE NAME PLEASE'
    ACCEPTIO, FILE
    FORMAT(16A1)
    OPEN(UNIT=1, NAME=FILE, ACCESS='SEQUENTIAL', TYPE='OLD')
    READ(1,*)M
    DO 20J=1,M
    READ(1,*)X(J),Y(J)
20  CONTINUE
    PI=4.0*ATAN(1.0)
    TYPE*, 'WHAT ORDER OF SERIES DO YOU WISH TO PURSUE?'
    ACCEPTI*, N
    DO30J=1,M
    DO25I=1,M
    A(J,I)=COS(I*PI*X(J)/12)
    AT(I,J)=A(J,I)
25  CONTINUE
30  CONTINUE
C   MULTIPLY THE MATRIX AND ITS TRANSPOSE TOGETHER
C
C   DO60I=1,M
C   DO60K=1,M
C   SUM=0.0
C   DO40J=1,M
C   SUM=SUM+A(J,I)*AT(K,J)
40  CONTINUE
C   B(K,I)=SUM
50  CONTINUE
60  CONTINUE
C   FORM AUGMENTED MATRIX BY ADDITION OF 'Y' VALUES
C   MULTIPLIED BY THE TRANSPOSED MATRIX 'AT'
C
C   DO80J=1,M
C   SUM=0.0
C   DO70I=1,M
C   SUM=SUM+AT(J,I)*Y(I)
70  CONTINUE
C   K=K+1
C   B(J,K)=SUM
80  CONTINUE
C   AUGMENTED MATRIX NOW FORMED WITH DIMENSIONS (M+1)*M
C   BEGIN SEARCH FOR THE LARGEST PIVOT ELEMENT
C
90  N=K-1
    IF(M.EQ.1)GO TO 100

```

```

JJ=1
BIG=ABS(B(1,1))
DO110I=2,N
AB=ABS(B(1,1))
IF(BIG-AB)100,110,110
100 BIG=AB
JJ=1
110 CONTINUE
IF(JJ-1)120,140,120
120 DO130J=1,M
TEMP=B(JJ,J)
130 B(1,J)=TEMP
140 DO150J=2,K
DO160I=2,M
150 C(I-1,J-1)=B(I,J)-B(1,J)*B(1,1)/B(1,1)
DO160J=2,K
160 C(N,J-1)=B(1,J)/B(1,1)
K=K-1
C
C ASSIGN THE 'C' MATRIX TO THE NAME 'B'
C
DO170J=1,K
DO170I=1,M
170 B(I,J)=C(I,J)
IF(K-1)90,180,90
C
C PRINT THE SOLUTION VECTOR
C
180 WRITE(6,190) (B(I,1),I=1,M)
190 FORMAT(' *10X,F14.7)
DO210I=1,126
SUM=0.0
DO200J=1,M
SUM=SUM+B(J,1)*COS(J*PI*X(I)/12.)
200 CONTINUE
YFIT(I)=SUM
210 CONTINUE
DO220I=1,126
WRITE(6,230)X(I),Y(I),YFIT(I)
WRITE(7,*)X(I),YFIT(I)
OPEN(UNIT=7,NAME='FOUR.DAT',STATUS='NEW')
230 FORMAT(3F12.8)
220 CONTINUE
ERROR=0.0
DO240I=1,126
ERROR=ERROR+(YFIT(I)-Y(I))**2
240 CONTINUE
TYPE*, 'COMPOUNDED ERROR (SQUARED) = '
WRITE(6,*)ERROR
STOP
END

```

A.7. System Equations Solution Program

```

*****
* SOLUTION OF THE SYSTEM SIMULTANEDUS EQUATIONS*
* BY GAUSS-JORDAN ELIMINATION METHOD
*****

```

```

      DIMENSION A(50,50),B(50,50),C(50,50)
      TYPE *, 'HOW MANY EQUATIONS DO YOU WISH ME TO SOLVE?'
      ACCEPT *, N
      N=N+1
      TYPE *, 'WHAT ARE THE VALUES OF THE AUGMENTED MATRIX?'
      ACCEPT *, ((C(I,J),J=1,N),I=1,N)
      GO TO 90
80    TYPE *, 'WHAT IS THE INTERFERENCE VALUE FOR THIS RUN?'
      ACCEPT *, PUSH
      C(N,N)=PUSH
      TYPE *, 'IS THERE ANY OTHER VALUE YOU WISH TO CHANGE (1 FOR YES)'
      ACCEPT *, CHANGE
      IF(CHANGE.NE.1) GO TO 90
      TYPE *, 'INPUT I,J MATRIX COORDINATES OF CHANGING VALUE'
      ACCEPT *, U
      ACCEPT *, V
      TYPE *, 'INPUT NEW VALUE'
      ACCEPT *, GNU
      C(U,V)=GNU
90    DO 20 I=1,N
      DO 20 J=1,N
      A(I,J)=C(I,J)
      WRITE(6,*)C(I,J),A(I,J)
20    CONTINUE
      SEARCH FOR LARGEST PIVOT ELEMENT
      K=M-1
6      IF(K.EQ.1) GO TO 11
      JJ=1
      BIG=ABS(A(1,1))
      DO 8 I=2,K
      AB=ABS(A(I,1))
      IF(BIG-AB) 7,8,8
7      BIG=AB
      JJ=1
8      CONTINUE
      IF(JJ-1) 9,11,9
9      DO 10 J=1,M
      TEMP=A(JJ,J)
10     A(I,J)=TEMP
11     DO 12 J=2,M
      DO 12 I=2,N
12     B(I-1,J-1)=A(I,J)-A(I,J)*A(I,1)/A(1,1)
      DO 13 J=2,M
13     B(N,J-1)=A(I,J)/A(1,1)
      M=M-1
      ASSIGN THE 'B' MATRIX TO THE NAME 'A'
      DO 14 J=1,M
      DO 14 I=1,N
14     A(I,J)=B(I,J)
      IF(M-1) 6,13,8
      PRINT THE SOLUTION VECTOR

```

```
15  DO 100 I=1,M
    TYPE *, ' '
    WRITE(6,*)A(I,1)
100  CONTINUE
    BETA=A(1,1)*180./3.1412
    TYPE *, ' '
    WRITE(6,*)BETA
    TYPE *, 'IF FINISHED, TYPE 1'
    ACCEPT *,Q
    IF (Q.EQ.1)GO TO 17
    M=M+1
    GO TO 80
17  STOP
    END
```

